Investigation of the Role of Pds5 and Wapl in Sister Chromatid Separation in Mammalian cells

Thesis submitted for the degree of Doctor of Philosophy at the University of Leicester

By

Naif Abdulaziz Binjumah

Department of Biochemistry

College of Medicine, Biological Sciences and Psychology

University of Leicester

University Road, Leicester, LE1 7RH

June 2013

Declaration

The accompanying thesis submitted for the degree of Doctor of Philosophy, entitled "Analysis of the Role of Pds5 in Sister Chromatid Cohesion" is based on work conducted by the author in the Department of Biochemistry at the University of Leicester mainly during the period January 2009 and June 2013. All of the work recorded in this thesis is original unless otherwise acknowledged in the text or by references. None of the work has been submitted for another degree in this or any other University.

Signed: 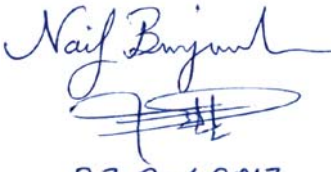

Date: 23 Oct 2013

Department of Biochemistry

University of Leicester

Lancaster Road

Leicester

LE1 9HN

Abstract

The key element of sister chromatid cohesion (SCC) is the cohesin complex composed of Smc1, Smc3, Scc1 and Scc3 (SA1 and SA2 in vertebrates). However, additional proteins such as Pds5 and Wapl are also known to regulate SCC. Most of our knowledge of Pds5 function derives from studies in yeasts and humans, and its role in SCC, although explored, remains unclear. Previous studies have implicated Pds5 in maintaining SCC in budding yeast and fungi (*Sordaria*). In *Xenopus* egg extracts, however, Pds5 is reported to be required for sister chromatid resolution during prophase. Since the role of Pds5 in regulating SCC in mammalian cells remains unclear, the aim of this project was to characterize the function of the two human Pds5 homologues, Pds5A and Pds5B and human Wapl in the regulation of sister chromatid cohesion.

Here using mammalian cells, I show that the Wapl protein level is cell cycle regulated and the protein dissociates from chromatin during prophase. In contrast, Pds5A and Pds5B protein levels are constant throughout the cell cycle and dissociate from chromatin in a consecutive manner during mitosis. siRNA-mediated depletion of Pds5A, Pds5B and Wapl individually prevented mitotic chromosome separation and activated the spindle assembly checkpoint (SAC), although some cells circumvented the SAC and exhibited mitotic defects. However, unlike Wapl, depletion of Pds5 proteins was also found to slow S-phase progression and induce apoptosis through activation of the DNA damage checkpoint. I also found that the association of Wapl with Pds5A increased after S-phase and continued until Wapl degradation after mitosis. Inhibition of either Cdk1/cyclin B1 or Plk1 abolished the association between Wapl and Pds5A.

The current model of vertebrate cohesin dissociation from chromosomes indicates a role for Sororin and SA2 phosphorylation in the removal of the cohesin complexes from chromosomal arms. Interestingly, I show that Wapl is a new substrate for Cdk1/cyclin B1 and Plk1. My data imply that Wapl phosphorylation at prophase is also required for the removal of cohesin complexes from chromosomal arms. Taken together, my results suggest that a reconsideration of the current model may be required to explain the mechanism of cohesin removal from chromosomes at mitosis.

Acknowledgment

I would like to thank my parents, wife Ghadeer, son Rayan, brothers and sisters for their support and encouragement over the past four years.

I would also like to thank my supervisor Dr Raj Patel, for his support and guidance throughout my Ph.D, and committee members Prof. Andrew Fry and Dr. Shaun Cowley. Many thanks to Dr. Kees Straatman and Tara Hardy for their help with image analysis. Dr. Laura O'Regan for her help in carrying out the kinase assay. Dr. Xiaowen Yang for his help with generation of constructs. PNACL laboratory, University of Leicester for mapping phosphorylation sites by mass spectrometry.

I am truly thankful to my colleagues and friends Dr Sameeh Al-Sarayreh, Abdulwahab Binjumah and Mohammed Alamro and all who gave invaluable support specially Dr Khawla Al-Kuraya, Dr Shahab Uddin and KFSH&RC.

Contents

List of figures

List of tables

Abbreviations

aa	Amino acid
APC/C	Anaphase-promoting complex/cyclosome
APS	Ammonium persulphate
AT	Adenine-thymine
ATM	Ataxia telangiectasia mutated
ATP	Adenosine triphosphate
ATR	Ataxia telangiectasia and Rad3 related
BLAST	Basic Local Alignment Search Tool
bp	Base pair
BRCA1	Breast cancer 1
BSA	Bovine serum albumin
BUB	Budding uninhibited by benzimidazole
BUBR1	Budding uninhibited by benzimidazole Related 1
C-terminal	Carboxy-terminal
CAF	Chromatin assembly factor
CAR	Cohesion attachment regions
Cdc2	Cell division control protein 2 homolog
Cdc20	Cell division cycle protein 20
Cdc25A	Cell division cycle protein homolog A
Cdh1	Cdc20 homologue 1
Cdk	Cyclin dependent kinase
cDNA	Complementary DNA
ChiP	Chromatin immunoprecipitation
Chk1/2	Checkpoint kinase 1/2
CKIs	Cyclin dependent kinase inhibitors
cm	Centimetre
Co-IP	Co-Immunoprecipitation
CO_2	Carbon Dioxide
CPC	Chromosome passenger complex
CSC	Checkpoint sliding clamp
CSF	Cytostatic factor
CSK	Cytoskeleton
DMEM	Dulbecco's Modified Eagle's Medium

DMSO	Dimethyl sulphoxide
DNA	Deoxyribonucleic acid
dNTP	Deoxynucleotide triphosphate
DP	Differentiation regulated transcription factor proteins
DSB	DNA double-strand breaks
E. coli	Escherichia coli
EBNA2	Epstein-barr nuclear antigen 2
EGFP	Enhanced green fluorescent protein
ESCO1/2	Establishment of cohesion homolog 1/2
FACS	Fluorescence-activated cell sorting
FGF	Phenylalanine-glycine-phenylalanine
FISH	Fluorescence in situ hybridization
FITC	Fluorescein isothiocyanate
FOE	Friend-of-Epstein-Barr nuclear antigen 2
g	Gram
G1	Gap 1
G2	Gap 2
h	Hour
HEAT	Huntington, Elongation Factor 3, PR65/A, TOR
HEK 293T	Human Embryonic Kidney 293T
HeLa	Henrietta Lacks
HMG	High mobility group
HPV	Human papilloma virus
HR	Homologous recombination
HRP	Horseradish peroxidase
hrs	Hours
INCENP	Inner centromere protein
IP	Immunoprecipitation
kDa	kilo Daltons
M (unit)	Molarity
M	Mitosis
m/z	Mass/charge ratio
mA	Milliamps
MAD1/2/3	Mitotic arrest- deficient protein 1/2/3
min	Minute
ml	Millilitres

mm	Millimetre
mM	Millimolar
mRNA	Messenger ribonucleic acid
N-terminal	NH2-terminal
ng	Nanogram
nm	Nanometre
Noc	Nocodazole
NP40	Nonyl phenoxypolyethoxylethanol 40
O.A	Okadaic acid
°C	Centigrade
p21	Protein 21
p53	Protein 53
PARP	Poly (ADP-ribose) polymerase
PASC	Parallel sister chromatids protein
PBD	Polo box domain
PBS	Phosphate buffered saline
PCNA	Proliferating cell nuclear antigen
PCR	Polymerase chain reaction
Pds5	Precocious dissociation of sisters protein 5
PI	Propidium Iodide
Plk1	Polo-like kinase 1
PMSF	Phenylmethylsulphonly fluoride
PP2A	Protein phosphatase 2A
RB	Retinoblastoma protein
RBS	Roberts' syndrome
Rfc	Replication factor C
RIPA	Radio-immunoprecipitation assay
RNA	Ribonucleic acid
RNAi	RNA interference
rpm	Revolutions per minute
RT	Room temperature
S-phase	SynthesiS-phase
S	Serine
S. cerevisiae	Saccharomyces cerevisiae
S. pombe	Schizosaccharomyces pombe
SA1/2/3	Stromalin antigens 1/2/3

SAC	Spindle assembly checkpoint
Scc	Sister chromatid cohesion
SCC-112	Sister chromatid cohesion protein 112
SD	Standard deviation
SDS-PAGE	Sodium dodecyl sulphate polyacrylamide gel electrophoresis
sec	Second
Ser	Serine
Sgo1	Shugoshin 1
siRNA	Small interfering RNA
Smc	Structural maintenance of chromosomes
SOC	Super Optimal Broth with Catabolite
T	Threonine
Temed	Tetramethylethylenediamine
TST	Tris-Saline-Tween
V	Voltage
v/v	Volume in volume ratio
w/v	Weight in volume ratio
Wapl	Wings apart-like
μCi	Microcurie
µg	Microgram
µl	Microliters

Chapter 1

Introduction

1.1. Sister chromatid cohesion

The sister chromatid cohesion (SCC) apparatus ensures that the sister chromatids of replicated chromosomes are physically paired, which is crucial for regulating different events during interphase, such as gene expression and development (Dorsett, 2007) and cell division in both mitosis and meiosis. Without this pairing, precocious separation of sister chromatids may occur before chromosomes are attached to the spindle fibers and equal distribution of the genetic material into the two daughter cells would be impossible. The establishment and dissolution of SCC is tightly controlled in health and any aberrant regulation may lead to chromosome missegregation, aneuploidy or genomic instability, which are the hallmarks of cancer cells (Pfau and Amon, 2012). Characterizing and identifying the molecular mechanisms regulating the dissolution of SCC is therefore essential for better understanding of the regulation of cell division control.

Recently, many proteins have emerged as fundamental regulators of SCC and its dissolution (Losada and Hirano, 2005, Nasmyth, 2005, Nasmyth and Haering, 2005, Hirano, 2005b). Research into the molecular mechanism of how sister chromatids are separated is required to understand the underlying basis of various causes of cancerous phenotypes. This can be accomplished by understanding the functional properties of the regulatory proteins implicated in the regulation of SCC. The main focus of this project is to characterize the role of cohesin regulatory proteins, Pds5 and Wapl, in the regulation of SCC and to shed light on the mechanism that triggers sister chromatid separation in early mitosis. This introduction to the thesis seeks to explain the basic principles of cell cycle control, the cohesin complex and the cohesin-related proteins.

1.2. The mammalian cell cycle

Mammalian cells have multiple mechanisms by which quiescent cells are prompted to enter the cell cycle through the G1-phase (Figure 1.1). A sequence of biochemical events contributes to this process. Phosphorylation of target proteins is carried out by a family of cyclin-dependent kinases (Cdks) that are regulated at each stage of the cell cycle. As long as extracellular stimuli such as growth factors are present, cyclin D is synthesised and binds to and activates Cdk4/6. The central cell cycle regulator Cdk4, 6/cyclin D complex is sufficient to convert the unphosphorylated RB/E2F-1/DP complex to the hypophosphorylated form. After the activation of cyclin D-Cdk4/6, growth factors elevate other genes, such as cyclin E, which binds to Cdk2, resulting in the hyperphosphorylation of retinoblastoma protein (RB) and causes its dissociation from E2F. The release of hyperphosphorylated RB from the E2F/DP complexes allow activation of the E2F-responsive genes, which is required to drive the cell cycle through the G1/S transition and to induce DNA synthesis (Hinds et al., 1992, Lundberg and Weinberg, 1998).

During S-phase, the newly replicated DNA is rapidly packed into condensed chromatin fibers. The basic packing unit of chromatin is the nucleosomal repeat, consisting of 147 base pairs of DNA wrapped around an octamer of histones. These nucleosomes mediate assembly of newly replicated DNA with the aid of chromatin assembly factors (CAFs), proteins associated with the replication fork machinery. In eukaryotes, there are five basic types of histones (H1, H2A, H2B, H3, and H4), which are synthesized mainly in S-phase. Two each of the core histones H2A, H2B, H3, and H4 come together to form a central octamer, which binds and wraps approximately 146 base pairs of DNA. The histone H1 (linker histone) binds to DNA on the outside of the nucleosomes, then these interact with each other, causing chromatin to be packed further into higher order structures. Eukaryotic chromatin contains two distinct domains, euchromatin and heterochromatin. Euchromatin is less condensed, contains more genes and other unique sequences, is more accessible and is generally more easily transcribed, whereas heterochromatin is typically highly condensed, has highly repetitive satellite sequences and forms structural functions such as forming centromeres or telomeres. The centromere is the region of each chromosome that attaches to spindle fibers during mitosis and meiosis (Olins and Olins, 1974, Olins and Olins, 2003).

Mitosis is a highly regulated process that includes various stages during which the cell divides its contents into two resulting in the generation of two daughter cells from a parent cell. This process comprises the six stages of mitosis: prophase, prometaphase, metaphase, anaphase, telophase and cytokinesis. In prophase, the centrosomes separate and form a mitotic spindle.

During prometaphase, the kinetochore attaches to the chromosomes while the microtubules attach to the kinetochore on the other side of the chromosomes. During metaphase, the chromosomes are aligned and organised between the mitotic spindles, then the cell duplicates its chromosomes (sister chromatids), which separate at anaphase and move to opposite sides by shortening and depolymerising the mitotic spindles, before the cell undergoes cytokinesis (Figure 1.1), dividing into two daughters, each with one centrosome and one set of chromosomes (Alberts, 2002).

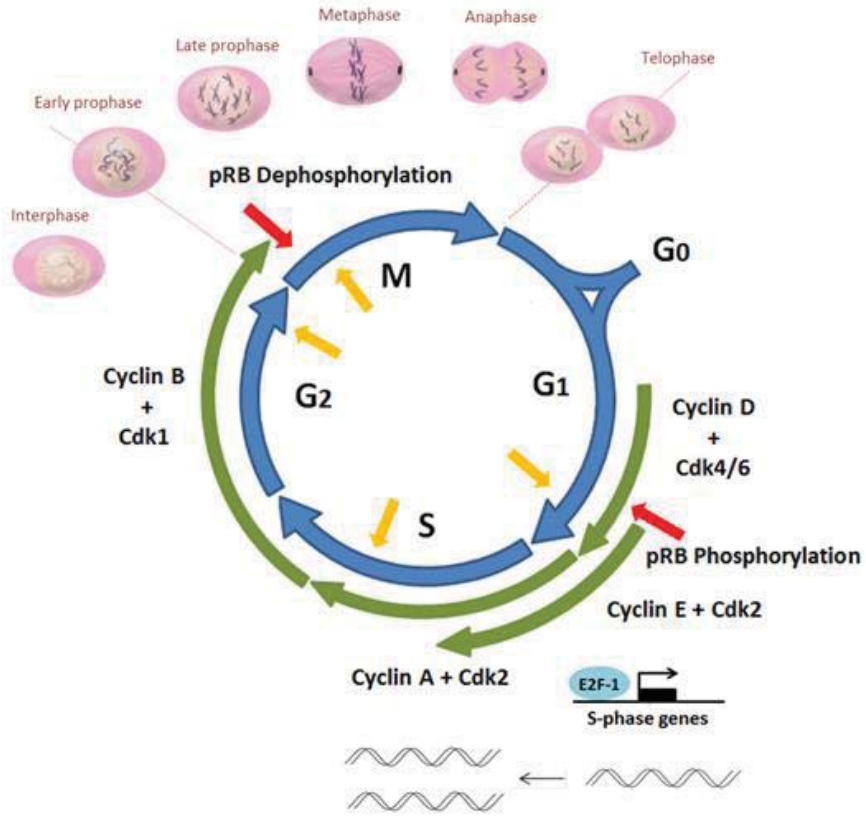

Figure 1.1: The regulation of the eukaryotic cell cycle.

The cell cycle is an ordered set of events, consisting of interphase and mitosis (M). Interphase is divided into three distinct phases: Gap 1 (G1) also called the growth phase, Synthesis (S) and Gap 2 (G2). The cell cycle is monitored by three DNA damage checkpoints during interphase and one spindle assembly checkpoint (SAC) during mitosis (yellow arrows). Non-proliferative cells generally exit the cell cycle and enter the quiescent G0 state, and may remain quiescent for long periods of time, until growth factors are present, when they re-enter the cell cycle. The growth factors also activate Cdk4/6 and Cdk2, which hyperphosphorylate and dissociate Rb from E2F-1. E2F-1 now is able to perform its transcription factor functions and allows the G1-to-S-phase transition. After DNA synthesis, the cell enters the G2-phase, where they continue to grow and prepare for cell division. When a cell enters mitosis, the chromosomes condense (Early prophase), the nuclear envelope breaks down and spindle microtubules attach to kinetochores (Prophase). The chromosomes then align at the metaphase plate (Metaphase), separate and pull apart to the spindle poles (Anaphase). The nuclear envelope reforms for each daughter cell (Telophase) and the two daughter cells are now divided (Cytokinesis) (Alberts, 2002).

1.2.1. Cell cycle checkpoints

Eukaryotic cells have evolved a set of feedback control mechanisms or checkpoints, to ensure that genetic information is copied faithfully and transmitted from the mother to the daughter cells. These regulatory pathways monitor the successful completion of events in one phase of the cell cycle before allowing the cell to proceed to the next phase. This involves monitoring DNA damage and spindle assembly. The DNA damage checkpoints recognize the presence of damaged DNA at G1 (before the S-phase) and at G2, and progress through the cell cycle is halted until the problem is solved, whereas the spindle assembly checkpoint detects improper alignment of chromosomes, or any failure of the attachment between the mitotic spindle and kinetochores, and arrests the cell in metaphase until they attached correctly.

1.2.2. The DNA damage checkpoints

In the presence of damaged DNA during G1, sensor genes RAD17, RAD9, Rad1 and HUS1 form a heterotrimeric checkpoint sliding clamp (CSC) similar in structure to the DNA polymerase clamp PCNA (Proliferating Cell Nuclear Antigen) (Shiomi et al., 2002), while Rad17 forms a complex with four replication factor C (Rfc) subunits, Rfc2, Rfc3, Rfc4 and Rfc5 (Rfc-related complex), which act as a clamp loader that is related to PCNA (Kondo et al., 1999, Griffith et al., 2002). These complexes are recruited to the damage site and trigger the DNA damage checkpoint response by activating the signal transducer kinase ATM/ATR, which in turn activates several kinases including Chk1 and Chk2 (Liu et al., 2000, Matsuoka et al., 2000). Activation of Chk1 involves phosphorylation at Ser 317 and Ser 345 in response to blocked DNA replication or certain forms of genotoxic stress (Lopez-Girona et al., 2001, Zhao and Piwnica-Worms, 2001). Chk1 is now able to phosphorylate the C-terminal portion of Cdc25A and inhibits its phosphatase activities toward Cdk2 and 4 (Chen et al., 2003), thus stopping the progression of the cell cycle until the damage is repaired. In contrast to Chk1, Chk2 phosphorylates Cdc25A at Ser^{123}, BRCA1 at Ser^{988} and p53 at several sites, including Ser^{20} (Bartek and Lukas, 2003). p53 is thought to be essential for G1 arrest in response to DNA damage. Activation of p53 directly induces the expression of the Cdk inhibitor, p21, which inhibits cyclin E-Cdk2 activity, thereby inhibiting G1/S transition (Bartek and Lukas, 2003).Chk1 and Chk2 are the major effectors of the G2/M DNA damage checkpoint response by phosphorylating Cdc25C on Ser^{216} and down-regulating its phosphatase activity (Furnari et al., 1997, Matsuoka et al., 1998, Sanchez et al., 1997), so that it can no longer activate Cdk1/Cdc2.

1.2.3. The spindle assembly checkpoint (SAC)

The spindle assembly checkpoint (SAC) is thought to suppress the metaphase-anaphase transition in the presence of a damaged mitotic spindle (e.g. microtubule depolymerizing and stabilizing drugs such as nocodazole and taxol) or in the presence of unattached kinetochores (Jordan et al., 1992, Jordan et al., 1993, Rieder et al., 1994, Rieder et al., 1995). Microtubule depolymerization causes spindle checkpoint activation and cell cycle arrest in metaphase. The SAC is also activated if cells fail to biorient sister chromatids on the spindle and fail to align at the metaphase plate (Rieder et al., 1994) (Figure 1.2).

Several groups of SAC proteins have a crucial role in a pathway that is active during prometaphase until alignment of the chromosomes occurs during metaphase. These proteins include the mitotic-arrest deficient proteins (Mad1, Mad2 and Mad3/BubR1 in humans) and the budding uninhibited by benzimidazole proteins (Bub1 and Bub3) (Hoyt et al., 1991, Li and Murray, 1991). Cdc20, a substrate-specific activator of the ubiquitin ligase, anaphase-promoting complex/cyclosome (APC/C) is the direct target of SAC activation and polyubiquitylates two key substrates, cyclin B and securin (Yu, 2002). Degradation of the ubiquitylated securin causes the activation of separase and subsequent cleavage of the cohesin subunit, Scc1, which holds sister chromatids together (Uhlmann et al., 1999). In contrast, the proteolysis of cyclin B is required for down-regulation of the master mitotic kinase, Cdk1, which is necessary for exit from mitosis in diverse systems (Peters, 2006). The SAC prevents this basic chain of events by prolonging prometaphase through the inactivation of Cdc20 to make sure that cells do not enter anaphase until all chromosomes have biorientated spindle attachment at the metaphase plate. When chromosome biorientation is established, the SAC is inactivated, allowing cells to enter anaphase (Li et al., 1997).

During prometaphase, Cdc20 and all SAC proteins localize at unattached kinetochores (Simonetta et al., 2009, Hewitt et al., 2010, Maldonado and Kapoor, 2011) and some SAC proteins are immediately removed upon the attachment of the microtubule to the kinetochores. For instance, Mad2 localizes to unattached kinetochores in prometaphase after binding Mad1 (Hewitt et al., 2010) and it is implicated in the mechanism by which the SAC induces mitotic arrest in response to spindle damage (Gorbsky et al., 1998). Moreover, the APC/Cdc20 is a target of the Mad2-dependent SAC, which is required for the degradation of cyclin B and securin.

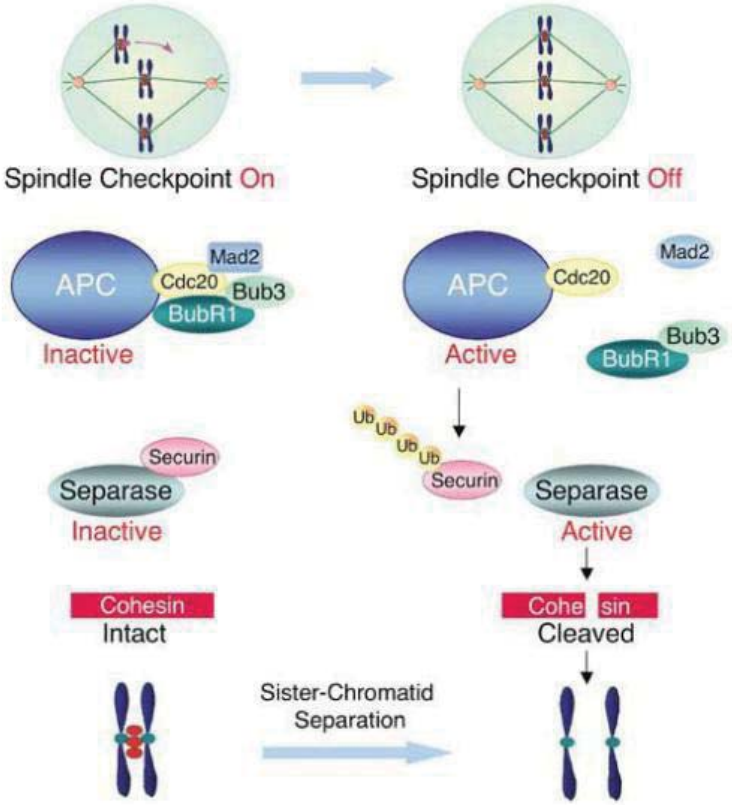

Figure 1.2: Spindle assembly checkpoint activation.

Separase is held inactive until the onset of anaphase through its binding to the inhibitor protein securin. (A) Unattached kinetochore causes spindle checkpoint activation and cell cycle arrest in metaphase. (B) Biorientated attachment of kinetochores silences the spindle assembly checkpoint; the APC becomes active and indirectly triggers the degradation of cohesin by targeting securin, which results in sister chromatid separation at anaphase (Bharadwaj and Yu, 2004).

1.3. The cohesin complex

The key structural component of SCC is a chromosomal protein complex known as cohesin (Figure 1.3). The cohesin complex consists largely of the flexible structural maintenance of chromosome (SMC) family of ATPases, Smc1/Psm1 and Smc3/Psm3. These two subunits bind to each other, head to head through interactions between their hinge domains and tail to tail through interactions with non-SMC subunits, sister chromatid cohesion protein-1 Scc1/Mcd1/Rad21 (a member of the kleisin family of proteins) and stromal antigens Scc3/Psc3/SA (SA1 and SA2 in vertebrates) (Haering et al., 2002, Gruber et al., 2003). The N- and C-terminal sequences of the SMC heads are linked to the globular ATPase heads that play a role in cohesin complex assembly (Weitzer et al., 2003). There are different models to explain the mode of interaction between cohesin complex and chromatin (Figure 1.4). Studies of the crystal structure of a complex between ATPase heads of Smc1 and C-terminal domains of Scc1 reveal that Scc1 forms a folding motif known as winged helix domain that connects a pair of β strands in ATPase heads of Smc1 (Haering et al., 2004, Arumugam et al., 2006). Thereby, a ring-shaped structure (in the most acceptable model) with a diameter of approximately 50 nm is formed and holds sister chromatids together until mitosis, when the chromosomes separate (Figure 1.4C) (Haering et al., 2002). The protein sequences and structures of SMC proteins are highly conserved among a wide range of species with divergence of 0.0-0.1 % (Hirano, 2005a, White and Erickson, 2006), indicating the relationships between structure and function of cohesin across species. Table 1.1 summarizes the cohesin subunits and associated protein nomenclatures among species (Onn et al., 2008, Peters et al., 2008).

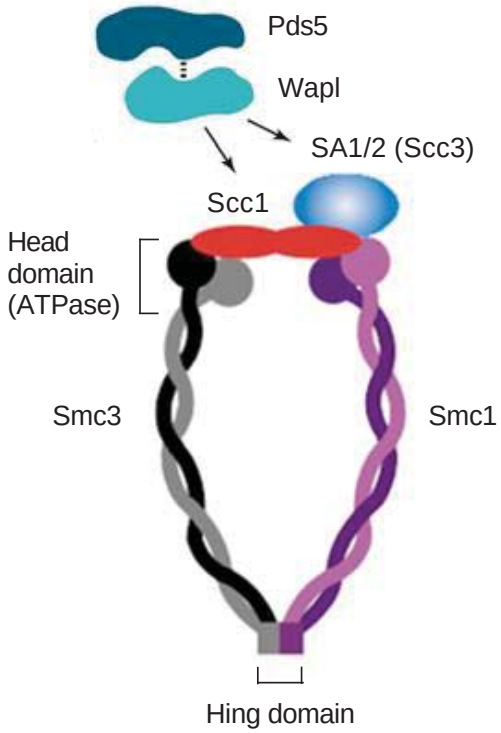

Figure 1.3: The cohesin complex.

The cohesin complex consists of a flexible coiled coil of the structural maintenance of chromosome proteins Smc1 and Smc3. These two proteins bind to each other head to head through the hinge domain and tail to tail through their interaction with Scc1 and SA1 or 2 (Campbell and Cohen-Fix, 2002). Cohesin regulatory protein Wapl association with the core complex depends on Scc1 and SA1, and there is evidence that Wapl directly interacts with Pds5 (Kueng et al. 2006).

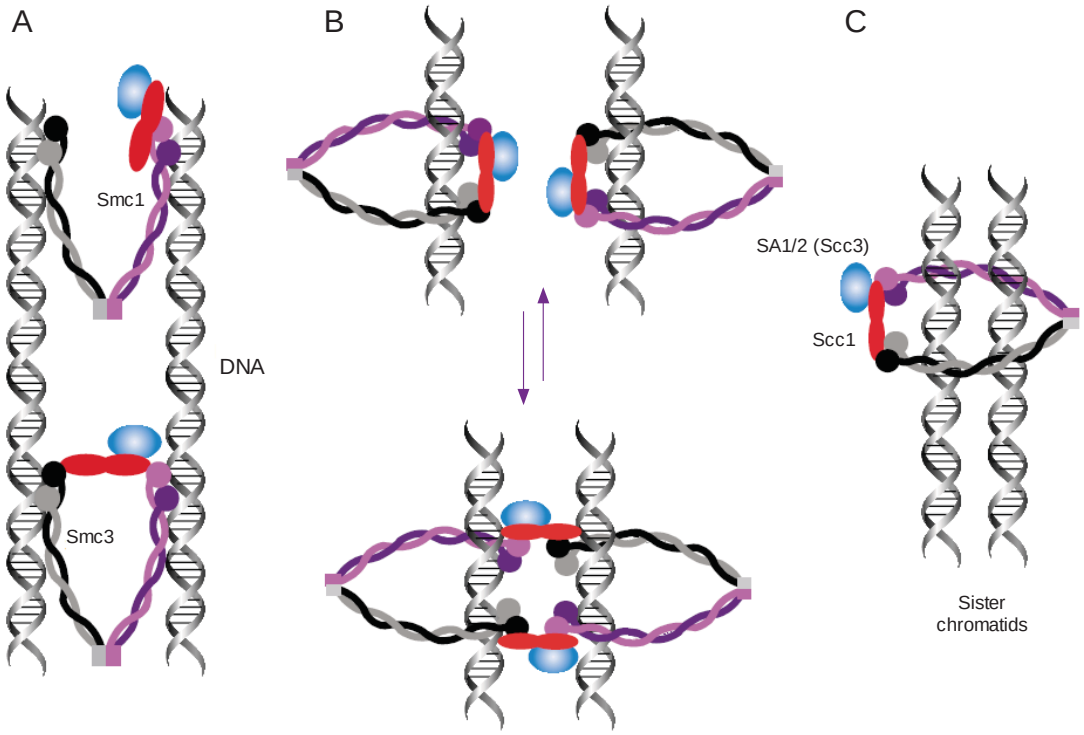

Figure 1.4: Models of cohesin interaction with chromatin.

(A) The SMC proteins interact directly with chromatin (direct binding model) to form a physical bridge between the sister chromatids (Anderson et al., 2002, Haering et al., 2002). (B) The cohesin complex loops around individual chromatids and cohesion is established by a change in the Scc1 association from intra-complex interactions (top panel) to inter-complex interactions (bottom panel) (Double-ring model). (C) The currently accepted model, the cohesin complex binds by encircling and embracing the two sister chromatids (ring model) (Haering et al., 2002).

Table 1.1: Cohesin subunits and its regulatory proteins.

Function	*Homo sapiens*	*Saccharomyces cerevisiae*	*Schizosaccharomyces pombe*	*Drosophila melanogaster*	*Xenopus laevis*	*Kilodaltons*
Cohesin subunits	Smc1 α	Smc1	Psm1	Smc1	Smc1	143/160
	Smc1 β*					144
	Smc3	Smc3	psm3	Smc3	Smc3	140
	RAD21 (Scc1)	MCD1	Rad21	Rad21	Rad21	72 /120
	SA1 (STAG1)	Scc3	Psc3	SA	SA1	145
	SA2 (STAG2)			SA2	SA2	138
	SA3 (STAG3)		Rec11*			139
	Rec8 (Scc1)*	Rec8*	Rec8*	c(2)M*	Rec8*	63
Loading factors	Nipbl	Scc2	Mis4	Nipped-B	Scc2	316
	hScc4 (Mau2)	Scc4	Ssl3	Scc4	Scc4	69
Acetyl transferases	Esco1	ECO1 (CTF7)	Eso1	Deco	Esco1	95
	Esco2			San	Esco2	27/ 68
Cohesin deacetylases	HDAC8**	Hos1				
Cohesion establishment	Sororin (CDCA5)			Dalmatian		28/35
Cohesion maintenance	PDS5A	*PDS5*	pds5	pds5	PDS5A	151
	PDS5B				PDS5B	165
Cohesion removal	WAPAL	Wpl1 (Rad61)	Wapl	Wapl	Wapl	140/180
	Plk1	CDC5	Plo1	Polo	Plx1	66
	Separin	ESP1	Cut1	Separase	Separin	233

* Cohesin subunits (meiosis) *Saccharomyces cerevisiae*
** Histone deacetylase 8

1.3.1. Regulation of the cohesin complex during the chromosome cycle

During the cell cycle, the chromosomes undergo a series of dynamic changes known as the chromosome cycle, involving replication, cohesion and segregation. In vertebrate cells, the cohesin complex is loaded onto chromatin during telophase following reformation of the nuclear envelope (Losada et al., 1998, Darwiche et al., 1999, Sumara et al., 2000, Gerlich et al., 2006), whereas in budding yeast the cohesin complex is loaded onto chromatin during late G1-phase (Guacci et al., 1997, Michaelis et al., 1997) (Figure 1.5). In all species studied so far, loading of cohesin onto chromatin requires loading factor comprising a protein complex of Scc2 and Scc4 (Gillespie and Hirano, 2004, Takahashi et al., 2004). The interaction between cohesin and chromatin is enriched at specific loci known as cohesion attachment regions (CARs). These regions are typically 500-800 base pairs long and occur approximately every 9 kilobases along the chromosome arms. High levels of cohesin interaction are also observed at the centromeric region (Cohen-Fix, 2001, Wang and Christman, 2001). However, this interaction is dynamic and not sufficient to ultimately link the sister chromatids to one another.

The stable binding of cohesin to chromatin takes place once the replication fork passes through the cohesin ring with the aid of replication fork-associated acetyltransferase Eco1/Ctf7 (Esco1/Esco2 in humans) (Skibbens et al., 1999, Toth et al., 1999, Ivanov et al., 2002, Unal et al., 2007). This enzyme lacks the ability to load cohesin onto chromatin, but it must be present during S-phase to establish cohesion and becomes dispensable when cohesion has been established, suggesting that Eco1 has a specific function during DNA replication. It has been shown that Eco1 acetylates the cohesin complex component Smc3 on two lysine residues on the ATPase head domain (Unal et al., 2007, Unal et al., 2008).

During prophase, the bulk of cohesin is dissociated from sister chromatid arms through a pathway that requires polo-like kinase 1 (Plk1), Aurora B and wings apart-like protein (Wapl) (Losada et al., 2002, Sumara et al., 2002, Gandhi et al., 2006), whereas cohesin at the centromeric region is protected by shugoshin (Sgo1), which targets protein phosphatase 2A (PP2A) to cohesin and prevents cohesin phosphorylation (Rivera and Losada, 2009). In both fission and budding yeast, Sgo1 associates with the protein phosphatase PP2A and protects centromeric cohesin in meiosis I by counteracting the phosphorylation of Rec8 (a member of the kleisin family of SMC) by Plk1 (Riedel et al., 2006). In humans, Sgo1 at the centromere recruits PP2A to counteract the Plk1-mediated phosphorylation of the SA1/2 cohesin subunits, thereby preventing their dissociation from the centromeric region (Rivera and Losada, 2009). The centromeric cohesin subunit Scc1 is cleaved during metaphase by separase, following its

activation by anaphase-promoting complex (APC/C) which allows the transition to anaphase (Rivera and Losada, 2009).

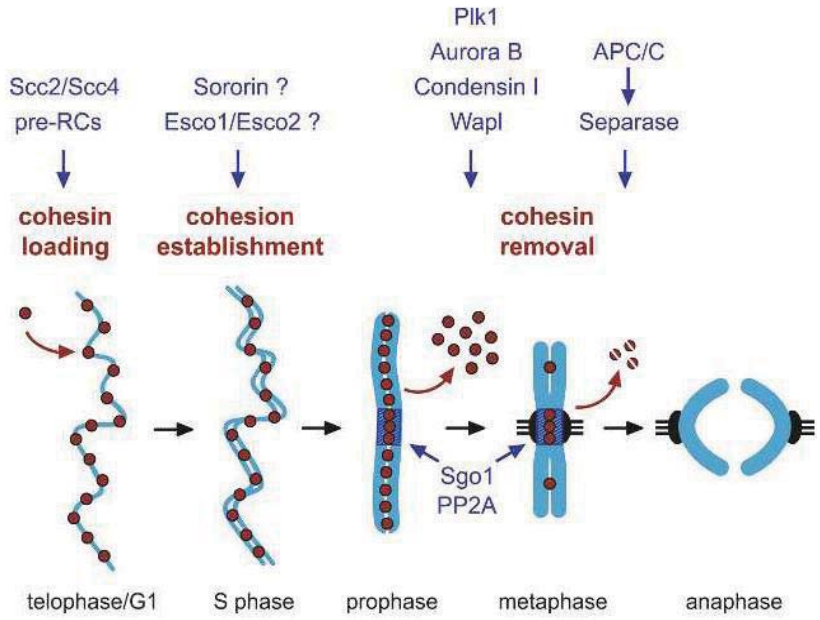

Figure 1.5: Cohesin regulation during the chromosome cycle.

The cohesin complex is loaded onto chromatin during telophase and G1, which requires the essential function of adhering complex Scc2/Scc4. The association of cohesin with chromatin at this stage is dynamic. The cohesion between sister chromatids is established and this requires additional factors such as Esco1/2 and Sororin. The bulk of cohesin dissociates from chromosome arms during prophase via the prophase pathway, involving Plk1, Aurora B and Wapl. However, the centromeric cohesin is protected by Sgo1-PP2A complex. The centromeric cohesin is removed during metaphase by separase, following its activation by anaphase-promoting complex (APC/C) which allows the transition to anaphase (Peters et al., 2008).

1.3.2. Cohesin and DNA-damage repair

The first indication of cohesin involvement in DNA double strand break (DSB) repair was discovered before cohesin was reported to mediate cohesion between replicated sister chromatids. The cohesin subunit Scc1/Mcd1 ortholog from *Schizosaccharomyces pombe* (*S. pombe*) was first identified in genetic screens for proteins whose mutation rendered *S. pombe* cells hypersensitive to radiation, because damaged DNA cannot be correctly repaired; thus, it was called Rad21 (Radiation-sensitivity) (Birkenbihl and Subramani, 1992). It has been suggested that repair of DSB by homologous recombination (HR) requires holding sister chromatids together by the cohesin complex. Cohesin assembly around the DSB requires DNA damage sensing complex MRX/N (Mre11/Rad50/Xsr2/Nbs1) (Figure 1.6), phosphorylation of histone H2AX by Mec1/Tel1, and cohesin loading factors (Strom et al., 2004, Unal et al., 2004).

In the presence of DNA damage, the DNA damage checkpoint promotes their physical proximity and spreads signals around the DSB site by histone H2AX phosphorylation (γH2AX) in humans (H2A in yeast). The cohesin complex is recruited to DSB sites with the aid of a loading factor Scc2/Scc4 loading complex (Strom et al., 2004). Cohesin binding to the phospho-H2AX domain is enabled by DSB repair endonuclease Mre11 (Unal et al., 2004), as well as functional loading factors (Strom et al., 2004). Yeast strains expressing a non-phosphorylatable H2A (H2AX in mammals) fail to recruit cohesin, suggesting that the phosphorylatable H2A may act as a signal for cohesin assembly (Unal et al., 2004). In addition, modifications such as acetylation and phosphorylation of the cohesin core subunits are also necessary for specific cohesin functions (Kitagawa et al., 2004). Eco1/Esco1 acetyltransferase is required to promote efficient cohesion establishment (Heidinger-Pauli et al., 2009). Eco1/ESCO1 acetyltransferase activity is generally restricted to S-phase and postreplication DNA damage may promote Eco1/ESCO1 activity via DNA damage checkpoint kinase, Mec1/ATR (Strom et al., 2004, Unal et al., 2007).

A recent study in budding yeast suggested that the cohesin complex that is established in S-phase is unable to maintain cohesion after a DSB in G2. Therefore, the S-phase cohesins must be removed by the protease separase for efficient repair of DSB. This was demonstrated when cells expressing the Mcd1 separase-resistant allele (non-cleavable mutant of Mcd1) failed to undergo DSB resection and impaired DNA repair events (McAleenan et al., 2013). In both budding and fission yeast, the protease separase is responsible for cohesin's removal from the chromosomes during mitotic anaphase (Uhlmann et al., 1999, Tomonaga et al., 2000, Uhlmann et al., 2000). In contrast, in vertebrates, most cohesins are removed from the chromosomes during prophase in a separase-independent process (Waizenegger et al., 2000,

Losada et al., 2002). These facts raise the question of how the S-phase cohesin is removed in the presence of DSB's in vertebrates. Perhaps this mechanism is different in vertebrates, because cohesin removal during prophase relies on cohesin regulatory proteins Pds5 and Wapl.

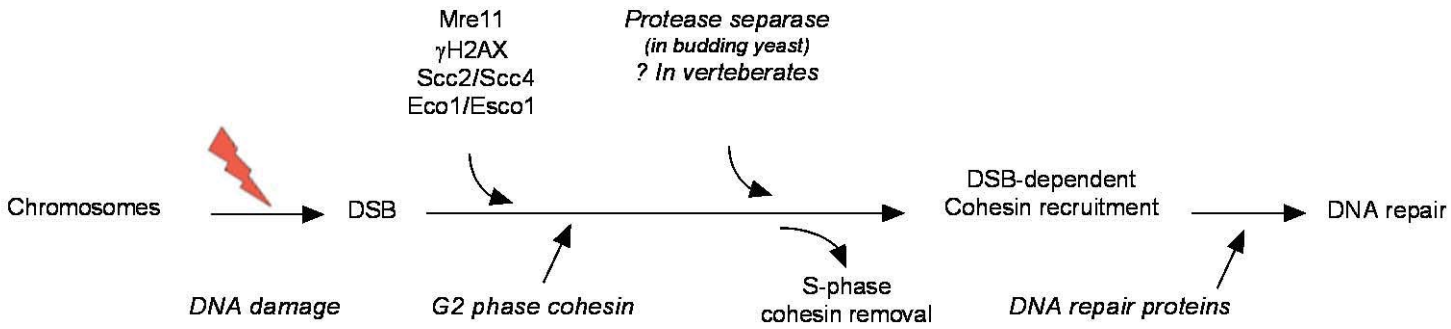

Figure 1.6: Cohesin metabolism during DNA-damage repair.

DNA damage sensor Mre11 promotes signalling pathways that activate DNA damage checkpoints. DNA breaks promote dissociation of cohesin loaded during the previous S-phase by separase (in budding yeast). H2AX phosphorylation (called γH2AX) marks the site of DNA damage and facilitates cohesin assembly around the DSB. Another specific cohesin loading factor, such as Scc2/Scc4, is also required for cohesin loading. Eco1/Esco1 acetyltransferase is activated via DNA damage checkpoint signalling and promotes the establishment of sister chromatid cohesion, which is required for the efficient DNA repair.

1.3.3. Regulation of the cohesin complex by prophase pathway

Several serine/threonine (S/T) protein kinases including Cdk1, Plk1, Aurora A and Aurora B are implicated in regulating cellular processes at mitosis (Takaki et al., 2008, Taylor and Peters, 2008, Hochegger et al., 2008). It has been shown that prophase pathway is facilitated by two mitotic kinases, Plk1 and Aurora B (Losada et al., 2002, Sumara et al., 2002), while Plk1 is likely to directly phosphorylate cohesin at SA1/2 (Rivera and Losada, 2009) and Cdk1 is essential for mitotic entry and cooperates with Plk1 to facilitate cohesin removal; however, the role of aurora B in this process remains unknown.

1.3.3.1. Aurora B kinase

Aurora B forms a comlex with INCENP (inner centromere protein), Survivin, and Borealin which is known as the chromosome passenger complex (CPC) (Carmena et al., 2009). This complex plays a key role in chromosome interactions with microtubules, chromatid cohesion, spindle stability, cytokinesis (Ruchaud et al., 2007) and bipolar chromosome orientation (Adams et al., 2000). It localizes at kinetochores during prophase and metaphase, then transfers to the central spindle and the midbody during anaphase (Cooke et al., 1987). The expression levels of Aurora B increase at the G2/M-phase and its maximum activity occurs during the transition from metaphase to anaphase (Terada et al., 1998, Goepfert et al., 2002).

Aurora B regulates many processes important for cell division. For example, Aurora B phosphorylates multiple substrates including histone H3 at Ser^{10} on chromatin (Giet and Glover, 2001, Goto et al., 2002). Chromatin plays an important role during cell differentiation and is controlled by specific epigenetic modifications of the core histones, such as phosphorylation and methylation, causing dysregulation of transcription factors (Turner, 2007). A recent study shows that phosphorylation of histone H3 at ser^{10} by Aurora B requires haspin (a mitotic kinase), to create a docking site for the BIR domain of survivin, allowing Aurora B positioning at inner centromeres in mitosis (Wang et al., 2012).

1.3.3.1.1. Aurora B and sister chromatid cohesion

It is known that release of cohesin from chromatin at the onset of mitosis correlates with phosphorylation of the SA/Scc3 subunits in *Xenopus* egg extracts without cleavage of the Rad21/Scc1 subunit (Losada et al., 2000). Other research in *Xenopus* egg extracts has shown a requirement for Aurora B in the prophase pathway to facilitate cohesin removal (Losada et al., 2002). Sperm chromatin was incubated with interphase extracts that had been depleted of Aurora B and the assembly mixtures were then converted into a mitotic state by adding

cytostatic factor (CSF) to cause metaphase arrest. The analysis of each sample and chromatin fractions by immunoblotting revealed that most cohesin dissociated from chromatin in the mock-depleted extracts, whereas depletion of Aurora B blocks cohesin release from chromatin (Losada et al., 2002), suggesting that Aurora B is required for cohesin removal at prophase.

A recent study of chicken DT40 cells indicated that Aurora B cooperates with Aurora A to coordinate chromosome separation (Hegarat et al., 2011). This was investigated by time-lapse microscopy analysis using cells expressing histone H2B-GFP after inhibition of Aurora A and/or Aurora B. The relative length of mitosis was 82 min in the absence of Aurora A, while the absence of Aurora B caused a shorter delay (40 min) and the absence of both kinases completely blocked chromosome segregation. Given that Bub1 and BubR1 are essential components of the SAC and that their recruitment to kinetochores is dependent on Aurora B (Hauf et al., 2003), the chromosomal passenger complex (CPC) subunits may take over a direct role in the SAC function. In an attempt to determine whether Aurora B affects SAC function, HeLa cells were treated with the antibiotic actinomycin D to displace endogenous Aurora B and other CPCs from centromeres/inner kinetochores while preserving Aurora B kinase activity. This was found to cause a premature loss of the checkpoint proteins BubR1 and Bub1 from the kinetochores, as well as chromosome misalignment and cytokinesis failure (Becker et al., 2010). Moreover, the inhibition of Mps1 (SAC kinase) and/or co-depletion of Mad2 did not interfere with chromosome separation, but reduced the time to complete mitosis and exhibited a number of lagging chromosomes (Hegarat et al., 2011). These results indicate a direct function of Aurora B in SAC activation and chromosome segregation.

1.3.3.2. Polo-like Kinase (Plk1)

Plk1 is a member of family of highly conserved serine/threonine kinases, first described in mutants that display abnormal mitotic spindle in *Drosophila melanogaster* (*polo*) (Sunkel and Glover, 1988, Llamazares et al., 1991) and *Saccharomyces cerevisiae* (*cdc5*) (Kitada et al., 1993). In mammalian cells there are four polo-like kinases: Plk1, Plk2, Plk3 and Plk4. The regulation of Plks depends on proteins that are important for cell division and controlled by phosphorylation and ubiquitin-dependent proteolysis (Nigg, 2001, Peters, 2002). Like many other kinases, Plks are activated by phosphorylation within a short region of the catalytic domain known as the activation loop (or T-loop). This occurs at T^{210} in *Homo sapiens* Plk1 (Jang et al., 2002) or T^{201} in *Xenopus laevis* Plx1 (Qian et al., 1999). Studies have shown that Plk1 is activated by the Aurora A kinase and its activator, bora, in a pathway that also operates in unperturbed cell cycles in human cells (Seki et al., 2008, Macurek et al., 2008).

Plk1 is the best characterized member of this family that plays a role in mitosis, including separation of sister chromatids (Barr et al., 2004, Garland et al., 2006, Lera and Burkard, 2012). In *S. cerevisiae*, most of the cohesins are dissociated from chromatin during anaphase. The Plk1/Cdc5 phosphorylates cohesin subunit Scc1 on specific serine residues that are adjacent to separase protease cleavage sites, facilitating the separation of sister chromatids (Alexandru et al., 2001). In addition, the depletion of Cdc5 almost abolishes Scc1 cleavage and greatly delays the separation of sister chromatid (Alexandru et al., 2001). In vertebrates, Plk1 similarly promotes the cleavage of cohesin subunits Scc1 and SA1/SA2 to promote its dissociation from chromatin, but in this system the cohesin complex is already dissociated from the chromosome arms during prophase. This cohesin removal depends not on separase, but instead on the activated Plk1 in early mitosis (Losada et al., 2002, Sumara et al., 2002). In *Xenopus*, the Plk1/Plx1 is required for the removal of cohesin from chromatin by phosphorylating mitotic cohesin subunits Scc1 and SA1/SA2, but not for chromosome condensation. Moreover, depletion of Plx1 from interphase and CSF extracts prevents cohesin dissociation from chromosome arms fraction, although phosphorylation of histone H3 on serine 10 and association of condensin subunit SMC4 on chromosome fractions are detected (Sumara et al., 2002). In human cells, Plk1 phosphorylates and activates Cdc25C, a phosphatase that dephosphorylates and activates the cyclin B1/CdK1 complex (Barr et al., 2004), and subsequent phosphorylation of early mitotic inhibitor 1 (EMI1), an inhibitor of the APC, creating a degradation signal that is recognized for ubiquitylation and subsequent degradation of EMI1 (Hansen et al., 2004).

Studies of the role of mammalian Plk1 have identified the consensus phosphorylation sites for Plk1. The C-terminal polo-box domain (PBD) found in the Plk family binds to phosphorylation sites for which the consensus is S-[pT/pS]-[P/x] (Nakajima et al., 2003), (E/D/Q)-x-(S/T) Φ (Barr et al., 2004) or (E/D)-x-(S/T) Φ-x-(E/D) (Nakajima et al., 2003), where Φ signifies a hydrophobic amino acid. These consensus sequences are thought to be phosphorylated follwoing priming by kinases such as Cdk1 for subsequent recognition by Plk1. Once bound to the substrate, Plk1 is thought to phosphorylate sites that are distinct from the one that is recognized by the PBD. Based on this, Nakajima et al. (2003) have suggested two phosphorylation sites in Scc1 (T^{144} and T^{312}) to match the consensus (E/D)-x-(S/T) Φ-x-(E/D), whereas Barr et al. (2004) have proposed an additional one in Scc1 (Ser^{454}) and three in SA2 (T^{1109}, Ser^{1137} and Ser^{1224}) to match the consensus (E/D/Q)-x-(S/T) Φ. These findings are consistent with the hypothesis that Scc1 and SA2 are directly phosphorylated by Plk1. Subsequently, the expression of a nonphosphorylatable mutant of SA2 reduces dissociation of cohesin from chromosomes in prophase and prometaphase, whereas expression of nonphosphorylatable Scc1 does not cause such an effect (Hauf et al., 2005).

1.3.3.3. Cyclin-dependent kinase 1 (Cdk1)

Cdk1 is a member of the cyclin-dependent kinase family of serine/threonine protein kinases that control critical cell cycle events such as DNA replication and chromosome segregation. These protein kinases are activated by the formation of a complex with their cyclin partners and phosphorylate a variety of target substrates. Many of the genes encoding cyclins and Cdks are conserved between all eukaryotic species. For instance, up to six conserved Cdks in the budding yeast *S. cerevisiae*, Cdc28, Pho85, Kin28, Ssn3, Ctk1 and Bur1, are similar to mammalian Cdk1, Cdk5, Cdk7, Cdk8 and Cdk9 respectively, where Ctk1 and Bur1 both correspond to mammalian Cdk9 (Lorincz and Reed, 1984, Simon et al., 1986, Tohe et al., 1988, Lee and Greenleaf, 1991, Liao et al., 1995, Liu and Kipreos, 2000, Yao et al., 2000). Moreover, human Cdk1 can substitute for Cdk1 in *S. cerevisiae* and *S. pombe,* indicating the evolutionary conservation of cell cycle control (Lee and Nurse, 1987, Wittenberg and Reed, 1989). Cdk1 is best understood in budding yeast *S. cerevisiae* (known as Cdc28) and in fission yeast *S. pombe* (known as Cdc2) (Nasmyth, 1993, Lee and Nurse, 1987). The other Cdks are thought to function mainly in a transcriptional regulatory network (Meinhart et al., 2005). Budding yeast Cdk1, the first Cdk to be identified (Hartwell et al., 1973, Hartwell, 1974), plays important roles in mitosis and can drive S-phase in the absence of Cdk2, the master regulator of S-phase (Aleem et al., 2005).

The pattern of Cdk1 activity is pivotal for proper cell cycle progression. The cyclin-dependent kinase inhibitors (CKIs) Sic1 and Far1 are expressed from the M to G1-phases to keep Cdk1 activity low (Schwob et al., 1994, Alberghina et al., 2004). From the period of late G1 through mitotic anaphase, the activity of Cdk1 increases, when cyclin concentrations rise and the CKIs are degraded (Mendenhall and Hodge, 1998). Accordingly, Cdk1 is thought to be implicated in several important processes such as chromosome cohesion and dissolution. Genetic evidence has revealed the interaction between cohesin subunit Scc1/Mcd1/rhc21 and Cdk1/Cdc28 in *S. cerevisiae*, suggesting that Cdc28 may be an upstream regulator of Scc1 (Heo et al., 1999). A later study in *S. pombe* found that Scc1/Rad21 contained Cdc2/Cdk1 consensus T^{147}PSR. The phosphorylation of the T^{147} site was not detected by mass spectrometry due to the short tryptic peptide which was used, but was instead detected by the anti-phospho T^{147} antibody in mitotic extracts. Additionally, the phosphorylation level of T^{147} was abolished in starved G0 arrested cells, then sharply raised during S-phase, indicating that it may be phosphorylated during S and M-phases (Adachi et al., 2008), although the function of this phosphorylation remains unknown.

Given that Cdk1 is an upstream regulator of the cohesin complex, Eco1 (Esco1 in humans) is an attractive candidate because it is required for cohesion establishment after DNA

replication. Despite the central role of Eco1 in regulating cohesion establishment, Eco1 and Eco2 are phosphorylated during mitosis and Eco2 is subsequently ubiquitinated by the ubiquitin ligase APC^{Cdh1} (Lafont et al., 2010). In contrast, overexpression of Eco1 causes re-establishment of cohesion in mitotic yeast cells (Unal et al., 2007). It is known that yeast Eco1 is a target of Cdk1 (Ubersax et al., 2003) and that mutation of the Cdk1 consensus sites in Eco1 has no apparent effect on sister chromatid cohesion, whereas mutations that reduce the activity of Cdk1 are synthetically lethal with an Eco1 mutation (Brands and Skibbens, 2008). Thus, the role of Cdk1 is to regulate Eco1 degradation and hence to limit the establishment of cohesion to S-phase (Lyons and Morgan, 2011). In vertebrates, however, cohesin regulatory subunit SA1/Scc3 is also targeted for phosphorylation by Cdk1 *in vitro*. This phosphorylation prevents the cohesin complex from rebinding to chromatin after dissociation. Like SA1, recent studies indicate that Sororin, a cohesin-association protein, is regulated by Cdk1-mediated phosphorylation. Moreover, dissociation of Sororin from the chromatids during mitosis is prevented when Cdk1/cyclin B1 phosphorylation sites in Sororin are mutated to alanines. However, these mutations have no apparent effect on the degradation of Sororin (Schwob et al., 1994).

Cdk1 is a proline-directed kinase which phosphorylates substrates with the consensus sequence S/T-P-x-K/R (where is any amino acid) or S/T-P (Nigg, 1993, Harvey et al., 2005). Many of the known Cdk1 substrates frequently contain several phosphorylation sites clustered in their primary sequence, and their exact position in the protein has not been conserved during evolution, suggesting that precise positioning of phosphorylation sites is not very precisely conserved (Moses et al., 2007, Holt et al., 2009).

1.3.3. Cohesin related proteins

Cohesin is a multi-protein complex comprising Smc1, Smc3, Scc1 and Scc3, as well as a number of associated proteins that support its function. The maintenance of sister chromatid cohesion during interphase depends on a cohesin-interacting protein, Sororin (Rankin et al., 2005, Schmitz et al., 2007). Previous studies in human cells have reported that Wapl interacts physically with cohesin and plays a critical role in promoting chromosome segregation (Gandhi et al., 2006). In vertebrates, the association of Wapl with the core complex depends on Scc1 and Scc3 (Kueng et al., 2006). Three homologues of Scc3, known as SA1, SA3 (reserved for meiotic cohesion) and SA2, have been found in vertebrates and are associated with the cohesin subunits (Losada et al., 2000, Pezzi et al., 2000, Sumara et al., 2000). In fungi (*Sordaria*), Pds5 is another protein implicated in cohesin regulation. It was initially discovered as a protein associated with chromatin in a cohesin-dependent manner (Panizza et al., 2000).

1.3.3.1. Sororin

Sororin is a regulator of sister chromatid cohesion that associates with cohesin complex to increase its stability on chromatin after DNA replication (Schmitz et al., 2007). It was first identified from a screen for proteins degraded by the APC/C in *Xenopus laevis* extracts, using an *in vitro* transcription and translation protein expression system (Rankin et al., 2005). Sororin is conserved in vertebrates but no homologues have been identified in lower eukaryotes (Zhang and Pati, 2012). The expression level of Sororin is regulated during the cell cycle; it is expressed from the S to G2-phase and degraded in early G1 and displays intracellular localization (Nishiyama et al., 2010, Zhang et al., 2011). It is a nuclear protein in interphase cells and dissociates from chromosome arms in prophase with no detectable localization at metaphase, but persists on centromeres until metaphase (Nishiyama et al., 2010). During S-phase, Sororin is recruited to chromatin and causes a conformational rearrangement to stabilize bounded cohesin. When Scc1 is depleted from *Xenopus* egg extracts, the association of Sororin with chromatin is reduced. A similar phenotype was observed when Esco1 and Esco2 were depleted from HeLa cells, suggesting that Sororin is recruited to chromatin in a manner that depends on cohesin and Smc3 acetylation (Nishiyama et al., 2010).

Sequence alignment of Sororin from several vertebrate species indicates the presence of a KEN box in the N terminus, a Plk1 binding motif and FGF motif (Rankin et al., 2005). In addition, there are nine consensus sites (S^{21}, S^{75}, T^{48}, S^{79}, T^{111}, T^{115}, T^{159}, S^{181} and S^{209}) for Cdk1/cyclin B1 phosphorylation clustered in the N terminus and middle part of Sororin (Dreier et al., 2011, Zhang et al., 2011), suggesting that Sororin is regulated by

phosphorylation. Mutations in all nine of the putative Cdk1/cyclin B1 phosphorylation sites blocked the dissociation of Sororin from cohesin (Zhang et al., 2011), but did not increase the frequency of chromosome nondisjunction at anaphase. However, other studies indicate that Sororin is required for sister chromatid cohesion during S and G2-phases. When Sororin was depleted with siRNA from synchronized HeLa cells at S-phase, the distance between the chromosome arms was observed to be double in Sororin-depleted cells compared to the control cells (Schmitz et al., 2007, Nishiyama et al., 2010).

On the other hand, the Plk1 PBD is known to bind to the consensus motif S(pS/pT) (P/*X*), where pS is phosphoserine and pT is phosphothreonine (Elia et al., 2003). Accordingly, Sororin has five putative PBD binding sites: $ST^{115}P$, $SS^{125}S$, $SS^{126}K$, $ST^{157}S$ and $ST^{159}P$. Among these sites, $ST^{159}P$ is conserved in vertebrate Sororin and is also a Cdk1/cyclin B1 phosphorylation site (Zhang et al., 2011). In humans, the PBD of Plk1 interacts with Sororin only via its $ST^{159}P$ consensus motif after the T^{159} is phosphorylated by Cdk1/cyclin B1. Substitution of the threonine residue with alanine prevents the recruitment of Plk1 and inhibits the separation of chromosomal arms (Zhang et al., 2011). Although SA2 is directly phosphorylated by Plk1, no PBD binding site has been found on SA2 or other cohesin subunits. Therefore, it has been suggested that Sororin phosphorylation by Cdk1/cyclin B1 can create docking sites to bring Plk1 into proximity with SA2. Phosphorylation of SA2 by Plk1 during prophase is known to remove cohesin complexes from chromosomal arms (Zhang et al., 2011, Zhang and Pati, 2012).

The conserved FGF motif of Sororin makes it capable of interacting with Pds5. When this motif is mutated, Sororin-Pds5 interaction is reduced. Similarly, when Pds5 is depleted from *Xenopus* egg extracts, the association of Sororin with chromatin is greatly reduced (Nishiyama et al., 2010), indicating that Sororin's FGF motif is important for interaction with Pds5. Like Sororin, Wapl interacts with Pds5 via its FGF motif. Three FGF motifs have been found in the N terminus of vertebrate Wapl: the first is responsible for the interaction of Wapl with SA1 and Rad21, while the other two mainly interact with Pds5 (Shintomi and Hirano, 2009). Because Sororin and Wapl have opposite functions in regulating sister chromatid cohesion, Sororin appears to compete with Wapl to bind Pds5 and antagonize Wapl to maintain SCC during interphase. Once Sororin is phosphorylated during prophase/prometaphase, it loses its ability to antagonize Wapl, leading to the removal of cohesin (Nishiyama et al., 2010).

1.3.3.2. Wing apart-like (Wapl)

The Wapl gene was first identified as a gene product required for heterochromatin organization in *Drosophila melanogaster* and Wapl mutants show parallel sister chromatids with apparently loosened cohesion at their centromeres (Verni et al., 2000). Further study identified *Drosophila* Wapl as a factor essential for normal chromosome segregation (Dobie et al., 2001). Human Wapl has also been identified as a binding partner of the Epstein-Barr virus transformation-related protein (EBNA2) and named Friend-of-EBNA2 (FOE) (Kwiatkowski et al., 2004). FOE shows similarities to the Drosophila Parallel Sister Chromatids Protein (PASC) and corresponds to a protein of 1227 amino acids, differing from the original sequence of KIAA0261 by deletion of 126 bases near the 5´ end (Table 1.2). Human Wapl was predicted to comprise 1190 amino acids (accession # NM_015045) with molecular mass of 133 kDa (Oikawa et al., 2004).

It has been previously shown that Wapl has the characteristics of an oncogene and that its mRNA is overexpressed in uterine cervical cancer (Oikawa et al., 2004). This cancer is associated strongly with human papilloma virus (HPV), which encodes two oncoproteins, E6 and E7 (zurHausen, 1996). Kuroda et al. (2005) report that human Wapl is inducible by HPV E6 and E7 oncoproteins. Furthermore, Kwiatkowski et al. (2004) have suggested that human Wapl contributes to the abnormalities of Roberts' syndrome (RBS). This conclusion was based on the low level of Wapl protein with unperturbed nuclear distribution detected in RBS cells compared with normal cells, by both immunoblot and indirect immunofluorescence.

Table 1.2: Wapl Isoforms.

Isoform	*Size a.a*	*Name*	*Interaction*	*Expression*	*Difference from the canonical sequence*	*Reference*
1	1190	Wings apart-like protein (Wapl)	Interacts via FGF motifs with Pds5B and SMC3	Highly expressed in uterine cervix tumor	Canonical sequence	(Oikawa et al., 2004)
2	1227	Friend of EBNA2 (FOE)	Interacts with Epstein-Barr virus EBNA2	Highly expressed in placenta, thymus, kidney, lung and skeletal muscle	Extended N-terminal of 43 aa, 510-515 aa are missing.	(Kwiatkowski et al., 2004
3*	1275	KIAA0261	Not tested	Not tested	Extended N-terminal of 85 aa	(Nagase et al., 1996)

*Wapl isoform 3 Was determined by a chromosomal mapping of cDNA clones of unidentified human genes from human immature myeloid cell line KG-1. No experimental confirmation is available for this isoform.

On the other hand, recent studies have demonstrated that Wapl is physically associated with cohesin and promotes its removal from chromosome arms (Gandhi et al., 2006, Kueng et al., 2006). In mammalian cells, Wapl associates with cohesin by interacting to a specific amino acid sequence on SA1 via an FGF motif present in the N-terminus of Wapl (Figure 1.7). Combinations of mutations in the FGF motifs of Wapl prevent the resolution of sister chromatids (Shintomi and Hirano, 2009). Moreover, overexpression of Wapl leads to premature separation of sister chromatids (Gandhi et al., 2006) and contributes to tumour progression by induction of chromosomal instability (Ohbayashi et al., 2007). Taken together, Wapl appears to be required for the dissolution of cohesion. Thus, Wapl appears to be a cohesin destabiliser during the early stages of mitosis (Gandhi et al., 2006). Identifying the molecular mechanisms by which Wapl removes cohesin from chromosome arms is therefore a central issue for understanding cell division. It has been shown so far that the physical interaction of Wapl with Pds5 directly modulates conformational changes of cohesin and facilitates its dissociation from chromatin during prophase (Shintomi and Hirano, 2009). However, the mode of action of Wapl appears to depend on Sororin. During interphase, Sororin competes with Wapl for binding to Pds5 and displaces it to maintain sister chromatid cohesion. Conversely, when Sororin is phosphorylated in early mitosis, Wapl displaces it, binds with Pds5 and subsequently removes cohesin complexes from sister chromatid arms (Zhang et al., 2011). However, it has not been shown so far how Wapl is regulated during the mammalian cell cycle and the molecular mechanisms by which it removes cohesin from sister chromatid arms remain to be determined.

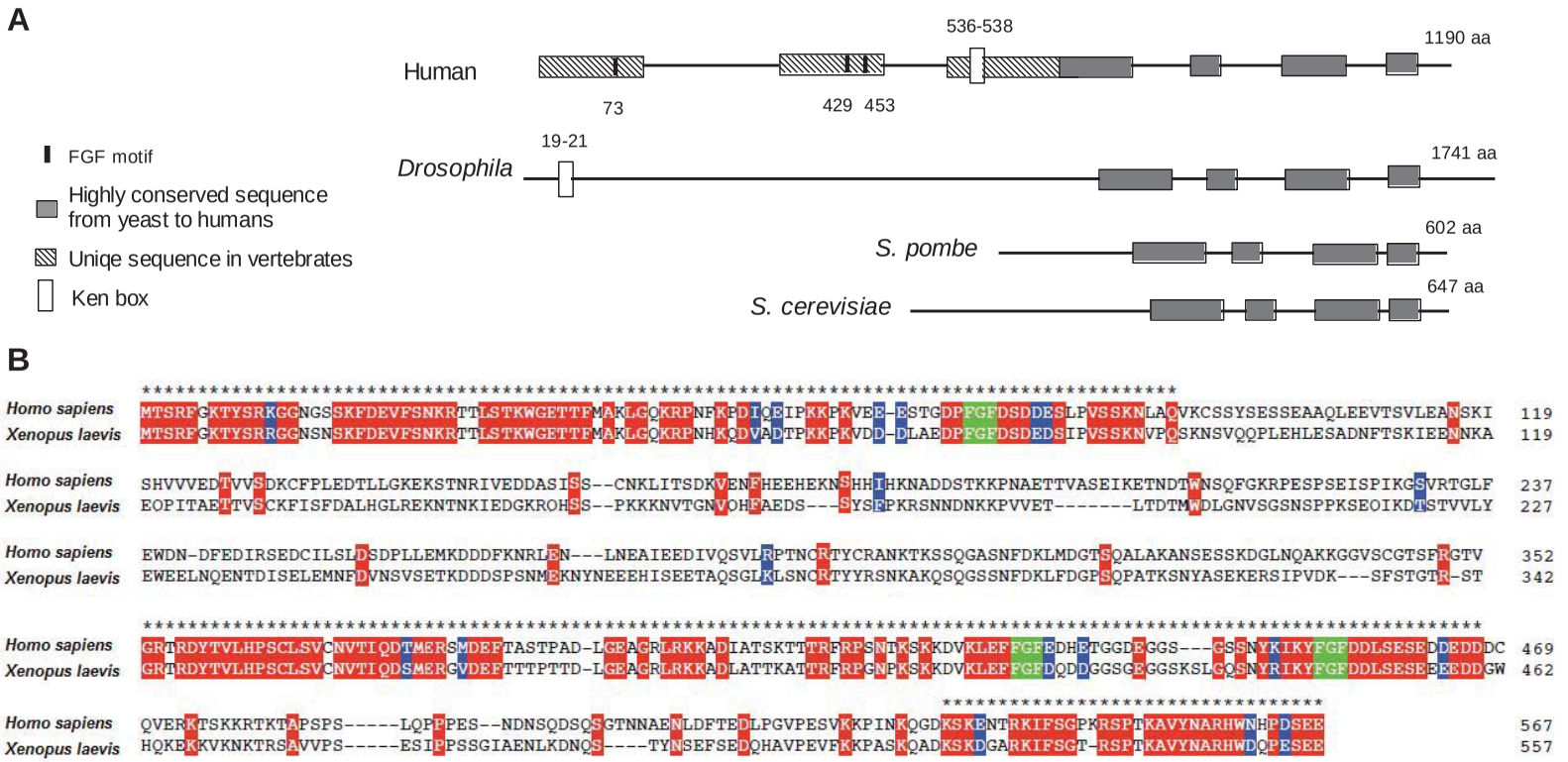

Figure 1.7: Schematic representation illustrating FGF motifs in Wapl.

(A) Primary structure of Wapl orthologs. Three FGF (phenylalanine-glycine-phenylalanine) motifs are conserved in the N-terminal domain of all of the vertebrate orthologs and coordinate a molecular interaction with the HEAT repeats of Pds5. (B) Sequence alignment of the human and *Xenopus laevis* Wapl N-terminal. The identical and similar residues are highlighted in red and blue respectively. The FGF-motifs are highlighted in green and the regions of high similarities are indicated with asterisks (Shintomi and Hirano, 2009).

1.3.3.3. Precocious dissociation of sisters protein 5 (Pds5)

Pds5 is a member of a highly conserved family of proteins with homologues in most, if not all, eukaryotic cells (Table 1.3), first identified in a genetic screen designed to identify genes important for chromosome structure (Denison et al., 1993). Pds5 is thought to be essential for the establishment and maintenance of sister chromatid cohesin during S-phase (Hartman et al., 2000). The temperature sensitive *S. cerevisiae* Pds5 mutants that enhance mitotic lethality were screened by FISH to identify those exhibiting precocious dissociation of sister chromatids. This was done using chromosome centromere distal probes to assay cohesion at the centromeric region. When the mutant cells were shifted from 23 °C to 37 °C, most mutant cells in mid-M-phase had two FISH signals, compared to one FISH signal per nuclear DNA mass in wild-type cells, indicating that sister chromatids had precociously dissociated in Pds5 mutant cells (Hartman et al., 2000).

It has been previously reported that Pds5 co-localizes with cohesin on interphase chromosomes (Panizza et al., 2000) and form a stable sub-complex with Wapl during mitosis to directly modulate conformational changes of the cohesin complex (Shintomi and Hirano, 2009). However, the role of Pds5-Wapl complex in the regulation of cohesion complex appears paradoxical. It includes promoting cohesin association to chromosomes, anti-establishment of sister-chromatid cohesion and removal of cohesin from chromosomes during mitosis. Mutations in Pds5 and Wapl generate opposite phenotypes in *Drosophila*. For instance, the loss of Pds5 prevents sister chromatid cohesion, whereas the loss of Wapl prevents sister chromatid resolution in mitosis (Verni et al., 2000, Dorsett et al., 2005). In budding yeast, deletion of Pds5 and Wapl causes loss of SCC (Hartman et al., 2000, Stead et al., 2003) and cohesion defects (Rolef Ben-Shahar et al., 2008, Rowland et al., 2009, Sutani et al., 2009) respectively.

Table 1.3: Nomenclature of Pds5 protein in different species.

Name	*Size (amino acids)*	*Species*	*Identity (%)*	
			Homo sapiens	
			Pds5A	*Pds5B*
Pds5p	1277	*Saccharomyces cerevisiae*	19	19
Pds5+	1205	*Schizosaccharomyces pombe*	23	25
BimD	1506	*Aspergillus nidulans*	23	21
Spo76	1596	Sordaria *macrospora*	21	20
Pds5	1218	*Drosophila melanogaster*	37	37
Evl-14	1570	*Caenorhabditis elegans*	20	21
Pds5A	1323	*Xenopus laevis*	86	69
Pds5A	1333	Rattus norvegicus	97	72
Pds5A (SCC112)	1337	Homo sapiens	-	73
Pds5B	1447	Homo sapiens	73	-

Fission yeast Pds5 and Wapl have even more distinct functions. The deletion of Wapl has no effect on SCC establishment and maintenance (Feytout et al., 2011). While Pds5 is not essential for the establishment of SCC and mitotic growth, its loss reduces viability in G2-arrested cells (Tanaka et al., 2001, Wang et al., 2002), suggesting that Pds5 is required for maintenance of SCC. Consistent with the role of Pds5 in the establishment of SCC, physical interaction between Pds5 and Eso1 was observed using the yeast two-hybrid system, but not by immunoprecipitation. Eso1 is known to be required during the S-phase to acetylate the cohesin component Smc3/Smc3 on two lysine residues (K105 and K106 in fission yeast Psm3) and these acetylated residues are maintained throughout G2 (Feytout et al., 2011, Kagami et al., 2011). A recent study shows that immunopurified cohesin component Smc3/Psm3 from *S. pombe* cells reacts strongly with antibodies that recognizes the acetylated form of Psm3 ($Psm3^{K106Ac}$), but the reaction failed when Psm3 was purified from *S. pombe* cells lacking pds5 (Vaur et al., 2012), suggesting that Pds5 is required for Psm3 acetylation by recruiting Eso1.

1.3.3.3.1. Pds5-like proteins Pds5A and Pds5B

Pds5A was first described in humans and *Xenopus*, showing a strong similarity to its orthologs Pds5/BimD/Spo76 previously described in fungi and comprising 1337 amino acids with a molecular mass of 150 kDa (Sumara et al., 2000, Losada et al., 2005). Pds5A mRNA and protein levels were found to be up-regulated in tumour tissues of the oesophagus, stomach, liver and transverse colon (Zheng et al., 2008). In addition, the overexpression of Pds5A is associated with higher growth rates and may contribute to tumorigenesis. Transfection of 293T cells with Pds5A resulted in a high percentage of cells in G2-M when compared with controls, whereas depletion of Pds5A by siRNA showed the opposite (Zheng et al., 2008).

The second Pds5-like protein is Pds5B/APRIN, originally identified as androgen shutoff gene 3 (formerly AS3) from prostate cancer cell lines (Geck et al., 1999), which has been shown to be implicated in hormonal regulation and cancer cell arrest (Maffini et al., 2008). Pds5B is phosphorylated upon DNA damage on consensus sites recognized by ATM and ATR protein kinases (Matsuoka et al., 2007). It has high levels of similarity with Pds5A in the N-terminus (1-1140: 77 % identity and 88 % similarity), with the presence of HEAT repeats within the N-terminus, but it differs at the C-terminus (1141-1360: 17 % identity and 29 % similarity) by the presence of two AT-hook-type HMG box motifs in the Pds5B protein sequence, compared to only one degenerate HMG box motifs in Pds5A (Zhang et al., 2007, Zhang et al., 2009a) (Figure 1.8). Nevertheless, different transcript variants encoding distinct isoforms have been found for Pds5 genes in humans (Table 1.4).

So far, few relevant studies have been performed on Pds5A and Pds5B, but their homologues in lower organisms have been characterized and are required for SCC (Panizza et al., 2000, Tanaka et al., 2001, Zhang et al., 2005). In mammals, both Pds5A and Pds5B interact with cohesin and Wapl and regulate cohesin removal from chromatin (Kueng et al., 2006), although the molecular mechanism by which Pds5A and Pds5B regulate sister chromatid cohesion is largely unknown (Losada et al., 2005 (Losada et al., 2005).

Generation of either Pds5A or Pds5B-deficient mice causes many developmental defects (Zhang et al., 2007, Zhang et al., 2009a). These abnormalities include slow growth, cleft palate, skeletal defects, heart and neuronal defects, which are similar to those seen in human Cornelia de Lange syndrome (CdLS), a disorder caused by mutations in cohesion proteins (Jackson et al., 1993). Sequencing analysis of Pds5A and Pds5B in 114 individuals of familial cases of CdLS revealed one patient with mutation R1292Q within the AT-hook domain in Pds5B. This mutation is likely to have disrupted Pds5B binding and to have contributed to a familial case of CdLS (Zhang et al., 2009a).

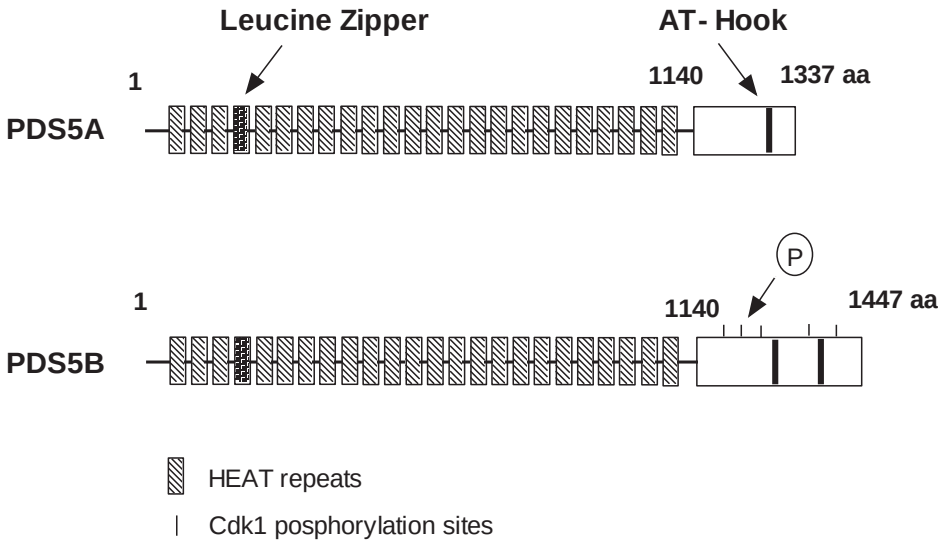

Figure 1.8: Schematic representation of human Pds5A and Pds5B protein sequences.

Pds5A and Pds5B are similar to each other at the N-terminal, which contains 23 HEAT repeats and one protein-DNA interaction motif (leucine zipper), but they differ at the C-terminal, where Pds5A has one adenine-thymine (AT)-hook domain, whereas Pds5B has two. The AT-hook is thought to bind to the minor groove of AT-rich DNA. There are five possible Cdk1 phosphorylation sites (threonine or serine followed by proline) at the C-terminus of Pds5B (Losada et al., 2005).

Table 1.4: Pds5 isoforms

Member	*Isoform*	*Size (aa)*	*Name*	*Expression*	*Difference from the canonical sequence*	*Reference*
Pds5A	1	1337	Pds5A or Sister chromatid cohesion protein 112 (SCC-112)	Highly expressed in human normal breast and renal tissues	Canonical sequence	(Gerhard et al., 2004)
	2	600		Expressed in kidney	Differ in region 591-600 aa, 601-1337 aa are missing.	(Kumar et al., 2004)
Pds5B	1	1447	Pds5B, APRIN, AS3, KIAA0979		Canonical sequence	(Nagase et al., 1999)
	2	1391	Androgen-induced prostate proliferative shutoff-associated protein AS3	Highly expressed in the early regulatory phase of androgen-induced proliferative shutoff	1392-1447 aa are missing.	(Geck et al., 1999)
	3*	529			Differ with region 491-529 aa 530-1447 aa are missing.	(Gerhard et al., 2004)
	4*	122			Differ with region 105-122 aa 123-1447 aa are missing.	(Gerhard et al., 2004)
	5*	125			1-1230 aa are missing. 1356-1447 aa are missing.	(Ota et al., 2004)

*No experimental confirmation available

1.4. Aims and objectives

The starting point for this project was a yeast 2-hybrid screen that was performed in collaboration with Dr Carsten Hageman, Tumorbiology Laboratory, Department of Neurosurgery, University of Würzburg, Germany, using the spindle checkpoint protein Mad2 as a bait and a Rat pheochromocytoma cells (PC12) cDNA library. A protein interaction was found between Pds5A (SCC-112) and human Mad2. Our initial studies did not find any in vivo interaction between Mad2 and Pds5A in co-immunoprecipitation experiments performed in either interphase or mitotic HeLa cell extracts. As the role of human Pds5 in the regulation of sister chromatid cohesion is currently unclear, the aims of this project were widened to include the following:

- Characterization of Pds5A and Pds5B during the mammalian cell cycle.
- Characterization of Wapl during the mammalian cell cycle.
- Study of the mechanism by which Pds5 and Wapl regulate sister chromatid separation.
- Study of the changes in the levels of Pds5 and Wap proteins throught the mammalian cell cycle.
- Live cell imagining of cells following Pds5A, Pds5B and Wapl siRNA.

1.4.1 The hypothesis

Based on the study performed in *Xenopus* egg extracts (Shintomi and Hirano, 2009), our hypothesis was that Pds5 is required for removal of cohesin at mitosis in mammalian cells.

Chapter 2

Materials and methods

2.1. Materials

2.1.1. Chemicals and reagents

Table 2.1: List of chemicals and reagents used in this study

Reagent	Supplier
2X Phusion High-Fidelity PCR Master Mix	ThermoScientific
Active Aurora B	Sigma
Active Cdk1/cyclin B1	Millipore
Active Plk1	Invitrogen
Agar	Gibco
Agarose	Melford
Ammonium persulphate (APS)	Fisher
Aphidicolin	Sigma
Aurora B Kinase Inhibitor ZM447439	Tocris Bioscience
Cdk1 Inhibitor RO-3306	Calbiochem
Cell dissociation solution (1X)	Sigma
Cisplatin	Sigma
Colloidal Coomassie Instant Blue Stain	Expedeon
DNA Ladder 1000 bp	New England Biolabs
DNA Loading Dye	ThermoScientific
Ethidium Bromide	Sigma
Ethylene Glycol Tetraacetic Acid (EGTA)	Fisher
Ethylenediaminetetraacetic acid (EDTA)	Fisher
EZ-ECL Chemiluminescence Detection Kit	Geneflow
Foetal Bovine Serum (FBS)	Gibco
FuGENE 6 Transfection Reagent	Roche
Fuji Super RX X-Ray film	Sigma
Hoechst 33342 dye	Sigma

Hybond-C Nitrocellulose Membrane	Amersham Biosciences
Interferin siRNA Transfection Reagent	Polyplus
Lipofectamine 2000 Reagent	Invitrogen
Methanol	Fisher
Nocodazole	Sigma
Okadaic acid	Calbiochem
Penicillin/Streptomycin (x10)	PAA Laboratories
Pierce Protein A/G Magnetic Beads	ThermoScientific
Plk1 Inhibitor BI 2536	Axon MedChem
Poly-L-Lysine	Sigma
Propidium Iodide	Sigma
Protein A Sepharose Beads	Sigma
Protein Ladder	ThermoScientific
Protogel (% acrylamide/% bis-acrylamide)	Gene flow
Qiagen Plasmid Purification Kit	QIAGEN
QIAprep Spin Miniprep kit	QIAGEN
QIAquick Gel Extraction Kits	QIAGEN
Ribonuclease (DNase free)	Sigma (R5503)
siRNA Transfection Medium	Santa Cruz Biotechnology
SOC medium	Promega
Taxol	Sigma
Tetramethylethylenediamine (TEMED)	Fisher
Tryptone	Sigma
Yeast Extract	Sigma
[ϒ-32P]-ATP	Amersham-Pharmacia

All other reagents were of analytical grade and purchased from either Fisher or Sigma.

2.1.2. Oligonucleotides

2.1.2.1. RNAi Oligonucleotides

The ON-TARGETplus set of four oligonucleotides for Pds5A, Pds5B and Wapl were purchased from Dharmacon. The sequence of each of the 4 sense strands of the siRNA duplexes were as follows:

Table 2.2: List of oligonucleotides used in this study

Name	Target sequence
Human Pds5A #1	5′-GAUAAACGGUGGCGAGUAA-3′
Human Pds5A #2	5′-CCAAUAAAGAUGUGCGUCU-3′
Human Pds5A #3	5′-GAACAGCAUUGACGACAAA-3′
Human Pds5A #4	5′-GAGAGAAAUAGCCCGGAAA-3′
Human Pds5B #1	5′-GAAAUAUGCUUUACAGUCA-3′
Human Pds5B #2	5′-UGAUAAAGAUGUUCGCUUA-3′
Human Pds5B #3	5′-GCAUAGUGAUGGAGACUUG-3′
Human Pds5B #4	5′-GGUCAAUGAUCACUUACUU-3′
Human Wapl #1	5′-GGAGUAUAGUGCUCGGAAU-3′
Human Wapl #2	5′-GAGAGAUGUUUACGAGUUU-3′
Human Wapl #3	5′-CAAACAGUGAAUCGAGUAA-3′
Human Wapl #4	5′-CCAAAGAUACACGGGAUUA-3′
ON-TARGETplus non-targeting siRNA	5′-UAGCGACUAAACACAUCAA-3′

2.1.2.2. PCR Primers

The primers were designed and analyzed for specificity using BLAST (http://www.ncbi.nlm.nih.gov/BLAST/).

Table 2.3: Cloning primers used for plasmid construction

Name	Forward Primer	Reverse Primer
Flag-Pds5A Full length	5′-GTATTTTCAGGGCGCCATCA AACGCCTGAAGATGGAT-3′	5′-ACGGAGCTCGAATTTCACCTT TGTAAGTCAATTTGTCT-3′
Flag-Pds5A N-terminus	5′-GTATTTTCAGGGCGCCATCA AACGCCTGAAGATGGAT-3	5′-GACGGAGCTCGAATTTCAGGA AACCTCTTCATCTGGAGACCA-3
Flag-Pds5A C-terminus	5′-GTATTTTCACGGCGCCTGGT CTCCACATGAAGAGGTTTCCC-3	5′GACGGAGCTCGAATTTCACCTTT GTAAGTCAATTTGTCT-3
Flag-Wapl Full length	5′-TATTTTCAGGGCGCCACATC C AGATTTGGGAAAACAT-3	5′-GACGGAGCTCGAATTTCACTAG CAATGTTCCAAATATT-3

2.1.3. Vectors

All vectors were provided by Dr. Xiaowen Yang (Protein Expression Laboratory (Protex), Biochemistry department, University of Leicester) (http://www2.le.ac.uk/departments/biochemistry/research-groups/protex) and (http://www2.le.ac.uk/colleges/medbiopsych/facilities-and-services/cbs/protein-and-dna-facility/protex/mammalian)

Table 2.4: List of vectors used in this study

Vectors	Application
pLEICS-12	Mammalian expression vector with Flag tag
pLEICS-13	Mammalian expression vector with Flag tag
pLEICES-14	Bacterial expression vector with GST tag

2.1.4. Bacterial strains

JM109 competent *Escherichia coli* (Promega).

2.1.5. Cell lines

HeLa (Henrietta Lacks) cells (a human epithelial cell line derived from a cervical carcinoma) were purchased from BioWhittaker. A HeLa cell line stably expressing histone H2B-mCherry and alpha-tubulin-EGFP was provided by Professor Andrew Fry (University of Leicester). HEK 293T cells (derived from human embryonic kidney cells) were provided by Dr Martin Dickens (University of Leicester).

2.1.6. Media

Table 2.5: List of cell culture media used in this study

Media	Supplier
Dulbecco's Modified Eagle's Medium (DMEM)	Sigma
Dulbecco's Modified Eagle's Medium (DMEM) + GlutaMAX 1X	Fisher
Opti-MEM + Glutamax	Fisher
Dulbecco's PBS (1X) without Ca^{2+}/Mg^{2+}	PAA Laboratories

2.1.7. Antibodies

Table 2.6: List of primary antibodies used in this study

Antibody	Concentration or Dilution used	Technique	Supplier
Anti-Pds5A Polyclonal *Catalog no. A300-088A*	0.5 µg/ml 5 µg/ml 2 µg/ml	Western Blot Immunofluorescence Immunoprecipitation	Bethyl Laboratories, Inc.
Anti-Pds5B Polyclonal *Catalog no. A300-537A*	0.5 µg/ml 5 µg/ml	Western Blot Immunofluorescence	Bethyl Laboratories, Inc.
Anti-WAPl Polyclonal *Catalog no. A300-268*	0.5 µg/ml 5 µg/ml	Western Blot Immunofluorescence	Bethyl Laboratories, Inc.

Anti-WAPl Monoclonal *Catalog no. sc-365189*	0.5 µg/ml 5 µg/ml	Western Blot Immunofluorescence	Santa Cruz Biotechnology, Inc.
Anti-Cohesin/Scc1 Monoclonal	1 µg/ml	Western Blot Immunofluorescence	MBL International Corporation
Anti-FLAG M2 Monoclonal *Catalogue No F3165*	1 µg/ml 4 µg/ml 2 µg/ml	Western Blot Immunoprecipitation Immunofluorescence	Sigma
Anti- Plk1 Monoclonal	1/2000 1/200	Western Blot Immunofluorescence	Sigma
Anti-ϒ-tubulin Polyclonal	1/2000 1/200	Western Blot Immunofluorescence	Sigma
Anti-α-tubulin Monoclonal	1/2000 1/400	Western Blot Immunofluorescence	Sigma
Anti-Centromere Human	1/200	Immunofluorescence	Europa Bioproducts Ltd
Anti-Caspase-3 Monoclonal	1:1000	Western Blot	Cell Signalling
Anti-Cleaved Caspase-3 Polyclonal	1:1000 1:300	Western Blot Immunofluorescence	Cell Signalling
Poly (ADP-ribose) polymerase (PARP) Polyclonal	1:1000	Western Blot	Roche
Anti-Chk1 Polyclonal	1:1000	Western Blot	Cell Signalling
Anti-phospho-Chk1 (Ser^{317}) Polyclonal	1:1000	Western Blot	Cell Signalling
Anti-Histone H3	1/2000	Western Blot	Cell Signalling
Anti-phospho-Histone H3 Polyclonal	1/5000	Western Blot	Cell Signalling

Anti-Aurora B Polyclonal	1/1000 1/200	Western Blot Immunofluorescence	Cell Signalling
Anti- Shugoshin Monoclonal	1/1000 1/200	Western Blot Immunofluorescence	Abcam
Cyclin B1 Polyclonal	1/1000	Western Blot	Santa Cruz Biotechnology, Inc.

Table 2.7: List of secondary antibodies used in this study

Antibody	Dilution used	Technique	Supplier
Goat Anti-Mouse IgG, HRP-linked antibody	1/1000	Western Blot	Cell Signalling Technology
Goat Anti-Rabbit IgG, HRP-linked antibody	1/1000	Western Blot	Cell Signalling Technology
Goat Anti-Mouse Alexa Fluor 488	1/1000	Immunofluorescence	Invitrogen
Goat Anti-Mouse Alexa Fluor 594	1/1000	Immunofluorescence	Invitrogen
Goat Anti-Rabbit Alexa Fluor 488	1/1000	Immunofluorescence	Invitrogen
Goat Anti-Rabbit Alexa Fluor 594	1/1000	Immunofluorescence	Invitrogen
Goat Anti-Human Alexa Fluor 594	1/1000	Immunofluorescence	Invitrogen

2.1.8. Blocking peptides

Table 2.8: List of blocking peptides used in this study

Blocking peptide	Concentration or Dilution used	Technique	Supplier
Pds5A blocking peptide *Catalog no. BP300-088A*	0.2 µg/µl	Western Blot	Bethyl Laboratories, Inc.
Pds5B blocking peptide *Catalog no. BP300-537A*	0.2 µg/µl	Western Blot	Bethyl Laboratories, Inc.
Wapl blocking peptide Catalog no. BP300-268	0.2 µg/µl	Western Blot	Bethyl Laboratories, Inc.

2.1.9. Buffers and Solutions

Table 2.9: Lysis buffers used for protein extraction

Buffer	Composition
Radio-Immunoprecipitation Assay (RIPA) Buffer	0.01 M Tris-HCl pH 7.0, 0.15 M NaCl, 2 mM EDTA, 0.1 mM sodium orthovanadate, 0.1 % w/v sodium dodecyl sulfate (SDS), 1 % v/v NP-40, 0.5 % w/v sodium deoxycholate, 50 mM sodium fluoride (NaF), 30 mM sodium pyrophosphate and protease inhibitors (1 mM PMSF, 10 µg/ml leupeptin, 10 µg/ml aprotinin, 10 µg/ml pepstatin).
Lysis Buffer A	0.01 M Tris-HCl pH 7.4, 0.05 M NaCl, 5 mM EDTA, 0.1 mM sodium orthovanadate, 30 mM sodium pyrophosphate, 50 mM NaF, 1 % v/v NP-40, 0.1 % w/v BSA and protease inhibitors (1 mM PMSF, 10 µg/ml leupeptin, 10 µg/ml aprotinin, 10 µg/ml pepstatin).
NEB Buffer	50 mM HEPES-KOH pH 7.4, 5 mM $MnCl_2$, 10 mM $MgCl_2$, 5 mM EGTA, 2 mM EDTA, 100 mM NaCl, 5 mM KCl, 1 % v/v NP-40 and protease inhibitors (1 mM PMSF, 10 µg/ml leupeptin, 10 µg/ml aprotinin, 10 µg/ml pepstatin).

Table 2.10: Buffers used for kinase assay

Buffer	Composition
Kinase Buffer	50 mM HEPES-KOH pH 7.4, 5 mM $MnCl_2$ or 10 mM $MgCl_2$, 5 mM β-glycerophosphate, 5 mM NaF, 4 mM ATP, 1 mM DTT, 10 μCi-γ-^{32}P-[ATP].

Table 2.11: Cell extraction buffers used for immunofluorescence

Buffer	Composition
Triton X-100 containing Buffer	0.5 % v/v Triton X-100, 20 mM HEPES pH 7.4, 3 mM $MgCl_2$, 50 mM NaCl, 300 mM sucrose.
CSK (Cytoskeleton) Buffer	10 mM Pipes-KOH pH 7.0, 100 mM NaCl, 3 mM $MgCl_2$, 300 mM sucrose.

Table 2.12: Buffers used for immunocytochemistry

Buffer	Composition
Mounting medium	Glycerol 9 ml, 1 M Tris-HCl (pH 8.0) 1 ml, n-propyl gallate 0.05g. The n-propyl gallate was dissolved by stirring the solution (placed in a light-proof container) overnight at room temperature. The mounting medium was then stored at 4 °C until required.
Preparation of glass coverslips	Glass coverslips (22 mm diameter, No 1, Fisher) were incubated with 1 M HCl for 30 min. The coverslips were then rinsed in distilled water and washed for 30 min in 100 % ethanol. The coverslips were air-dried and sterilised by heating in an oven at 180 °C for 30 min.

Table 2.13: Buffers used for agarose gel electrophoresis

Buffer	Composition
TAE Buffer (x50)	*TAE (50X)* Tris-HCl 242 g EDTA 37.2 g Glacial acetic acid 57.1 Distiled H2O to 1000 ml

Table 2.14: Buffers used for bacterial suspension and lysis

Buffer	Composition
Suspension Buffer	PBS pH 8.0, 100 mM NaCl. 0.2 % v/v Triton X-100, protease inhibitors (1 mM PMSF, 10 µg/ml leupeptin, 10 µg/ml aprotinin, 10 µg/ml pepstatin).
Solubilisation Buffer	20 mM phosphate buffer pH 8.0, 300 mM NaCl, 2 % v/v SDS, 2 mM DTT and protease inhibitors (1 mM PMSF, 10 µg/ml leupeptin, 10 µg/ml aprotinin, 10 µg/ml pepstatin).

Table 2.15: Solutions and buffers used for Western blotting

Buffer	Composition
Stacking gel	*For 10 ml* Protogel 1.6 ml 1 M Tris-HCl pH 6.8 1.2 ml SDS (10 % w/v) 0.1 ml APS (10 % w/v) 0.075 ml Temed 0.012 ml H2O 7 ml
Resolving (Running) gel	*% Gel* 8 / 10 / 12.5 / 15 Protogel 5.35 / 6.67 / 8 / 10 ml 1 M Tris-HCl pH 8.8 7.5 / 7.5 / 7.5 / 7.5 ml SDS (10 % w/v) 0.15 / 0.15 / 0.15 / 0.15 ml APS (10 % w/v) 0.1 / 0.1 / 0.1 / 0.1 ml Temed 0.02 / 0.02 / 0.02 / 0.02 ml H2O 6.9 / 5.6 / 4.2 / 2.2 ml
SDS-PAGE Running Buffer (1X)	0.025 M Tris-HCl, 0.192 M glycine, 1 % w/v SDS.
SDS-PAGE Transfer Buffer	25 mM Tris-HCl, 192 mM glycine, 20 % Methanol.
1x Tris-Saline-Tween (TST)	0.01 M Tris-HCl pH 7.4, 0.15 M NaCl, 0.1 % v/v Tween 20.
Blocking Buffer	5 % w/v Milk powder in TST buffer.

Table 2.16: Solutions used for Fluorescence-Activated Cell Sorting (FACS)

Solution	Composition
Stain Solution	9.5 ml of 1 X PBS, 0.5 ml of 10 µg/ml RNase solution and 200 µl of 0.02 µg/ml PI solution.

Table 2.17: Solutions used for staining chromosome spreads

Solution	Composition
Carnoy's solution	75 % methanol, 25 % acetic acid.
Giemsa Stain	4 ml Giemsa stain; 96 ml phosphate buffer (Gurr's tablets) pH 6.8.

2.2. Methods

2.2.1. Cell biology techniques

2.2.1.1. Cell culture

HeLa and HEK 293T cells were cultured in DMEM and DMEM + GlutaMAX, respectively, supplemented with 10 % v/v foetal bovine serum and 5 % v/v penicillin/streptomycin (100 IU/ml and 100 µg/ml). All cells were incubated at 37 °C in a humidified atmosphere containing 5 % CO_2 (CO_2 Incubator, SANYO). Cells were passaged every 3-4 days, whereas HeLa cells expressing histone H2B-mCherry/alpha-tubulin-EGFP were passaged every 2-3 days to keep them at a low confluency (50-60 %). For cell synchronization experiments, HeLa cells were synchronized at the G1/S boundary by treatment of an asynchronous population with aphidicolin (10 µg/ml) for 24 hrs. The cells were washed 5-6 times with Dulbecco's PBS and placed in DMEM to release them from the aphidicolin block. Mitotic cells were obtained by treatment of exponentially growing cells with nocodazole (0.1 mg/ml) for 18 h before the mitotic cells were harvested by shake-off. For some experiments, cells were incubated in DMEM containing an appropriate concentration of kinase inhibitor (polo-like kinase inhibitor BI 2536, Cdk1 inhibitor RO-3306 or aurora B kinase inhibitor ZM 447439) and nocodazole (0.1 µg/ml) and incubation for 18hrs.

2.2.1.2. RNAi Transfection

HeLa cells were plated in 6-well plates and incubated for 24 h before transfection. The appropriate concentration of siRNA was mixed with 200 µl of siRNA transfection medium and 8 µl of Interferin siRNA transfection reagent. The mixture was incubated for 20 min at room temperature (RT), and then added to the cells, which were incubated for up to 48 h. Control siRNA (transfection mixture containing either no siRNA or an equivalent concentration of non-targeting siRNA) and Lamin A/C were used as negative and positive silencing controls respectively. Conditions for siRNA transfection were optimized using a different concentration of each siRNA duplex set and different time points. The efficiency of siRNA-mediated knockdown was judged by Western blot. The transfection efficiency had previously been determined in our laboratory using an FITC-labelled lamin A/C siRNA (5'-ACCAGGUGGAGCAGUAUAA-3', Dharmacon) and found to be ≥ 90 %.

2.2.1.3. Preparation of chromosome spreads

48 h following siRNA treatment, HeLa cells were treated with either taxol (1 µM) for 24 h or with a mixture of taxol (1 µM) and okadaic acid (1 µM) for 12 h. The mitotic cells were collected by shake-off and swollen in hypotonic solution (75 mM sodium chloride) and

incubated for 10 min at 37 °C. The cells were collected by centrifugation at 1000 rpm for 10 min and the cell pellet resuspended in freshly made Carnoy's solution (3:1 (v/v) methanol: acetic acid) for 10 min. The fixation with Carnoy's solution was repeated twice. After the final fixation, the cell pellet was resuspended in a small volume (50-100 µl depending on the pellet size) of Carnoy's solution by gently tapping the bottom of the tube. 10 µl of the cell suspension was dropped onto glass slides held at a 45° angle and dried by placing them at an angle over a 37 °C water bath. The slides were stained with 4 % Giemsa in phosphate buffer at pH 6.8 for 7 min, washed in deionised water and air dried. The chromosome spreads were viewed using a light microscope (Nikon Eclipse TE 300 semi-automatic, Tokyo, Japan) and the number of nuclei displaying separated sister chromatids (at the arms and/or centromere) quantitated. For each treatment, at least 100 nuclei in randomly selected field were counted and nuclei in which ≥ 50 % of the sister chromatids remained unresolved were classified as unseparated. Representative images of the chromosomes were captured using a Hamamatsu ORCA-R^2 digital camera, 100 objective, NA 1.4, or 60 objective, NA 1.4, using Openlab or Volocity software (Improvision), and processed using Photoshop (Adobe Photoshop element 10).

2.2.1.4. Plasmid DNA transfection

HeLa cells and HEK 293T cells were plated either in 10 cm tissue culture dishes or in 6-well plates at least 24 h before transfection. The transfection mix was prepared as shown in Table **2.18** and

Table 2.19. The transfection mixture was incubated for 20 min at RT. Prior to transfection, fresh complete medium was added to the cells, and then the reaction mixture was added dropwise to the cells and incubated for 24 h to 48 h. For transfection with Lipofectamine, antibiotic-free DMEM was used throughout the transfection period. Complete medium was added 6 h following transfection and the cells incubated for an additional 24 h. The transfected cells were then either fixed for immunocytochemistry or lysed for Western blotting or immunoprecipitation.

Table 2.18: Plasmid DNA transfection in HEK 293T

Plate	DNA (µg)	FuGENE 6 transfection reagent	Serum-free medium
6-well plate	2 µg	6 µl	To 100 µl
10 cm plate	10 µg	30 µl	To 500 µl

Table 2.19: Plasmid DNA transfection in HeLa cells

Plate	DNA (µg)	Lipofectamine 2000 Reagent	Opti-MEM medium
6-well plate	4 µg	10 µl	To 100 µl

2.2.1.5. Immunofluorescence

Cells were grown on 6-well plates containing sterile glass coverslips under the culture conditions described above. Alternatively, the mitotic cells harvested by shake-off were attached to poly-L-lysine (1 mg/ml) coated coverslips. The cells were fixed with either ice-cold 100 % methanol for 30 min at -20 °C or with 3.7 % (v/v) formaldehyde at RT for 20 min followed by permeabilisation with 0.1 % (v/v) Triton X-100 for 20 min. Other fixation methods used included cell extraction with a Triton X-100 containing buffer (Table 2.11 on page 45) for 5 min at 4 °C followed by fixation with 3.7 % (v/v) formaldehyde for 20 min at 4 °C and lastly cold (-20 °C) methanol for 30 min. After blocking with 5 % (w/v) BSA, the cells were stained with the appropriate primary antibodies and secondary antibodies labelled with either with Alexa Fluor 488 or 954 fluorescent dyes. Cell nuclei were stained with Hoechst 33342 dye and mounted onto glass slides with mounting medium. The coverslips were sealed with clear nail varnish and stored in the dark at 4 °C until examination. The labelled cells were examined using a Nikon inverted fluorescence microscope (Nikon Eclipse TE 300 semi-automatic Microscope, Tokyo, Japan) and the images were captured using a Hamamatsu ORCA-R2 digital camera, 100 objective, NA 1.4, or 60 objective, NA 1.4, using Openlab or Volocity software (Improvision). The images were further processed using Adobe Photoshop (Adobe Photoshop element 10).

2.2.1.6. Time-lapse video microscopy for live cells

HeLa cells stably expressing mCherry-histone H2B and alpha-tubulin-EGFP were grown on 35-mm glass bottom plates (Matek) with complete DMEM at 37 °C. After 24 h, the medium was replaced and the cells transfected with either control, Pds5A, Pds5B or Wapl siRNA for at least 36 h. The medium was replaced with Opti-MEM + Glutamax containing 10 % v/v FBS and the cells incubated at 37 °C for 1 h prior to imaging. Live cell imaging was performed using a Confocal Leica DMI 6000 CS microscope equipped with a heated-stage and a Perspex chamber to maintain an atmosphere of 5 % CO_2 (Leica TCS SP5 Confocal Laser Scanning Microscope). Images were acquired using 63 x 1.4 - 0.6 NA oil-immersion objective lens every 8 min over a period of 24 hrs. Images were analysed, filtered and processed using ImageJ software (ImageJ 1.34s).

2.2.1.7. Fluorescence-activated cell sorting (FACS)

Cells were harvested, washed once with 1 X PBS, fixed with ice-cold 70 % v/v ethanol and stored at -20 °C. Prior to analysis the cells were washed once with Dulbecco's PBS, resuspended in 0.02 µg/ml propidium iodide (PI) staining solution and analysed using a FACScan (Becton-Dickinson). Data were analysed using CellQuestPro (BD CellQuestPro).

2.2.2. Molecular biology techniques

2.2.2.1. Polymerase chain reaction (PCR)

DNA was amplified using a Peltier thermal cycler (DYAD). PCR reactions (20 or 50 µl) were performed using the Phusion High-Fidelity DNA polymerase (Finnzymes).

The PCR reaction mixture and the cycling programme used are tabulated in Table 2.20 and Table 2.21. The amplicons were analyzed by 1 % w/v agarose gel electrophoresis.

Table 2.20: PCR reaction mixture

Component	20 µl	50 µl
H_2O	To 20 µl	To 50 µl
2x Phusion Master Mix with HF Buffer (0.04 U/µl Phusion DNA Polymerase, 2x Phusion HF Buffer containing 3.0 mM $MgCl_2$, 400 µM of each dNTP, 100 % DMSO (500 µl).	10 µl	25 µl
Forward primer	0.5 µM	0.5 µM
Reverse primer	0.5 µM	0.5 µM
Template DNA	50 ng	50 ng

Table 2.21: PCR reaction programme

Steps	Programme
Initial denaturation	98 °C for 3 min
Denaturation	98 °C for 10 sec
Annealing	Annealing 63 °C for 30 sec
Extension	72 °C for 1 min
Cycles	35
Final extension	72 °C for 10 min
Storage	4 °C

2.2.2.2. Agarose gel electrophoresis

The PCR product was combined with loading buffer (1: 5 ratio) and separated on a 1 % w/v agarose gel prepared by dissolving agarose in 1x TAE (Table 2.13 on page 46) supplemented with 10 mg/ml ethidium bromide. Electrophoresis was performed at 100 V for 1 hr and the resolved DNA was detected using UV light.

2.2.2.3. DNA extraction from agarose gels

For gel extraction and cleanup of DNA fragments, the PCR product was run on 1 % w/v agarose gel. The amplified product bands were cut from the agarose gel and placed in a sterile 1.5 ml tube. The purification of the PCR products was carried out using the QIAquick Gel Extraction Kit (Qiagen) according to the manufacturer's instructions.

2.2.2.4. DNA cloning

Plasmids constructs pLEICS-12 and pLEICS-13 (see appendix Figure A.1 and 4) were obtained from Dr. Xiaowen Yang (Protex, University of Leicester). Pds5A (full length) (purchased from Origene, Rockville, Maryland, USA as Myc/DDK tagged clone in pCMV6 (RCZ1113)) and Wapl (full length) (provided by Prof. Masahiko Koroda, Tokyo Medical University, Tokyo, Japan) were cloned into pLEICS-13 vector, while Pds5A-N-terminus and Pds5A C-terminus were cloned in pLEICS-12. The cloning was performed by Dr. Xiaowen Yang using the In-Fusion technique (Protex, Department of Biochemistry, University of Leicester) (www2.le.ac.uk/departments/biochemistry/research-groups/protex).

2.2.2.5. Transformation of Escherichia Coli cells

DNA (200-300 ng) was introduced into 50 µl of competent *E. coli* strain JM109 (Promega) and incubated on ice for 30 min. The cells were heat shocked at 42 °C for 45 sec and then incubated on ice for 5 min. SOC medium (200 µl) was added to the bacteria and the cells incubated at 37 °C for 1-1.5 h. 100 µl of the bacterial cell suspension was plated onto LB agar plates containing 100 µg/ml ampicillin at 37 °C in an incubator (NAPCO). After overnight incubation, a single bacterial colony was picked, inoculated into 10 ml of fresh LB medium containing ampicillin (100 µg/ml) and incubated overnight at 37 °C with shaking (Innova 4330). The overnight culture was either used for plasmid purification or added to 1 litre LB medium containing 100 µg/ml ampicillin for large-scale plasmid purification.

2.2.2.6. Plasmid DNA purification

Small-scale plasmid DNA purification (3-5 ml of overnight bacterial culture) was carried out using the QIAprep Spin Miniprep kit. For medium (500 ml) or large-scale (1000 ml) culture, the Qiagen Midi or Maxi Plasmid Purification Kit was used. All steps were performed according to the manufacturer's protocols.

2.2.2.7. DNA concentration measurement

DNA concentration was quantified using a Nano Drop spectrophotometer (Nano Drop 2000 C, Thermo Scientific) and measurement of its absorbance at 260 nm. 1 µl of deionised H_2O was used for blanking the instrument and 1 µl of the DNA sample was used for quantification.

2.2.3. Proteomics techniques

2.2.3.1. Preparation of cell extracts and chromatin-associated proteins

Cell extracts were prepared from HeLa or HEK 293 cells. Cells were resuspended in RIPA lysis buffer for Western blots. Alternatively, cells were resuspended in NEB buffer, Buffer A or NP40 lysis buffer for either immunoprecipitation (IP) or co-immunoprecipitation (Co-IP) (Table 2.9 on page 45), in the presence of protease inhibitor. The cell lysates were clarified by centrifugation (Eppendorf 5417R) at 14 000 rpm at 4 °C for 15 min. Supernatants were transferred to fresh pre-cooled 1.5 ml Eppendorf tubes and stored at either -20 or -80 °C. For preparation of soluble and chromatin fractions, cells were resuspended in NP40 lysis buffer, frozen (at-80 °C) and thawed three times before being clarified by centrifugation (14 000 rpm for 15 min at 4 °C). The supernatant was transferred to fresh pre-cooled 1.5 ml Eppendorf tubes (soluble fraction) and the pellet washed three times with NP-40 lysis buffer and resuspended in 200 µl of NP-40 lysis buffer containing 5 units of micrococcal nuclease and

0.4 mM $CaCl_2$. The pellet was incubated at 28 °C for 5 min with gentle mixing, then clarified by centrifugation at 14 000 rpm at 4 °C for 15 min and the supernatant was transferred to fresh pre-cooled (4 °C) 1.5 ml Eppendorf tubes (chromatin fraction). Both the soluble fraction and the chromatin-derived fractions were stored at -80 °C until required.

2.2.3.2. Protein concentration measurement

The protein concentration of the cell extracts was determined using a Bradford Assay (Bio-Rad) according to the manufacturer's protocol. The absorbance of the samples was measured at 595 nm using a spectrophotometer (SmartSpec 3000, Bio-Rad).

2.2.3.3. SDS-PAGE and Western blotting

Cell lysates containing 5 to 15 µg proteins was combined in a ratio of 1: 1 with X 2 Laemmli loading buffer, heated at 95 °C for 5 min and then centrifuged for 10 sec to collect condensed liquid. Samples were loaded onto 8 %, 10 % or a 15 % polyacrylamide gel depending on the size of the protein to be analysed. SDS-PAGE was carried out at RT at 150 V (Bio-Rad PowerPac 300) until the tracking dye had reached the bottom of the gel. The proteins in the gel were then transferred to a nitrocellulose membrane (Hybond-C Extra) using either the wet transfer method at 350 mA in the cold for 1 h or the semi-dry method (60 mA at RT for 1 h). Wet transfer was performed using a mini Trans-Blot Cell (Bio-Rad) or a Hoeffer semi-dry transfer apparatus (Amersham-Pharmacia). Protein bands were visualized by EZ-ECL Chemiluminescence Detection Kit (Geneflow) using an HRP-tagged secondary antibody. The blot was exposed to Fuji X-ray film (Sigma) and developed an automatic film processor (SRX-101A, Konica Minolta, UK). The blots were scanned (CanoScan LiDE 90) and processed using Photoshop.

2.2.3.4. Immunoprecipitation and Co-immunoprecipitation

IP with antibodies was carried out using either protein A Sepharose beads (Amersham-Pharmacia) or Protein A/G Magnetic Beads (Pierce). For Pds5A or Pds5B IP and Co-IP, approximately 0.25 mg of pre-equilibrated protein A Sepharose beads (washed twice with ice-cold NEB lysis buffer or lysis buffer A) were added to the pre-cleared cell lysate (250 µg of total protein extract) containing 1 µg of primary antibody, incubated overnight at 4 °C on a rotator. After overnight incubation, the beads were washed three times with ice-cold lysis buffer and resuspended in 40 µl of SDS-PAGE sample buffer and analysed by Western blot.

For Flag-Wapl IP and Co-IP, 25 µl (approximately 0.25 mg) of Protein A/G Magnetic Beads were transferred to a 1.5 ml Eppendorf tube and placed in a magnetic stand to collect the

beads. The supernatant was removed and the beads were washed twice with ice-cold lysis buffer (NEB or lysis buffer A). The pre-washed magnetic beads were resuspended with 250 µg of total protein extract containing 4 µl of monoclonal Flag antibody, and incubated overnight at 4 °C on a rotator. After overnight incubation, the beads were washed three times with lysis buffer and either used for a kinase assay or resuspended in 40 µl of SDS-PAGE sample buffer and analysed by Western blot.

2.2.3.5. Preparation of samples for mass spectrometry

The immunoprecipitated Flag-Wapl was run on a 10 % v/v SDS-PAGE and the gel was stained in colloidal Coomassie instant blue stain. The appropriate protein band was cut from the gel and sent to the Protein and Nucleic Acid Chemistry Laboratory (PNACL), University of Leicester, for peptide mass fingerprinting and phosphopeptide mapping using an LTQ-Orbitrap-Velos-ETD mass spectrometer.

2.2.3.6. In vitro kinase assays

The immunoprecipitated Flag-Wapl was washed three times in cold (4 °C) lysis buffer and three times in cold (4 °C) kinase buffer (Table 2.10 on page 45). After the final wash, the beads were resuspended in 40 µl of kinase assay buffer. As a positive control, 5 µg of histone H1 (Sigma) was used as a substrate for Cdk1, 5 µg of myelin basic protein was used as a substrate for both Plk1 and Aurora B1. 1 µl (1 μCi) of [γ-^{32}P]-ATP was added to each reaction and the reaction initiated by the addition of the appropriate recombinant protein kinase. 0.4 µg/µl of active Cdk1/cyclin B1, Plk1 or Aurora B were added individually to the beads. The tubes were incubated at 30 °C for 30 min. The reactions were stopped by adding 40 µl of 2 X sample buffer and boiled for 3 min at 95 °C. 40 µl of each reaction was run on a 10 % polyacrylamide gel. Following SDS-PAGE the gel was stained in Instant Blue colloidal Coomassie stain (Instant Blue) and dried on a gel dryer (Bio-Rad). The dried gel was exposed to X-ray film overnight and developed. For sequential kinase assay, the immunoprecipitated Flag-Wapl was incubated with either Cdk1 or Plk1 at 30 °C for 30 min in the presence of cold ATP (*Step 1*). The kinase was either washed away or depleted by adding either 1 µM of Plk1 Inhibitor BI 2536 (Axon MedChem) or 0.1 µg/µl of Cdk1 Inhibitor (RO-3306 Calbiochem) (*Step 2*). The substrate was co-incubated with either Plk1 or Cdk1 in a second kinase reaction in the presence of 1 µl (1 μCi) of [γ-^{32}P]-ATP as described above.

Chapter 3

Characterization of Pds5A and Pds5B in the mammalian cell cycle

3.1. Introduction

Given that Pds5 is required for maintenance of sister chromatid cohesion, it has been shown that Pds5 is essential for cohesin stabilization and SCC maintenance during the G2-phase (Tanaka et al., 2001, Vaur et al., 2012). Moreover, Vaur et al (2012) have tested the idea that Pds5 might be essential for the stable mode of cohesin binding in *S. pombe*. Cells lacking pds5 and carrying the thermosensitive mis4-367 mutation in the cohesin loader Mis4, to prevent the deposition of cohesin on chromatin, were arrested in G2 by the cdc25-22 mutation which prevents entry into mitosis at 37 °C. The chromatin-bound cohesin was monitored by nuclear spreads and chromatin immunoprecipitation (ChiP) at specific loci (major sites of cohesin binding) (Vaur et al., 2012). The data show that the level of chromatin-bound cohesin was substantially reduced with time compared to the wild type control and that even the deletion of Wapl did not correct the pds5 deficiency. In addition, cell survival was dramatically reduced after the release from cdc25-22 arrest (Vaur et al., 2012). Taken together, these observations suggest that Pds5 is required for stable mode of cohesin binding, although its function seems to differ substantially among different organisms. For instance, Pds5 cooperates with cohesin in maintaining SCC in fungi (*Sordaria*) (Panizza et al., 2000). In budding yeast, Pds5 plays an important role in meiosis and is required for SCC (Zhang et al., 2005). However, another study has shown that Pds5 is required for sister chromatid resolution during prophase in *Xenopus* egg extracts (Shintomi and Hirano, 2009). While Pds5 has been identified as a binding partner of Wapl (Kueng et al., 2006), it remains to be determined whether human Pds5 is also required for sister chromatid resolution and if so, by what mechanism the two proteins function. I therefore propose in this chapter to characterize the role of Pds5A and Pds5B in the human cell cycle.

3.2. Results

3.2.1. Characterization of antibodies

Pds5A and Pds5B commercial antibodies were tested for their specificity and each produced a single band on Western blots corresponding to the predicted sizes of the proteins (Figure 3.1A and B). When these antibodies were bound to their blocking peptide, they no longer detected their target on the Western blot. Specificity was further confirmed by siRNA depletion and subsequent decrease in the protein signals (Figure 3.1C and D).

3.2.2. The dynamic localization of Pds5A and Pds5B

Because the role of Pds5 in regulating SCC remains unresolved, I proposed to characterize the functional properties of Pds5 in mammalian cells. I therefore examined the levels of endogenous Pds5 proteins during the cell cycle using a synchronized population of HeLa cells (Figure 3.2). The results obtained from the time course experiment show clearly that Pds5A and Pds5B protein expression levels remained constant throughout the cell cycle, although cohesin was degraded in late mitosis (after 15 hrs) as expected. This suggests that SCC is not regulated by changes in the expression levels of Pds5 proteins (Figure 3.2B). I next examined whether the cellular localization of Pds5 changed during the HeLa cell cycle. The immunocytochemistry results revealed the predominantly nuclear localization of Pds5 proteins in interphase cells and their dissociation from chromatin at mitosis (Figure 3.3 and Figure 3.4). Pds5A and Scc1 localized to both the nucleus and cytoplasm and dissociated from chromatin at prophase, whereas Pds5B persisted on chromatin until metaphase. Both Pds5A and Pds5B re-associated with chromatin at telophase. This result suggests that Pds5A and Pds5B may be involved in regulating SCC.

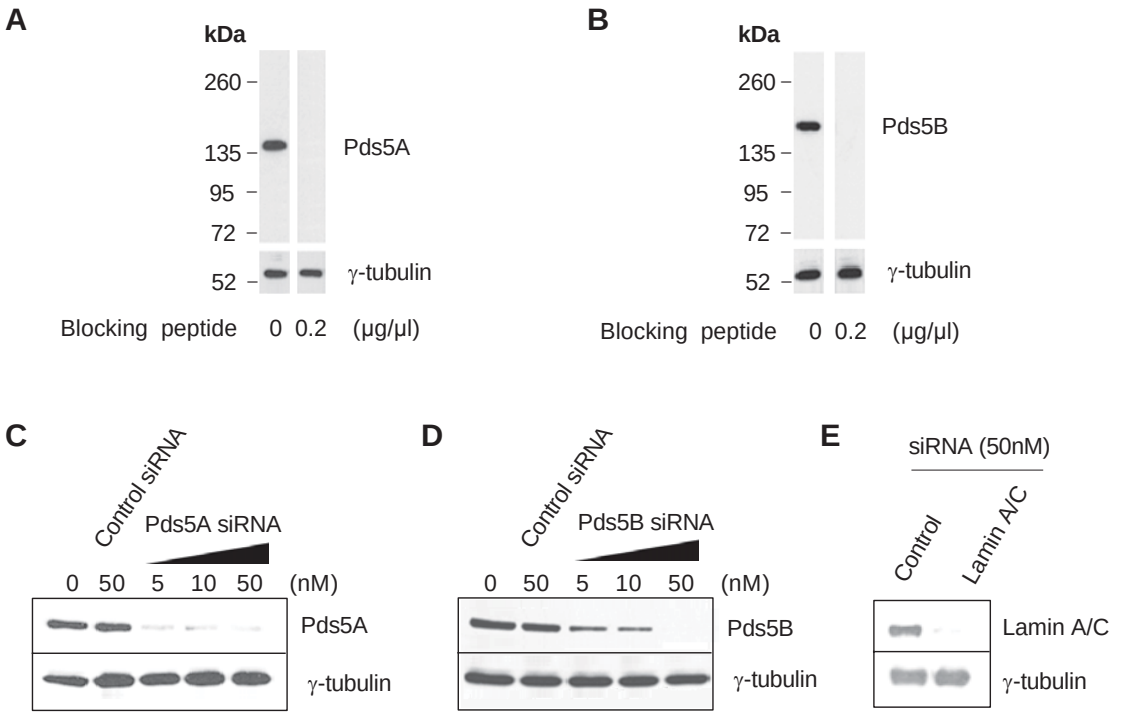

Figure 3.1: Testing the specificity of Pds5A and Pds5B antibodies by Western blot using HeLa cell extracts.

(A and B) HeLa cell extracts prepared from exponentially growing cells were Western blotted with antibodies to Pds5A and Pds5B. To test their specificity, Pds5A or Pds5B antibodies (0.5μg/ml) were incubated individually with the indicated concentrations of Pds5A or Pds5B blocking peptides for 3 hrs before probing the nitrocellulose membrane. Results are representative of three independent experiments. (C and D) HeLa cells were transfected with either control or SMARTpool siRNAs specific to Pds5A or Pds5B at the indicated concentrations for 48 hrs. Proteins were extracted as described in material and methods and loaded on an 8 % SDS-PAGE gel and Western blotted, then probed with antibodies against Pds5A, Pds5B and ϒ-tubulin. (E) Lamin A/C siRNAs (50 nM) were used to test the effectiveness of the transfection procedure. Results are representative of two independent experiments.

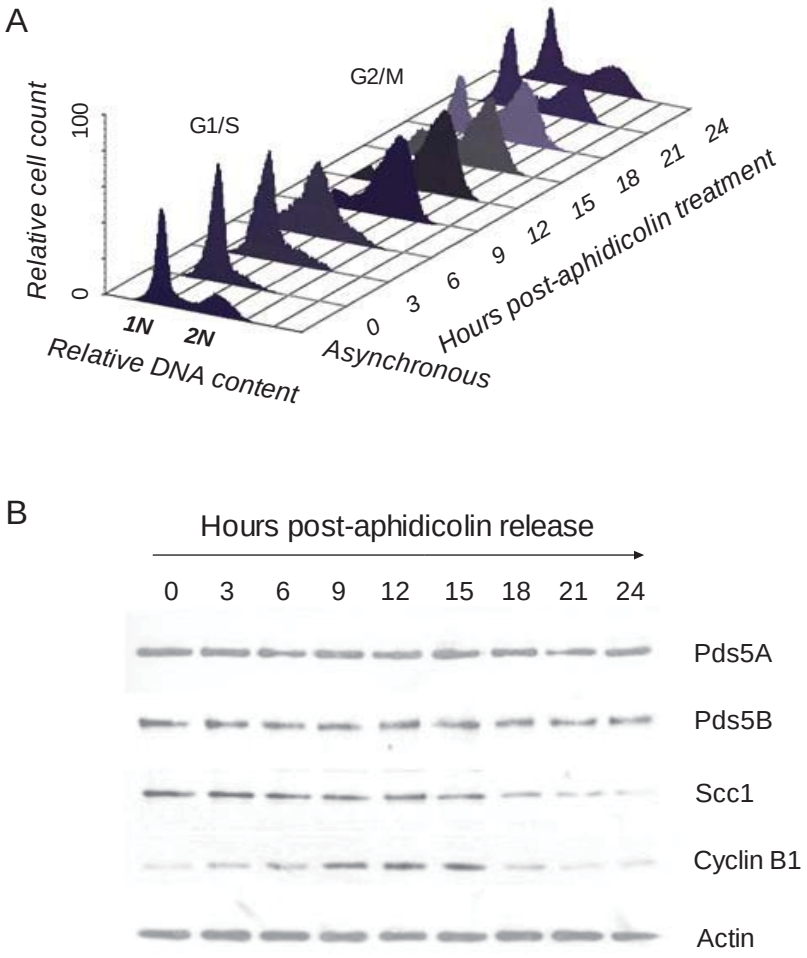

Figure 3.2: Analysis of endogenous Pds5A and Pds5B proteins expression during the HeLa cell cycle.

Asynchronously growing cells were arrested at the G1/S boundary with 10 µg/ml aphidicolin. After 24 hrs, the cells were washed three times with 1 % (v/v) PBS and fresh medium was added. (A) A FACS profile of propidium iodide stained nuclei at a series of time points after release from the aphidicolin arrest. (B) Total protein extracts were prepared at the indicated time points and Pds5A, Pds5B, Scc1, cyclin B1 and actin protein levels were analyzed by Western blot. Results are representative of four independent experiments.

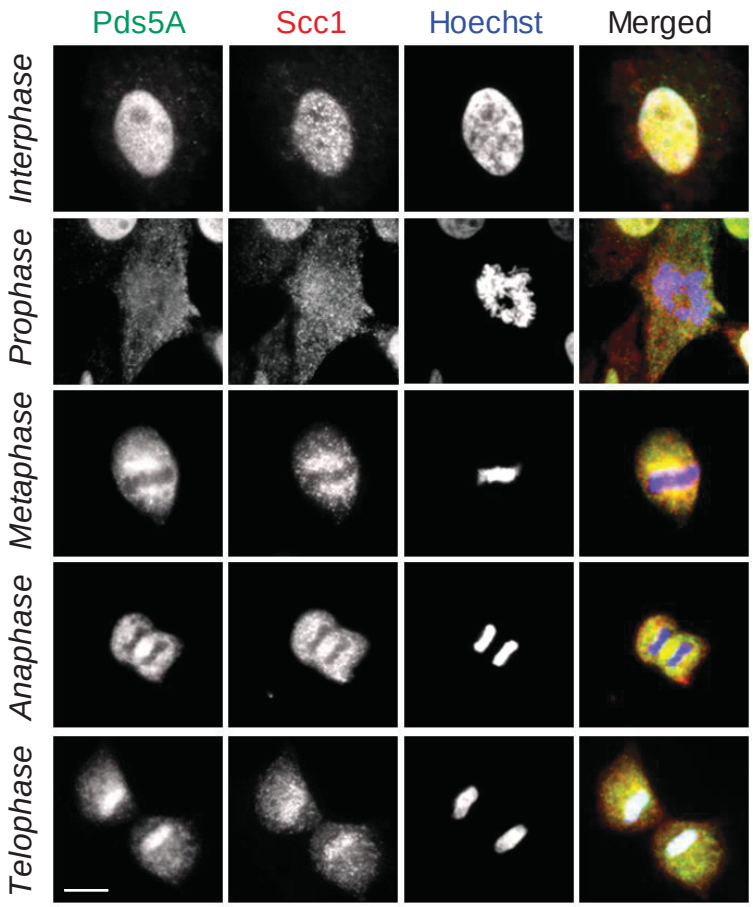

Figure 3.3: Immunofluorescence microscopy images showing the intracellular distribution of Pds5A and Scc1 at different stages of the cell cycle.

HeLa cells grown on cover slips were fixed with 3.7 % (v/v) formaldehyde for 20 min and treated with 0.1 % (v/v) Triton X-100 for 10 min. After blocking with 5 % (w/v) BSA, cells were co-stained with antibodies against Pds5A (green) and Scc1 (red). DNA was stained with Hoechst 33342 (blue). Merged images are shown (right panel). Scale bar: 8 µm. This figure is representative of three independent experiments.

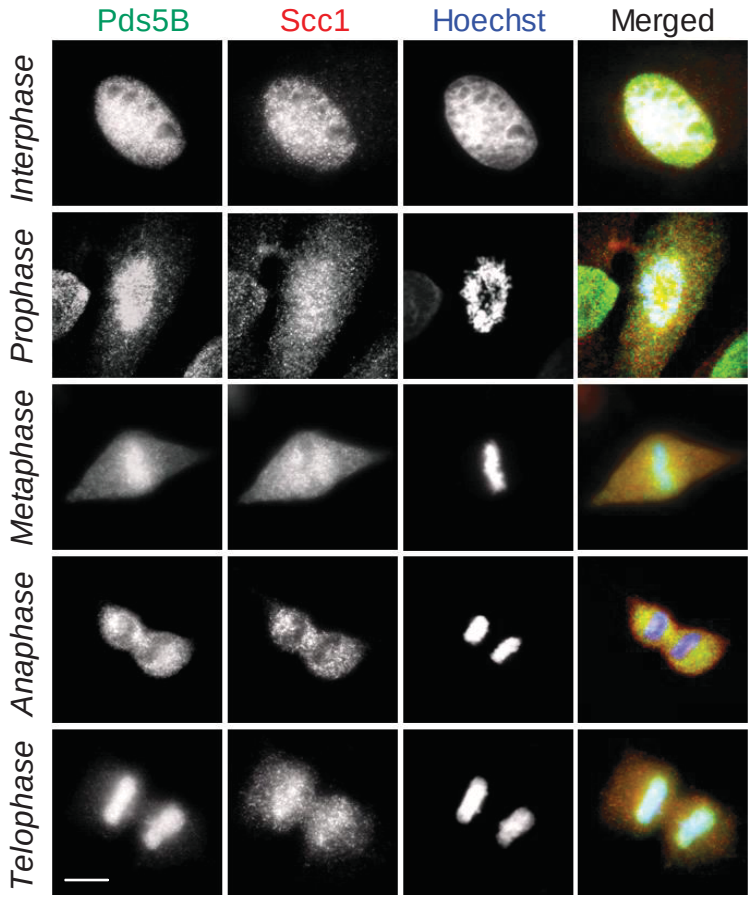

Figure 3.4: Immunofluorescence microscopy images showing the intracellular distribution of Pds5B and Scc1 at different stages of the cell cycle.

HeLa cells grown on coverslips were treated as described in Figure 3.3 on page 63, and then co-stained with antibodies against Pds5B (green), Scc1 (red) and Hoechst 33342 (blue). Merged images are shown (right panel). Scale bar: 8 µm. This figure is representative of three independent experiments.

3.2.3. Overexpression of Pds5A

Initially, I attempted several times to overexpress full-length Flag epitope-tagged Pds5A cDNA in HeLa cells to investigate its role in SCC. However, no significant levels of exogenous Pds5A could be detected by Western blot, so I sought to examine two additional truncated forms of Pds5A. To generate Flag-Pds5A N-terminus, I truncated the C-terminal residues after amino acid 789, which contains one AT-hook domain. For Flag-Pds5A C-terminus, I truncated the first 780 amino acids of the entire N-terminal region with nine amino acids overlapping (Figure 3.5A). Both truncated sequences were cloned into pLEICS-12 mammalian expression vector (see appendix, Figure A.1, 2, 3 and 5).

After surveying different transfection conditions not only for the transfection method, but also for different cell lines such as HeLa, MCF-7 and HEK 293T cells, I chose a condition in which the cells were transfected by FuGENE 6 transfection reagent to give high transfection efficiency (approximately ≥ 40 %) in HEK 293T cells, which was confirmed by Western blotting and immunofluorescence microscopy (Figure 3.5B and C). Despite this high transfection efficiency, HEK 293T cells were unsuitable for morphological analysis, since I tried several times and they attached poorly to coverslips, making it difficult to analyse the function of Pds5 proteins using this approach.

In some cases, the transfection efficiency of Lipofectamine 2000 reagent in HeLa cells was very low (only 2 - 5 %), which was assessed by immunofluorescence microscopy, and there was a high level of cell death (toxicity), even with mock-transfected cells. Using the anti-Flag antibody, the expression levels of overexpressed Pds5A could not be detected by Western blot, but using immunofluorescence microscopy the nuclear localization of full length and C-terminal Pds5A variant could be detected (Figure 3.5C, panel a and C, panel b). However, only interphase cells seen and no mitotic phenotypes observed when Pds5A (Full lengthe, N- or C-terminus) overexpressed. Since the N-terminal variant lacks the AT-hook domain and nuclear localization signal (Figure 3.5A; see appendix, Figure A.6), it was prevented from nuclear transport and accumulated only in the cytoplasmic compartments (Figure 3.5C panel b). This is consistent with previously reported data that the nuclear transport of APRIN/Pds5B depends on the AT-hook domains present in the C-terminal region (Maffini et al., 2008), suggesting a functional difference between the N-terminus and C-terminus of Pds5.

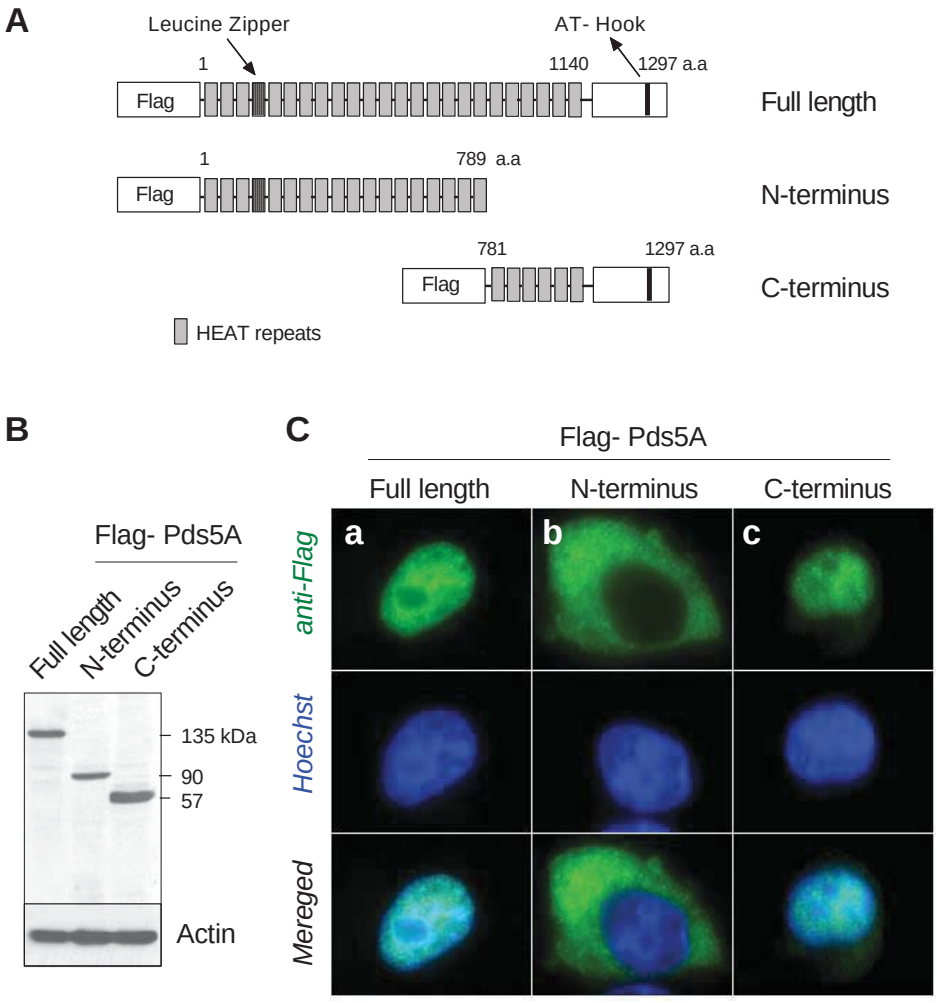

Figure 3.5. Expression and intracellular localization of Flag-tagged Pds5A.

(A) Schematic illustrations of Flag-tagged full-length Pds5A and its truncated variants. (B) Flag-tagged full-length Pds5A and its truncated mutants were transiently co-transfected into HEK 293T cells using FuGENE 6 and after 24 hrs their expression was confirmed by Western blot using an anti-Flag antibody. (C) Immunofluorescence microscopy images of interphase HEK 293T cells transfected separately with Flag-tagged full-length Pds5A and its truncated variants. Nuclear transport and chromatin localization of full-length Flag-tagged Pds5A (as shown in panel a) and FLAG-tag C-terminal Pds5A (as shown in panel c). (b) Accumulation of FLAG-tag N-terminal Pds5A in the cytoplasmic compartments. Merged images are shown in the lower panels. Scale bar: 8 μm. This data is representative of two independent experiments.

3.2.4. Pds5A and Pds5B are required for chromosome separation in human cells

The dynamic localization of the Pds5 proteins suggests their possible function in regulating SCC. In order to examine this, I used siRNAs to deplete Pds5A and Pds5B specifically, either individually or both together in HeLa cells. The protein levels of both Pds5A and Pds5B were markedly reduced within 36 hrs after siRNA treatment compared to controls (Figure 3.6A and B). The off-target effects were further minimized when I observed that the levels of the cohesin-related proteins were unaffected (Figure 3.7). When chromosome spreads were prepared from control siRNA-treated cells which had been subjected to Taxol, a potent microtubule stabiliser and proliferation that blocks the cell cycle at the metaphase/anaphase boundary (Jordan et al., 1993) (Figure 3.8A), a high frequency of resolved chromosome arms was observed (mean ± SD = 94 ± 1 %; n = 100 cells; Figure 3.8B and F), whereas the number of unresolved chromosomes was significantly increased with Taxol-treated cells in which Pds5A or Pds5B or both proteins were depleted by siRNAs (mean ± SD = 50 ± 21 %, 40 ± 21 % or 53 ± 12 % respectively; n = 100 cells; $P < 0.01$, $P < 0.05$, $P < 0.01$; Figure 3.8D and F). This observation would suggest that chromosome separation at the arms requires both Pds5A and Pds5B.

To further investigate the requirement of Pds5 proteins for centromeric cohesin removal, I nullified the action of PP2A by adding okadaic acid, a potent inhibitor of PP2A (Cohen, 1989) (Figure 3.8A). Treatment of cells with a combination of Taxol and okadaic acid causes high frequency of premature loss of cohesion at the arms and the centromere in control siRNA-treated cells (mean ± SD = 87 ± 7 %; n = 100 cells; Figure 3.8C and G), but this loss was significantly reduced at both regions in cells depleted of Pds5A, Pds5B or both, with respective increase in cells with unresolved chromosomes of 40 ± 26 % in Pds5A siRNA, 41 ± 17 % in Pds5B siRNA or 34 ± 12 % in both siRNAs (mean ± SD; n = 100 cells; $P < 0.01$, $P < 0.01$, $P < 0.05$ respectively ; Figure 3.8D and G). These results were confirmed using single oligonucleotide-mediated depletion of Pds5A and Pds5B (see appendix, Figure A.8). I conclude from these data that both Pds5A and Pds5B are required for chromosome separation at the chromosome arms and at the centromeric region. In response to Taxol and okadaic acid, later in the project I have shown that Pds5A and Pds5B are also required for separation during the normal cell cycle (see chapter 5).

To analyse further the effect of Pds5 proteins loss on cohesin, I monitored the removal of the bulk of cohesin from the chromosome arms, a process that depends on the prophase pathway (Losada et al., 2002, Sumara et al., 2002, Gandhi et al., 2006, Kueng et al., 2006, Shintomi and Hirano, 2009). I repeated the siRNAs treatment and the mitotic cells were harvested and attached to coverslips coated with poly-L-lysine (1 mg/ml) for immunofluorescence

microscopy. Interestingly, cohesin (Scc1) remained associated with the chromosome arms and maintained the SCC between the arms in Pds5A and Pds5B-depleted cells, even after mitotic arrest in Taxol-treated cells (Figure 3.8E), whereas in control siRNA-treated cells, cohesin was dissociated from the chromosomes except for the centromeric regions (Figure 3.8E). Taken together, these observations indicate that Pds5A and Pds5B have independent functions in regulating the cohesin complex and that both are required for the removal of human cohesin, both at the chromosome arms and at the centromeric region.

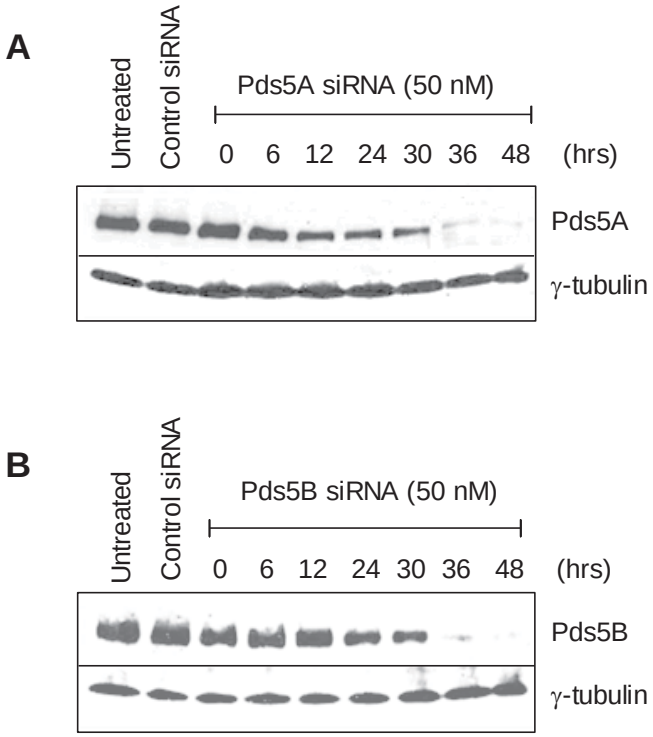

Figure 3.6: Pds5A and Pds5B levels were reduced by SMARTpool siRNAs after 36 hrs.

HeLa cells were transfected with 50 nM of either control or SMARTpool siRNAs specific for Pds5A (A) or Pds5B (B). Total proteins were extracted as described in material and methods, at various time points (6, 12, 24, 30, 36, 48 hrs), and were analyzed by Western blot using the antibodies indicated. This figure is representative of two independent experiments.

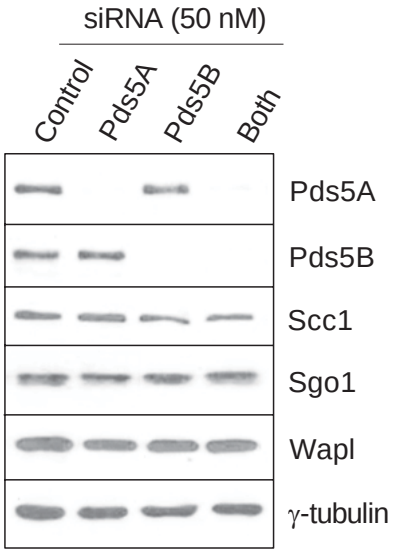

Figure 3.7: Specificity of Pds5A and Pds5B siRNA.

(A) HeLa cells were transfected with 50 nM of either control or a SMARTpool of Pds5A, Pds5B or a mixture of both siRNAs. Forty-eight hours later total protein was extracted and analysed by Western blot using the antibodies indicated. This figure is representative of three independent experiments.

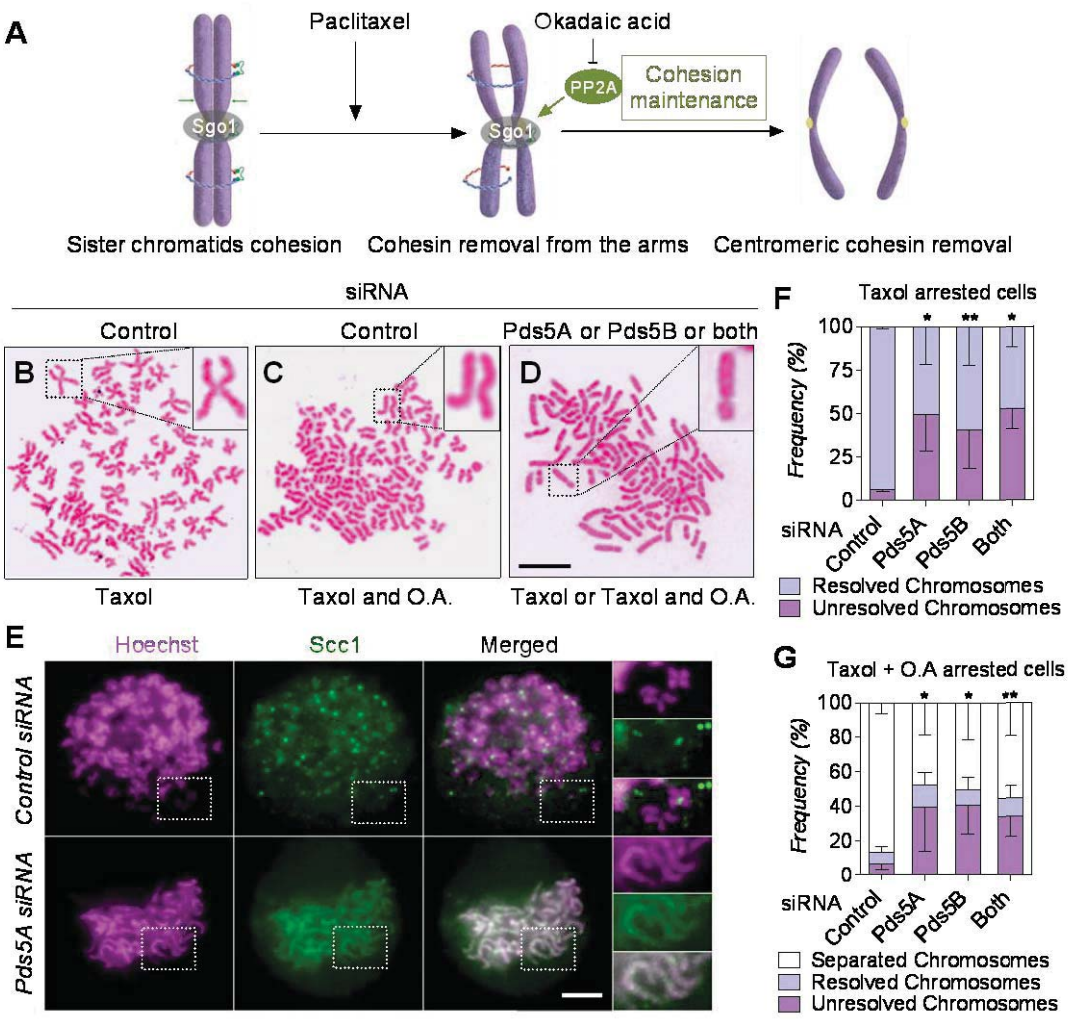

Figure 3.8: Both Pds5A and Pds5B are both required for sister chromatid resolution.

A) Schematic representation of the effect of Taxol and okadaic acid on chromosome separation. (B-D) Metaphase chromosome spreads were prepared from HeLa cells treated with 10 μM Taxol for 18 hrs or with 10 μM Taxol and 0.1 μM okadaic acid for 12 hrs in which Pds5A or Pds5B or both proteins were depleted by siRNA treatment (50 nM) for 48 hrs. Representative light microscopy images show the observed differences in the morphology of chromosomes; enlarged images are shown in the insets. Scale bar: 10 μm. (E) Immunofluorescence microscopy images showing the localization of Scc1 in cells treated with 10 μM Taxol in which Pds5A protein was depleted by siRNAs and stained with Scc1. DNA was stained with Hoechst 33342. (F and G) Histograms indicating the frequency of chromosome morphology in chromosome spreads obtained in (B -D). Error bars represent the mean values and standard deviations of measurements from at least 100 cells for each condition; *$P < 0.01$; **$P < 0.05$. P values were calculated using two-way ANOVA. This figure is representative of three independent experiments.

3.2.5. Loss of Pds5A and Pds5B alter the cell cycle and induce chromosomal abnormalities

The data obtained from the metaphase chromosome spreads raised the possibility that when Pds5 protein was depleted, it may have caused a cell cycle arrest at metaphase, because those cells were unable to segregate their chromosomes. To test this possibility, I performed a fluorescence-activated cell sorting (FACS) analysis after siRNA-mediated knockdown of the Pds5 proteins. Unexpectedly, the loss of Pds5A or Pds5B caused a slight change in the cell cycle profile during S-phase and an increase in the percentage of sub-G1-phase when compared to control siRNA-treated cells (Figure 3.9).

Cell cycle profile analysis was also performed following siRNA-mediated knockdown of both Pds5A and Pds5B, to establish whether the knockdown of both proteins had more effect on cell cycle progression. Following siRNA treatment for 48 hrs, Pds5A and Pds5B levels were reduced to similar levels compared to those obtained using a single treatment (Figure 3.6, on page 69 and Figure 3.7, on page 70), but the FACS data obtained showed a change in cell cycle progression similar to that seen when Pds5A and Pds5B were depleted individually (Figure 3.9). These data suggest that Pds5 proteins may be required for normal S-phase progression; however, the significance of this change is not clear. I therefore examined the morphology of cells following siRNA treatment by immunofluorescence microscopy.

The siRNA-mediated depletion of Pds5A, Pds5B or of both proteins dramatically raised the incidence of condensed and fragmented DNA, from 1.33 ± 0.75 % (mean ± SD; n = 100 cells) in control cells to 17 ± 3 %, 12 ± 1 % and 13 ± 5.5 % respectively (mean ± SD; n = 100 cells; $P < 0.01$; Figure 3.10A, panel b), in addition, there was an increase in interphase cells displaying irregularly shaped nuclei from 0.33 ± 0.75 % in control cells to 15 ± 3 % in Pds5A siRNA, 8 ± 1.5 % % in Pds5B siRNA and 12 ± 2 % in Pds5A and Pds5B siRNAs (mean ± SD; n = 100 cells; $P < 0.01$, $P < 0.05$, $P < 0.01$ respectively; Figure 3.10A, panel c). These enlarged multi-nucleated cells may indicate that these cells are models for aneuploidy caused by failure of chromosome segregation. Micronuclei were also frequently seen in interphase cells after depletion of Pds5A, Pds5B or both proteins (mean ± SD = 24 ± 8 %, 10 ± 1.5 % and 15 ± 2.5 % respectively; n = 100 cells; $P < 0.01$; Figure 3.10A, panel d). In contrast, the frequency of such events was very low in control cells (mean ± SD = 0.7 % ± 0.6).

On the other hand, the frequency of observing mitotic defects was less than that of observing defects in interphase cells, because of the low number of mitotic cells which can be seen in a single slide; therefore, only 20 to 50 cells were analysed in each experiment. However, the most common mitotic defect seen was the misalignment of chromosomes at the metaphase plate, with a respective increase of 22 ± 6 % in Pds5A siRNA, 15 ± 0.6 % in Pds5B siRNA and 14 ± 4 % in Pds5A and Pds5B siRNAs (mean ± SD; $P < 0.01$) (Figure 3.11A, panel a).

Although there were some other defects, such as lagging chromosomes during anaphase and cytokinesis (Figure 3.11B and C, panels b and c), the frequency of such defects might appear low due to the difficulty of finding cells at anaphase and telophase.

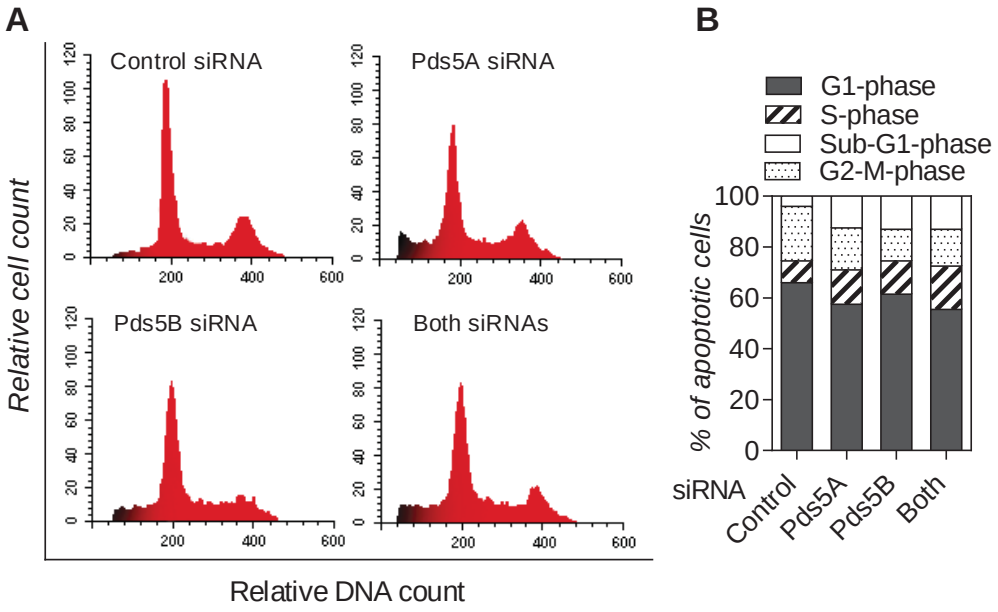

Figure 3.9: Depletion of Pds5 by siRNA proteins alters the cell cycle and induces an accumulation of cells in the sub-G1 population.

(A) A profile of propidium iodide-stained nuclei after 48 hrs treatment with Pds5A siRNA (50 nM), Pds5B siRNA (50 nM) or mixture of both siRNAs (50 nM each). (B) Histogram representing the percentage of cells in sub-G1, G1, S-phase and G2/M. Two independent experiments were analyzed and the mean is shown.

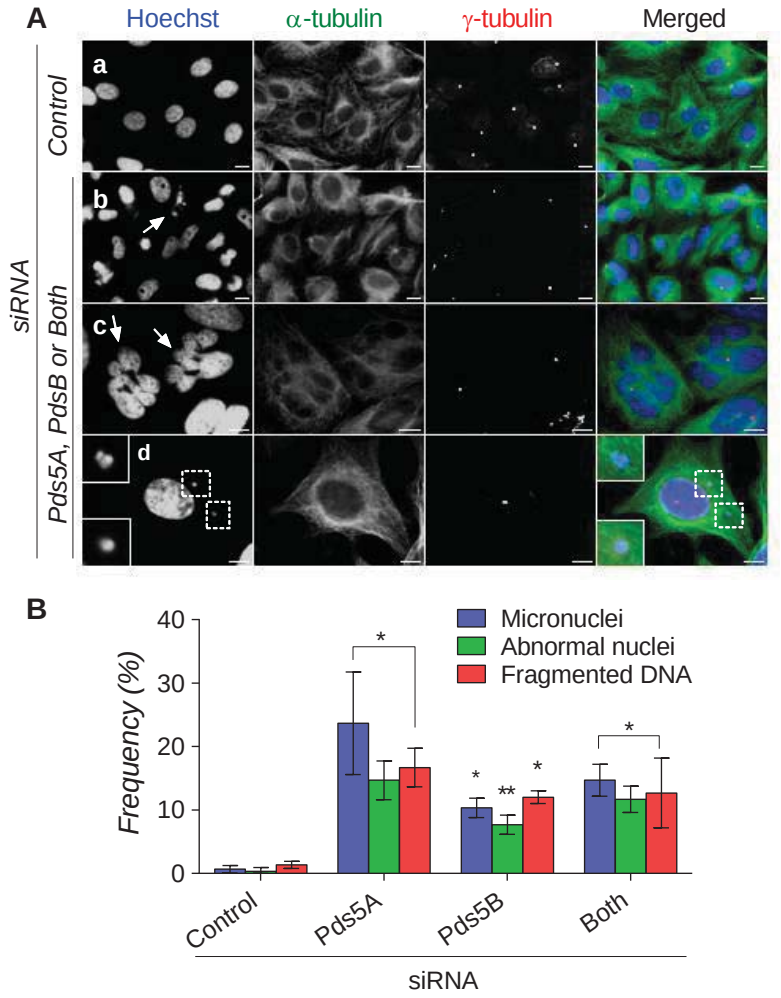

Figure 3.10: Depletion of Pds5 by siRNA induces aberrations in interphase nuclear morphology.

HeLa cells were treated for 48 hrs treatment with the indicated siRNAs. The cells were then fixed with -20 °C methanol and analyzed by immunofluorescence microscopy using anti-α-tubulin (green) to visualize the microtubules, anti-ϒ-tubulin (red) to visualize the centrosomes and Hoechst 33342 (blue) to visualize the DNA. (A) Loss of Pds5 proteins produced a significant increase in nuclear aberrations including fragmented DNA (shown in panel b), multinucleated cells (≥2 nuclei/cell) (shown in panel c) and micronuclei (shown in panel d). Merged images are shown in all panels. Scale bar: 8 μm. (B) Histogram indicating frequency of nuclear defects in interphase cells from three independent experiments; mean values ± standard deviation are shown of measurements from at least 100 cells; *$P < 0.01$, **$P < 0.05$. P values were calculated using two-way ANOVA.

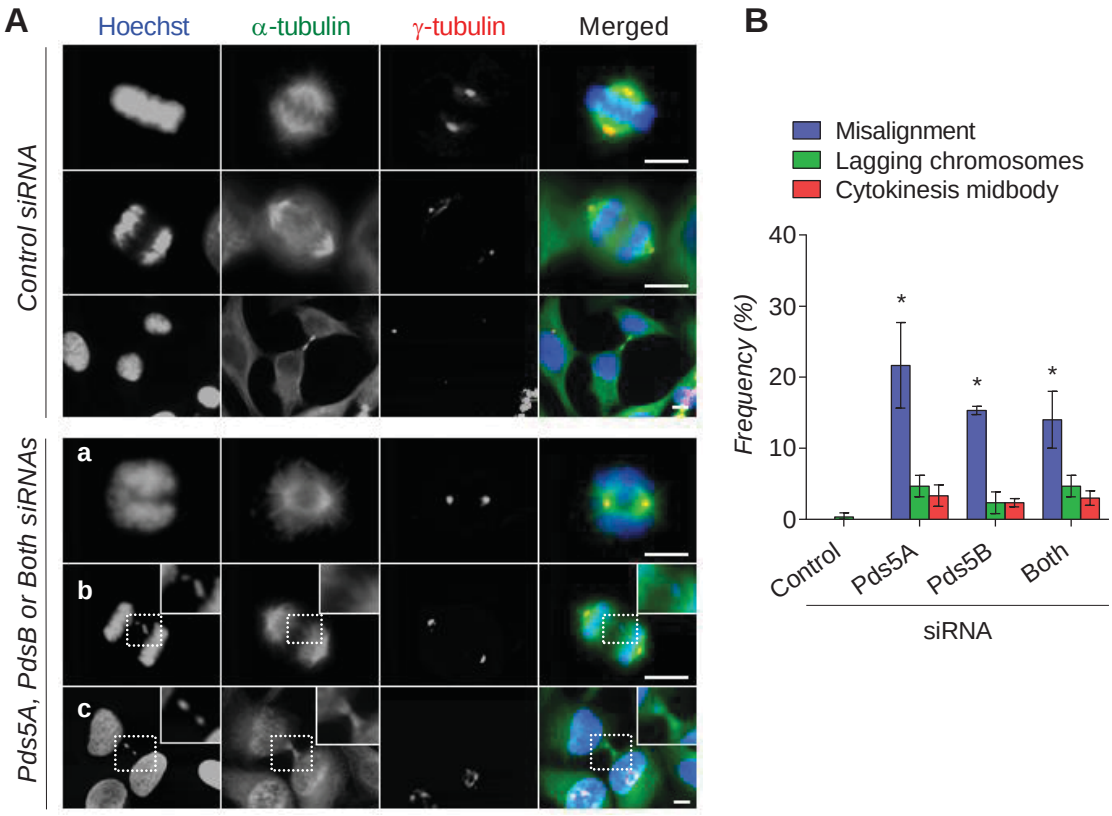

Figure 3.11: Depletion of Pds5A and Pds5B proteins induces abnormal mitosis.

Representative immunofluorescence images of mitotic Pds5 protein-depleted cells. Cells were fixed with -20 °C methanol following 48 hrs siRNAs treatment and co-stained with anti-α-tubulin (green) to visualize the microtubules, anti-ϒ-tubulin (red) to visualize the centrosomes and Hoechst 33342 (blue) to visualize the DNA. (A upper panel) Normal metaphase, anaphase and cytokinesis cells depicted from control siRNA-treated cells. (A, panel a) Chromosome misalignment in metaphase, (A, panel b) lagging chromosome in anaphase and (A, panel c) cytokinetic midbody with lagging chromosomes and interconnecting DNA bridge were observed after Pds5 protein depletion. Merged images are shown; scale bar: 10 μm. (B) Histogram showing frequency of defective mitotic cells. Three independent experiments were analysed (20 to 50 cells per experiment were analysed). Mean values ± standard deviation are shown; *$P < 0.01$, **$P < 0.05$. P values were calculated using two-way ANOVA.

3.2.6. Loss of Pds5A and Pds5B induces apoptosis via activation of the DNA damage checkpoint

The increase in the percentage of sub-G1-phase cells may be related to the observation of those cells showing DNA fragmentation (as observed in Figure 3.10 on page 75) and the presence of floating cells observed under a light microscope in the culture medium 48 hrs after siRNA treatment. Both these observation suggested that loss of Pds5 proteins may be lethal to HeLa cells. Since DNA fragmentation is an important hallmark of apoptotic cells, I assessed the levels of apoptosis at 48 hrs after transfection with Pds5A or Pds5B siRNA. Both adherent and floating cells were harvested, combined and seeded onto poly-L-lysine-coated coverslips, fixed and stained with Hoechst 33342 and a caspase-3 antibody that only detect a 19 kDa fragment of cleaved caspase 3 for immunofluorescence analysis. An increase in the proportion of apoptotic cells could be detected in both Pds5A and Pds5B-depleted cells (Figure 3.12). These results were further validated by Western blot detection of cleaved fragments of caspase-3 and poly (ADP-ribose) polymerase (PARP) (Figure 3.13A). Taken together with the cell cycle profiles (Figure 3.9), the data suggested that the loss of Pds5A and Pds5B may have caused a delayed passage through S-phase and activated the apoptotic signalling pathways. It would therefore be important to understand the molecular mechanisms leading to the activation of the apoptotic response in the absence of functional Pds5 proteins.

Given that SCC is required for the integrity of the DNA damage checkpoints (Lightfoot et al., 2011), I next sought to establish whether the absence of any cohesin regulatory factors might activate a DNA damage checkpoint response. To test this hypothesis, I blotted for phosphorylated Chk1 ser^{317}, using a phospho-specific antibody that recognizes Chk1, a kinase activated by ATR in response to DNA damage (Smits et al., 2010), when it is phosphorylated on ser^{317}, following depletion of Pds5 proteins. As judged by the results of the Western blot (Figure 3.13B), Chk1 was found to be phosphorylated on ser^{317} in Pds5 protein-depleted cells. This indicates that the absence of Pds5 proteins may cause replication stress or other types of DNA damage, which then triggers an apoptotic response through activation of the DNA damage checkpoint. It is also possibile that the loss of Pds5 causes the accumulation of cells in S-phase due to the defective DNA replication and slowed the progression of the S-phase. It is possible that because the cells were not synchronized after the loss of Pds5 proteins and were randomly distributed within the cell cycle, the cell cycle profile (Figure 3.9 on page 74) shows only a small accumulation of cells in S-phase. Following these arguments, both the control and Pds5 protein siRNA-treated cells were synchronized at the G1/S boundary by aphidicolin treatment and release in order to monitor their progression through S-phase. DNA content analysis by flow cytometry indicated that

control cells completed S-phase in approximately 8 hrs upon release from the aphidicolin block (Figure 3.14), whereas Pds5-depleted cells were unable to progress to mitosis. However, some cells completed S-phase in approximately 15 hrs, perhaps due to slower DNA replication caused by Pds5 protein depletion and activation of the DNA damage checkpoint response. This leads us to conclude that Psd5 function is not restricted to mitosis but may also be required for DNA replication integrity and this may depend on its ability to maintain SCC during the S-phase.

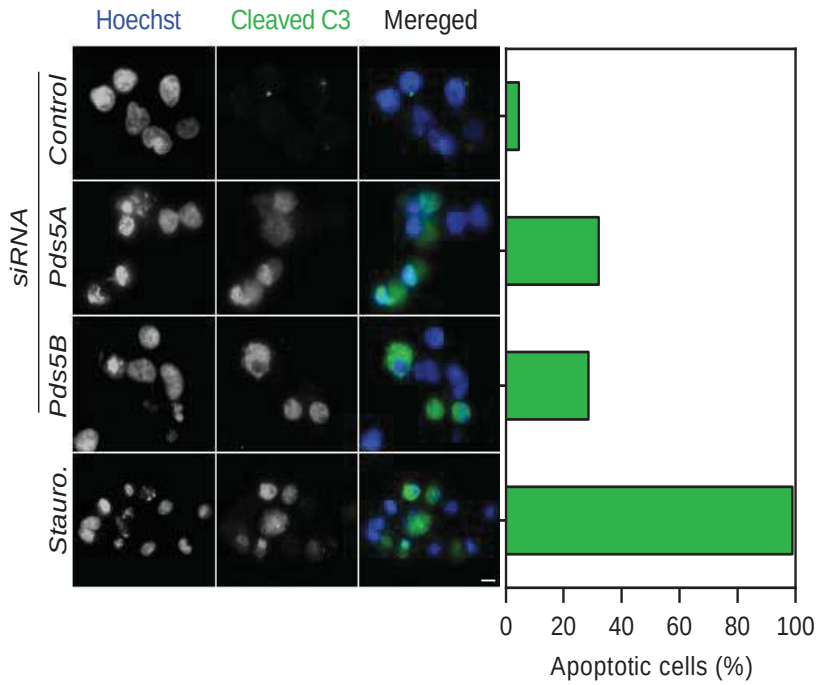

Figure 3.12: Depletion of Pds5A and Pds5B induce apoptosis.

Exponentially growing HeLa cells were transfected with control, Pds5A or Pds5B siRNA (50 nM) for 48 hrs. After 48 hrs both adherent and floating cells were attached on poly-L-lysine-coated coverslips with 100 % (v/v) cold methanol. Apoptotic cells were detected by cleaved caspase-3 antibody (green) using immunofluorescence microscopy. DNA was visualized by staining with Hoechst 33342 (blue). As a positive control for apoptosis, cells were treated with prototypical ATP-competitive kinase inhibitor staurosporine (1 µM for 6 hrs). Merged images are shown in the right-hand panels. Scale bar: 8 µm. The percentage of apoptotic cells is represented by a histogram in the right panel. Two independent experiments were analyzed and the mean of measurements from at least 100 cells is shown.

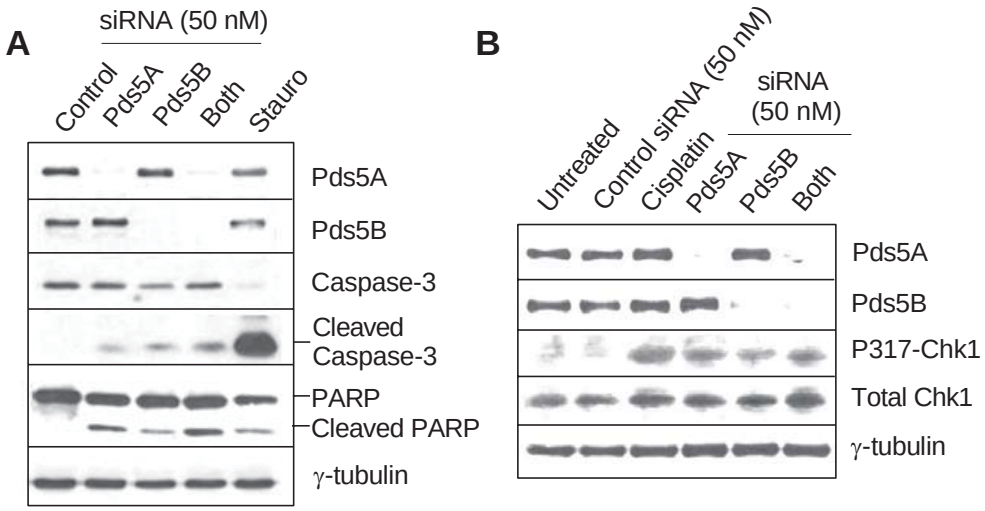

Figure 3.13: Depletion of Pds5A and Pds5B by siRNA induces apoptosis through the activation of the DNA damage checkpoint.

(A) HeLa cells were treated for 48 hrs treatment with the indicated siRNAs. Western blot analysis with antibodies against: Pds5A, Pds5B, full-length caspase-3, cleaved caspase-3, PARP and γ-tubulin. As a positive control for apoptosis, cells were treated with a prototypical ATP-competitive kinase inhibitor, staurosporine (1 μM for 6 hrs). (B) Cells were examined for phosphorylation of Chk1 at Ser^{317} by Western blot after 48 hrs siRNA treatment. As a positive control for the effects of a DNA-damaging agent, cells were treated with 10 μM cisplatin for 6 hrs. This figure is representative of three independent experiments.

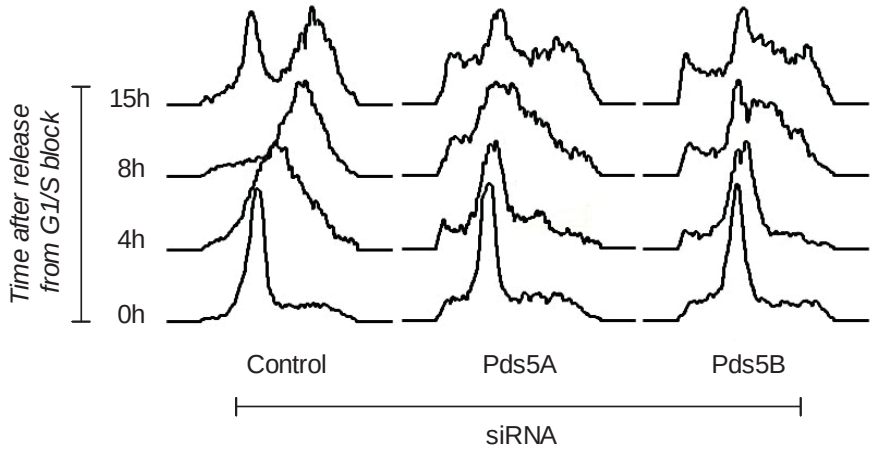

Figure 3.14: Depletion of Pds5A and Pds5B impairs S-phase progression.

Exponentially growing HeLa cells were transfected with control, Pds5A or Pds5B siRNA (50 nM) for 48 hrs. The cells were then synchronized at G1/S boundary by the adding of aphidicolin (10µg/ml for 24 hrs). The aphidicolin was removed and the cells were washed three times with 1 % (v/v) PBS and fresh medium was added. Cells were collected at the indicated times and DNA content was analysed by FACS as described in material and methods. This figure is representative of two independent experiments.

3.3. Discussion

Sister chromatid cohesion is a process that links two chromatids during interphase and is thought to be a prerequisite for maintenance until its partial reversal during prophase and the complete separation of sister chromatids at the metaphase-to-anaphase transition. Unlike in yeast and fungi, Pds5 is required for sister chromatid resolution during prophase in *Xenopus* egg extracts (Panizza et al., 2000, Zhang et al., 2005, Shintomi and Hirano, 2009). Therefore, I cannot rule out the possibility that SCC is regulated similarly in mammalian cells, because in both mammals and *Xenopus* egg extracts the removal of the bulk of cohesin complexes is already initiated in prophase (Losada et al., 1998, Darwiche et al., 1999).

To address this issue I have sought to provide evidence that Pds5 is involved in the regulation of SCC by analyzing the subcellular localization pattern of the Pds5 proteins. Psd5A behaves like the cohesin complexes in this respect (Figure 3.3 on page 63), dissociating from chromatin at prophase and rebinding to it in telophase before cohesion is established in S-phase. This behaviour is similar to that reported for Pds5 homologue in *Sordaria* (van Heemst et al., 1999) and Pds5A in human Caco cells (Sumara et al., 2000). However, unlike Scc1 which is cell cycle regulated and decline after mitosis, the expression levels of Pds5 proteins remained relatively constant throughout the cell cycle (Figure 3.2 on page 62).

Surprisingly, some Pds5B could still clearly be detected on chromosomes from prophase to metaphase, but not at anaphase (Figure 3.4 on page 64). This observation has not previously been reported. Additionally, during telophase Pds5B was detected on chromatin more intensely than cohesin and Pds5A (Figure 3.3 and Figure 3.4 on page 63 and 64), suggesting that Pds5A and Pds5B may play distinct roles during the cell cycle. Accordingly, the C-terminus sequence of Pds5 proteins contains nuclear localization signals (see appendix, Figure A. 7). I have shown that the C-terminus of Pds5A plays an essential role in mediating subcellular localization (Figure 3.5C, panel c on page 66). Pds5A contains a single degenerate AT-hook-type high mobility group (HMG), whereas Pds5B contains two AT-hooks (Zhang et al., 2009a). The positively charged Arg within the AT-hook domain in HMG is known to be crucial for DNA binding (Metcalf and Wassarman, 2006), suggesting a higher binding affinity for Pds5B than for Pds5A. It has been previously speculated but not demonstrated that Pds5B has cdk1 phosphorylation sites (Losada et al., 2005); these sites may mediate a post-translational modification of cohesin-bound Pds5B, causing it to dissociate from chromatin. Taken together, this all supports the hypothesis that Pds5B is bound to chromatin during telophase (probably before Pds5A) and it may be able recruit Pds5A to chromatin. Pds5A in this case may be serving as a scaffold to recruit other proteins such as

Wapl. Cohesin-bound Pds5A and Pds5B are both dissociated during prophase following their post-translational modification (probably by cdk1). At the metaphase-to-anaphase transition, Pds5B-bound chromatin may be targeted by an unknown second wave of post-translational modification (perhaps by cdk1 or Plk1), causing complete dissociation of Pds5B from chromatin.

Although I have so far been unable to overexpress Pds5A in HeLa cells efficiently to further analyse its role in SCC regulation, I was able to knock down Pds5 proteins efficiently. In this project, I have provided evidence that Pds5A and Pds5B are both required for chromosome separation, both at the chromosome arms and at the centromeric region, because the loss of either Pds5A or Pds5B prevented cohesin removal both from chromosomal arms and from the centromeric region in Taxol and Okadaic acid-arrested mitotic cells. Although I expected to see redundant functions for Pds5A and Pds5B in the regulation of SCC, the interpretation of the results regarding the different localization patterns between Pds5A and Pds5B may explain why Pds5A did not rescue the loss of Pds5B phenotype and vice versa. It seems that Pds5A and Pds5B are localized in such a way that Pds5A can recruit aditional proteins such as Wapl to trigger the removal of cohesin. This interpretation is supported by the evidence that Wapl interacts preferentially with Pds5A rather than Pds5B (Kueng et al., 2006). On the other hand, Pds5B may still be able to form a complex with Wapl to trigger the removal of cohesin, but due to a higher binding affinity for Pds5B, it may also be required for correct localization of Pds5A to allow its binding with Wapl. Therefore, the correct localization of either Pds5A or Pds5B may be affected by the absence of the other.

In fission and budding yeasts and in human cells, the localization of Pds5 proteins to chromosomes is cohesin dependent (Hartman et al., 2000, Losada et al., 2005) (Wang et al., 2002) and it is most likely that localization must occur before the process of DNA replication, because fission yeast Pds5 was found to interact with the establishment factor Ctf7/Esco1, which is known to recruit proteins involved in DNA replication such as Ctf18 and PCNA. Moreover, the loss of Pds5 function negates the requirement for Ctf7/Esco1 (Tanaka et al., 2001, Skibbens et al., 1999). The Ctf7/Eco1-mediated acetylation of the cohesin subunit Smc3 is known to be important for recruiting Sororin to stabilize bound cohesin during S-phase. At the same time, Pds5 can interact with the conserved FGF motif of Sororin to mediate conformational rearrangement to stabilize bound cohesin (Nishiyama et al., 2010). This suggests that Pds5 may be indirectly involved in the DNA replication mechanism by its ability to hinder the establishment of cohesion until it recruits Ctf7/Esco1 and Sororin. This would also be consistent with my observation that Pds5A and Pds5B-depleted cells accumulated at S-phase which was followed by induction of apoptotis through activation of

the DNA damage checkpoint signaling. The evidence for this was the phosphorylation of Chk1 at ser^{317} in response to blocked DNA replication caused by the loss of functional Pds5.

On the other hand, the evidence that cohesin is involved in repairing DNA damage by its ability to mediate SCC (Birkenbihl and Subramani, 1992) does not rule out the requirement for Pds5. The first step of the repair mechanism is that cohesin is loaded onto sites of DNA double-strand break (DSB) to mediates SCC with the aid of Esco1 (Strom et al., 2004). Since Pds5 is required to recruit Ctf7/Esco1 to the cohesin complex, I can also argue that after DNA DSB, Pds5 may be required to establish a state permissive of G2-phase cohesion, to ensure that the sister chromatids are physically connected and can thus undergo homologous pairing. While the most recent study in budding yeast has proposed that post-replicative DNA repair requires the protease separase to remove cohesin that is established in S-phase in the presence of DSB (McAleenan et al., 2013), I can speculate that the system may be different in vertebrates. In both budding and fission yeasts, separase is responsible for the removal of cohesins from the chromosomes during mitotic anaphase (Uhlmann et al., 1999, Tomonaga et al., 2000, Uhlmann et al., 2000), whereas in vertebrates, most cohesins are removed from the chromosomes during prophase in a separase-independent process which relies on the cohesin-regulatory proteins Pds5 and Wapl (Waizenegger et al., 2000, Losada et al., 2002). Based on the apoptosis data and cell cycle analysis of Pds5-depleted cells in this study, perhaps the post-replicative DNA repair mechanism in vertebrates requires Pds5; however, it remains to be determined whether Wapl is involved in the DNA repair mechanism.

Examination by immunofluorescence microscopy did not reveal whether Pds5-depleted cells are sensitive to metaphase arrest, because I did not observe an increase in number of mitotic cells. (Figure 3.9 on page 74). However, the S-phase phenotypes and the fact that Pds5 depletion causes a delay in S-phase that is mediated by a checkpoint response lead me to speculate that chk1 inhibition may allow cells to progress into mitosis. Therefore, it would have been interesting if I had addressed whether the depletion of both Pds5 and Chk1 might increase the incidence of mitotic arrest. Perhaps some cells have completed mitosis after a defective anaphase, especially for those cells that displayed mitotic abnormalities (Figure 3.11 on page 76) due to incomplete loss of SCC. This phenomenon may be the eventual cause of the production of cells displaying micronuclei or macronuclei (Figure 3.10 on page 75). Micronuclei are common indicators of genomic instability and are associated with chromosome loss and unstable chromosomes (Ford et al., 1988).

It is highly likely that a correlation exists between the frequency of misalignment and the frequency of micronuclei in Pds5 depleted-cells. Therefore, an investigation is required to monitor the dynamic processes of chromosome movement and separation using live-cell

imaging. However, the interpretation of these results raises the question of how the loss of Pds5 proteins causes such mitotic errors responsible for chromosome misalignments. To address this question, it may be worth examining whether the loss of Pds5 proteins has a direct effect on the localization of a key factor required to prevent chromosome misalignment, such as Bub1 (Klebig et al., 2009). If so, this may help to explain why the spindle checkpoint function was lost.

Chapter 4

Characterization of Wapl in the mammalian cell cycle

4.1. Introduction

The cohesin regulatory factors Wapl and Pds5 co-localize with cohesin on interphase chromosomes to form a complex which dissociates cohesin from chromosomes during mitosis (Shintomi and Hirano, 2009). However, unlike Wapl, Pds5 is essential for sister-chromatid cohesion and chromosome condensation (Hartman et al., 2000). This suggests that Pds5-independent Wapl has a putative regulatory function in establishing SCC with the cooperation of Esco1 and Sororin during S-phase. However, during mitosis Pds5 has anti-establishent function with the aid of Wapl to disestablish SCC.

Two critical questions arise: how are Pds5 and Wapl regulated throughout the cell cycle and what is the mechanism that controls the interaction of Pds5 and Wapl and subsequent dissociation from chromatin during mitosis? Since it is known that Pds5B contains possible consensus sites for Cdk1 phosphorylation (Losada et al., 2005) (Fig 3A and B), preliminarily speculation was that the modifications of Pds5 function might be modulated by phosphorylation in early mitosis and that this modification could be upstream of conformational changes in cohesin.

A possible way to detect phosphorylation is the electrophoretic mobility shift on SDS-PAGE, as most phosphorylated proteins exhibit slower migration on SDS-PAGE compared to their non-phosphorylated forms (Wegener and Jones, 1984), although some other phosphorylated proteins may exhibit a faster electrophoretic mobility on SDS-PAGE than their non-phosphorylated forms (Ye et al., 1997). Therefore, I set out to examine whether Pds5B is phosphorylated during mitosis by testing the gel mobility shift of Pds5B protein on SDS-PAGE using a lysate prepared from nocodazole-arrested cells. The preliminary results from Western blot analysis showed no detectable gel mobility shift of Pds5B. Consequently, I was curious to establish whether there were any gel mobility shifts of Pds5A or Wapl. Surprisingly, I detected a marked gel mobility shift of Wapl protein in mitotic cell extracts, which suggests a possible crucial role of Wapl phosphorylation during mitosis. To better understand this phenomenon and how this post-translational modification of Wapl might influence Pds5 function, I decided to characterize the function of Wapl in HeLa cells.

4.2. Results

4.2.1. Characterization of Wapl antibodies

Wapl commercial antibody, anti-Wapl polyclonal (Bethyl Laboratories) was tested for its specificity and produced a single band on a Western blot corresponding to the predicted size of Wapl protein. When the anti-Wapl polyclonal is bound to its blocking peptide, it no longer detects its target on the Western blot (Figure 4.1A). Specificity was further confirmed by siRNA depletion and subsequent decrease in the protein signals using Wapl antibody (Figure 4.1B).

4.2.2. Wapl is post-translationally modified in mitotic HeLa cells extracts

In order to determine whether the cohesin-related proteins are phosphorylated at mitosis, the total protein extracts from asynchronous populations and mitotically-arrested cells using 20 nM nocodazole for 18 hrs, were analysed by Western blot to detect shifts in the mobility of Pds5A, Pds5B and Wapl proteins. I detected a marked gel mobility shift of Wapl protein only after 24 hrs of nocodazole treatment (Figure 4.2B). This shift is likely due to post-translational modification by phosphorylation and to validate this observation, I set out to examine the mobility shift of Wapl protein using various mitotic blocks such as 20 nM nocodazole for 18 hrs, 10 μM Taxol for 18 hrs or a combination of 10 μM Taxol and 0.1 μM okadaic acid for 12 hrs. The Western blot results confirmed the first observation: Wapl protein bands from the mitotic cell extracts exhibited slower migration on SDS-PAGE compared to Wapl protein bands from extracts prepared from an asynchronous populations (Figure 4.2C).

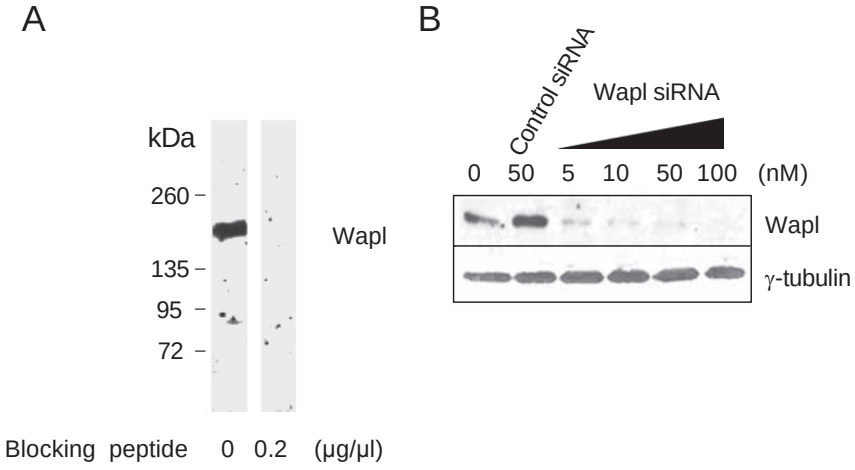

Figure 4.1: Specificity of the Wapl antibody.

HeLa cell lysates prepared from exponentially groing cells were wstern blotted with Wapl antibody (0.5 µg/ml; Bethyl Laboratories) which recognizes a region between residues 1125 and 1175 of human Wapl. To Wapl antibody specificity, Wapl antibody (0.5 µg/ml) was incubated with the indicated concentrations of Wapl blocking peptides for 3 hrs before probing the nitrocellulose membrane as shown in (A). Results are representative of three independent experiments. (B) HeLa cells were transfected with control or Wapl siRNAs at the indicated concentrations for 48 hrs. Protein extracts were prepared, loaded into 8 % SDS-PAGE gel for and probed with antibodies specific for Wapl and ϒ-tubulin. Results are representative of two independent experiments.

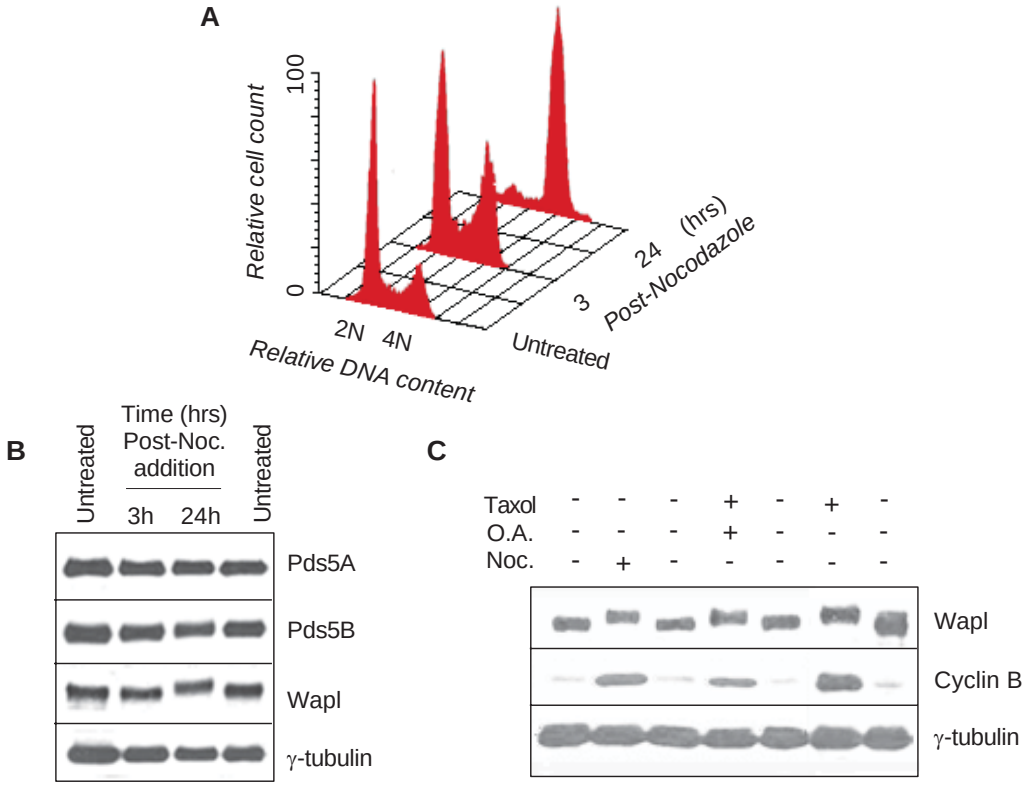

Figure 4.2: Wapl undergoes a mobility shift in mitotic HeLa cell extracts.

HeLa cells were arrested at mitosis by treatment with nocodazole (20 nM) for either 3 hrs or 24 hrs. (A) A FACS profile of propidium iodide-stained nuclei indicates cell cycle arrest at mitosis. (B) Total proteins were extracted using RIPA buffer supplemented with proteinase inhibitors and analysed by Western blot using the indicated antibodies. (C) Mitosis-specific mobility shift of Wapl was determined in HeLa cells arrested with various mitotic blockers. Cells were incubated with or without 20 nM nocodazole for 18 hrs, or a combination of 10 μM Taxol and 0.1 μM okadaic acid for 12 hrs, or 10 μM Taxol only for 18 hrs. Total proteins were extracted and analyzed by Western blot using the indicated antibodies. Result shown is representative of two independent experiments.

4.2.3. The intracellular localization of Wapl is cell-cycle-dependent

The intracellular localization of Wapl protein was assessed at various stages of the HeLa cell cycle. As Scc1, Wapl protein was detectable within the nucleus during interphase, but dissociated from chromatin from prophase to anaphase. Wapl re-associated with chromatin by late telophase (Figure 4.3). Interestingly, the expression level of Wapl protein was slightly elevated during mitosis, followed by destruction of the protein at exit from mitosis as assessed by degradation of cyclin B1 (Figure 4.4). A similar pattern of protein expression was seen with Scc1 (Figure 3.2 on page 62) upon release from aphidicolin block, suggesting that Wapl may also destroyed after mitosis.

4.2.4. Wapl is required for chromosome separation in human cells

In order to test whether Wapl is required for sister chromatid resolution, I used ON-TARGET plus SMARTpool siRNA strategy to specifically deplete Wapl from HeLa cells. Wapl protein was greatly reduced compared to controls following 48 hrs siRNA treatment (Figure 4.5A), while the levels of other cohesin-related proteins such as Pds5A, Pds5B and Scc1 were not affected by siRNA treatment (Figure 4.5B). When chromosome spreads were prepared from Wapl siRNA-treated cells which had been treated with either Taxol (10 μM) or a combination of Taxol (10 μM) and okadaic acid (0.1 μM), I observed a significant increase in the number of nuclei with unresolved chromosomes at the arms and at the centromeric region after the loss of Wapl protein (Taxol, mean ± SD = 31 ± 10 %; n = 100 nuclei; $P < 0.001$; Taxol and okadaic acid, 30 ± 8 %; n = 100 nuclei; $P < 0.001$) compared to control siRNA-treated cells (Taxol, 0.3 ± 0.5 %; n = 100 nuclei; $P < 0.001$; Taxol and okadaic acid, 0.3 ± 0.5 %; n = 100 nuclei; Figure 4.6). This observation was confirmed using single siRNA oligonucleotide-treated cells (see appendix, Figure A. 8). I conclude from these data that Wapl protein is required for chromosome resolution both at the chromosome arms and in the centromeric region.

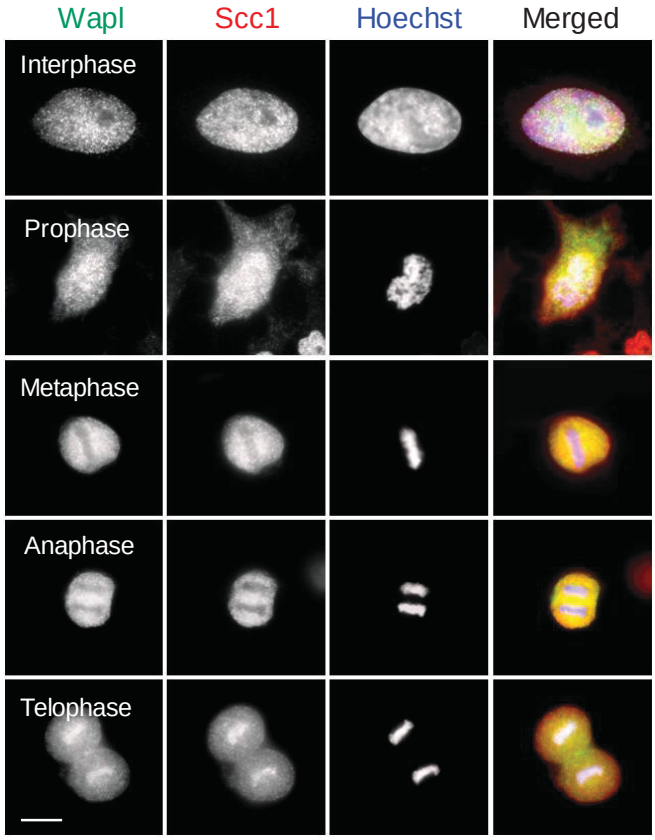

Figure 4.3: The intracellular distribution of Wapl and Scc1 during the cell cycle.

HeLa cells grown on coverslips were fixed with 3.7 % (v/v) formaldehyde and permeabilized with 0.1 % (v/v) Triton X-100. After blocking with 5 % (w/v) BSA, cells were co-stained with antibodies against Wapl (green) and Scc1 (red). DNA was stained with Hoechst 33342 (blue). Merged images are shown (right panel). Scale bar: 8 µm. This figure is representative of three independent experiments.

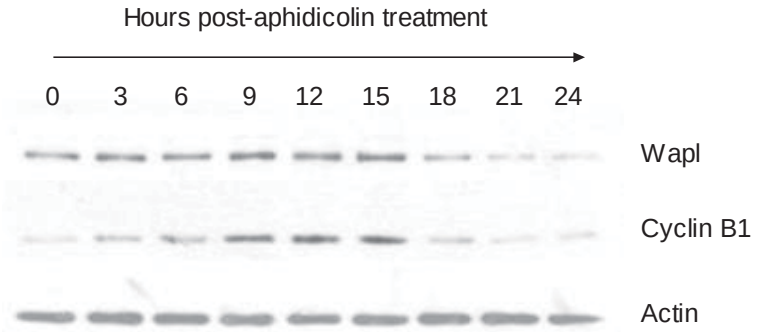

Figure 4.4: Analysis of endogenous Wapl protein levels during the cell cycle.

Asynchronously growing HeLa cells were arrested at the G1/S-phase boundary with 10 µg/ml aphidicolin. After 24 hrs, cells were washed three times with 1 % (w/v) PBS and fresh medium was added. Total protein extracts were prepared at the indicated time points. Wapl, cyclin B1 and ϒ-tubulin protein levels were determined by Western blot using specific antibodies. Results are representative of two independent experiments.

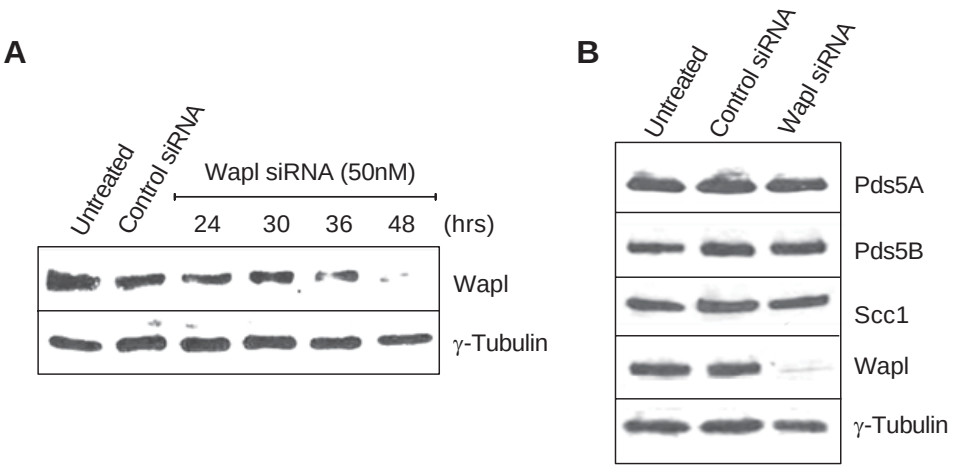

Figure 4.5: Wapl siRNA.

HeLa cells were transfected with either control or a SMARTpool of Wapl siRNA (50 nM) for the times indicated (A) or for 48 hrs (B). Total proteins were extracted using RIPA buffer supplemented with proteinase inhibitors and the cell lysates were analysed by Western blot using the indicated antibodies. This figure is representative of two independent experiments.

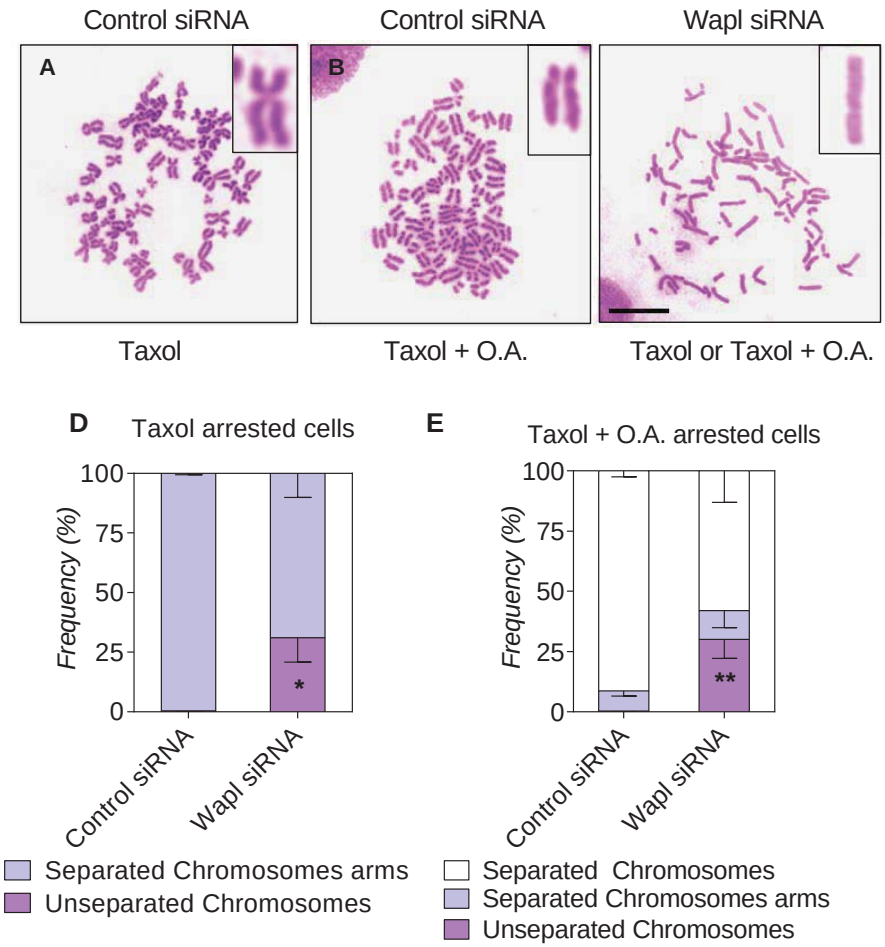

Figure 4.6: Wapl is required for sister chromatid resolution.

Chromosome spreads were prepared from HeLa cells treated with 10 µM Taxol for 18 hrs or 10 µM Taxol and 0.1 µM okadaic acid for 12 hrs in which Wapl was depleted by Wapl siRNAs (50 nM). (A-C) Representative light microscopy images showing the observed differences in morphology; enlarged images are shown in the insets. Scale bar: 8 µm. (D & E) Quantification of the chromosome spreads obtained in (A-C) and classified according to their morphology. At least 100 nuclei were analysed in each of three independent experiments. Means and standard deviations are shown; *$P < 0.005$; **$P < 0.001$. P-values were calculated using two-way ANOVA.

4.2.5. Loss of Wapl induces abnormal mitosis

Forty-eight hours after Wapl siRNA treatment, in contrast with Pds5A and Pds5B siRNA, neither remarkable dead cells floating in the culture medium observed (using light microscopy) nor an increase in the percentage of sub-G1-phase cells were detected by FACS analysis. These results suggests that Wapl loss might not be lethal to the HeLa cells (Figure 4.7A). A validation by Western blot using cleaved caspase-3 and PARP antibody indicated that loss of Wapl did not trigger an apoptotic response in HeLa cells (Figure 4.7B). However, examination by immunofluorescence microscopy revealed an increased number of interphase cells with one or more micronuclei (mean = 21 %) and nuclear buds (mean = 32 %; Figure 4.8Aa and B) in Wapl-depleted cells. Additionally, I could see abnormal chromosome segregation such as chromosomal bridge formation during anaphase and cytokinesis (mean = 24 %; Figure 4.8A, panels b and c, and C; appendix Figure A. 9). However, it is unclear at what stage of the cell cycle the micronuclei were formed. They may have been generated after abnormal chromosome segregation, as remnants of the chromosomal bridge formed during anaphase, as shown in Figure 4.8A, panel c. Furthermore, no prophase/metaphase/anaphase cells were observed, but instead cells undergo abnormal division and having Pds5A, Pds5B and Scc1 stably associated with chromosomes accompanied by a reduction of their levels in the cytoplasmic compartments, in which constriction of the cleavage furrow had advanced considerably and an anaphase bridge had formed (Figure 4.9A and B).

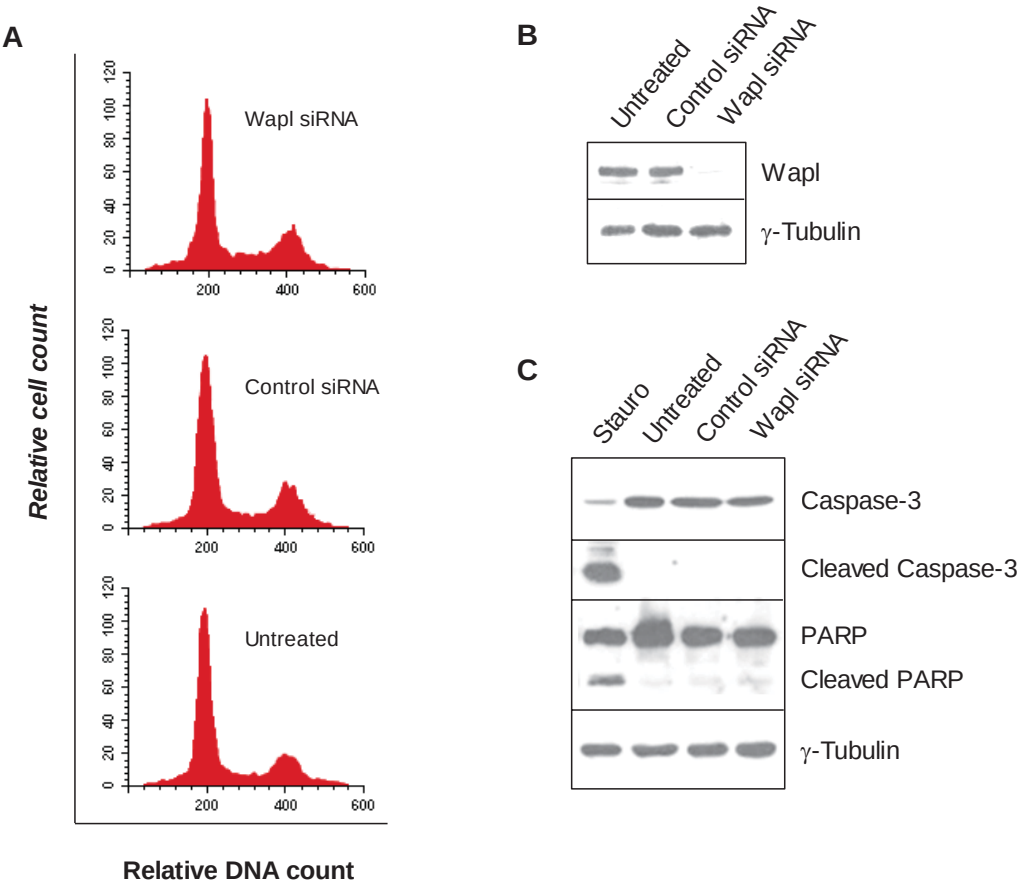

Figure 4.7: Wapl depletion does not affect cell cycle progression.

(A) Profile of propidium iodide-stained HeLa cell nuclei after 48 hrs Wapl siRNA treatment. (B & C) HeLa cells were transfected with either control or a SMARTpool of Wapl siRNA (50 nM) for the 48 hrs and cell lysates were analysed by Western blot using the indicated antibodies. This figure is representative of one experiment.

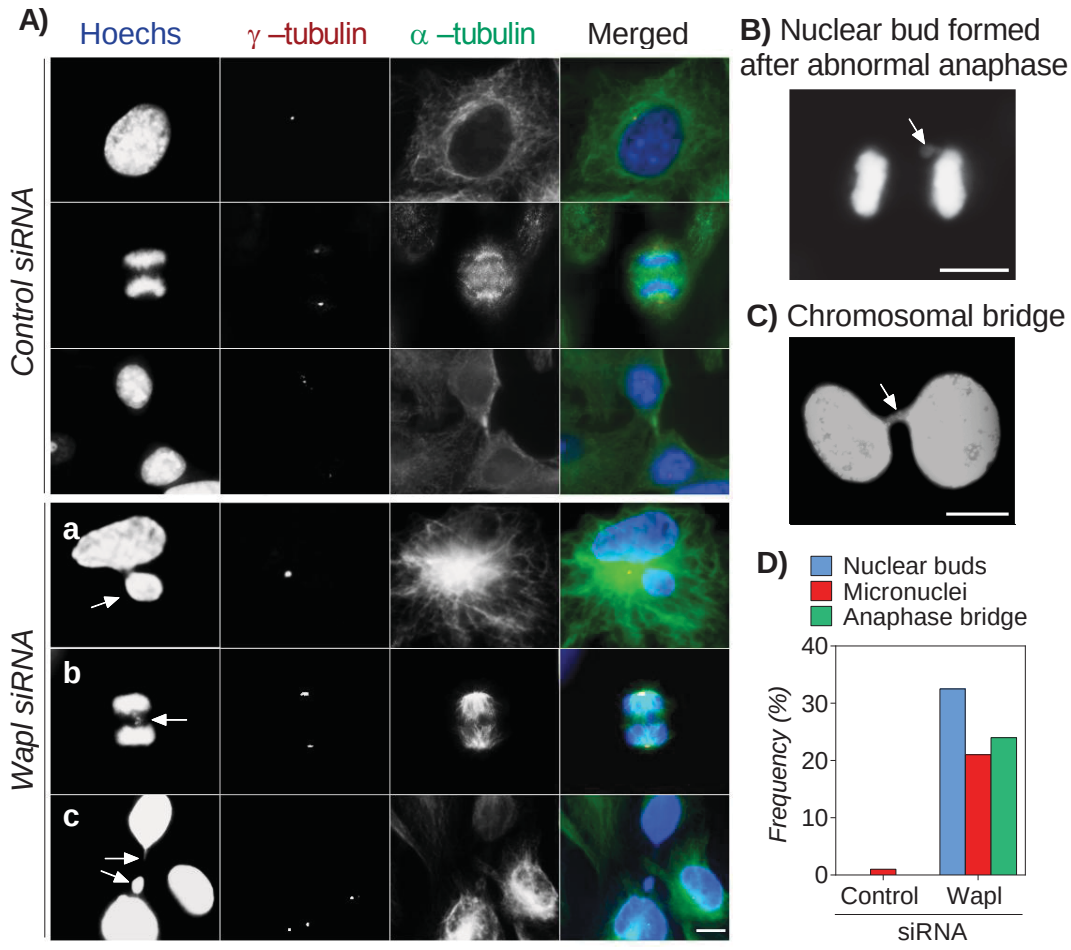

Figure 4.8: Wapl depletion induces an abnormal mitosis.

Representative immunofluorescence images of Wapl-depleted cells. HeLa cells were fixed with -20 °C methanol following 48 hrs Wapl siRNA treatment and co-stained with anti-α-tubulin antibody (green) to visualize the microtubules, anti-ϒ-tubulin antibody (red) to visualize the centrosomes and Hoechst 33342 (blue) to visualize the chromosomes. (B and C) HeLa cells were stained with Hoechst 33342 only. The arrows in (A, panel a, and B) indicate nuclear buds, in (A, panel b, and C) they indicate chromosomal bridge formation and in (A c) they indicate micronuclei and nuclear buds as remnants of chromosomal bridge. Scale bar: 8 µm. (D) Percentage of cells displaying chromosomal bridge, nuclear buds and micronucleation. Two independent experiments were analysed and the mean is shown of measurements from at least 50 cells.

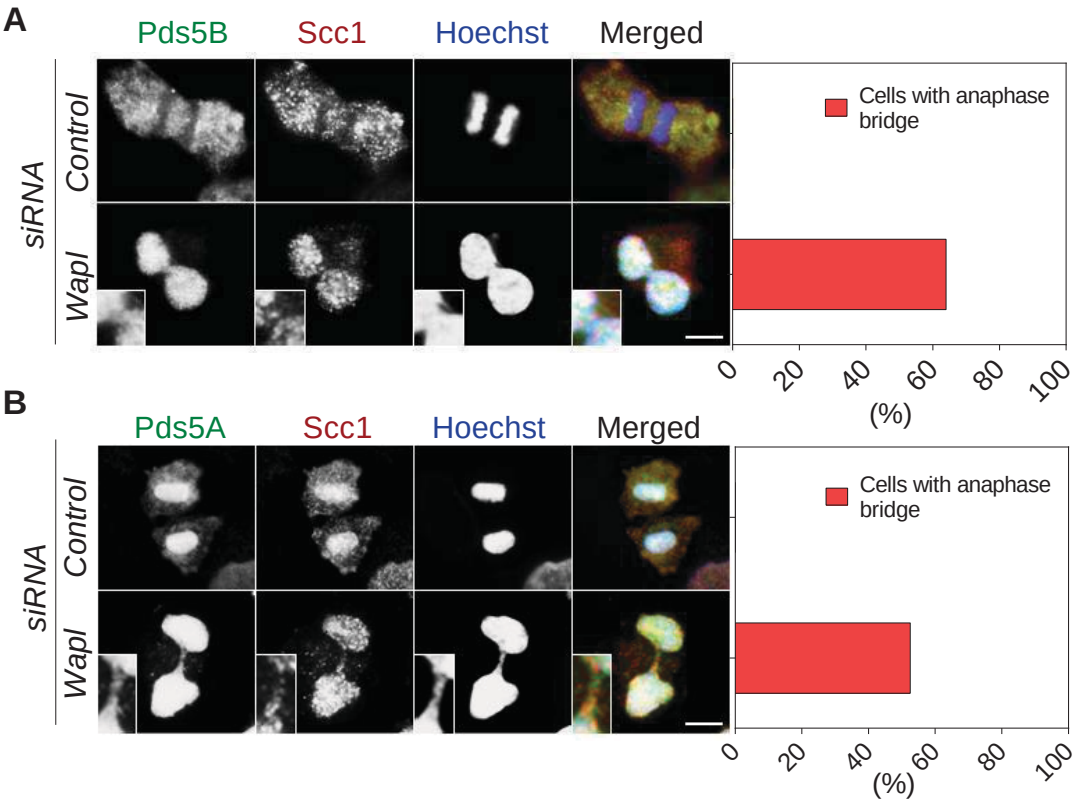

Figure 4.9: Pds5A, Pds5B and Scc1 are stably associated with chromatin in Wapl-depleted cells.

HeLa cells were transfected with either control siRNA (50 nM) or SMARTpool Wapl siRNAs (50 nM). After 48 hrs, cells were fixed with 3.7 % (v/v) formaldehyde and permeabilised with 0.1 % (v/v) Triton X-100. After blocking with 5 % (w/v) BSA, cells were co-stained with Scc1 and either Pds5A or Pds5B antibodies. DNA was stained with Hoechst 33342. Merged images are shown. Scale bar: 8 µm. (A) Upper panel: Control anaphase cell shows normal chromosomes separation with distribiution of Pds5B in the cytoplasmic compartment; lower panel: Abnormal anapase with chromosomal bridge formation and Pds5B is stably associated with chromosomes accompanied by a reduction of its level in the cytoplasmic compartments. (B) Upper panel: Control cell shows normal telophase and localization of Pds5A on chromatin and in the cytoplasmic compartment; lower panel: Abnormal telophase cell with chromosomal bridge formation and Pds5A is stably associated with chromosomes accompanied by a reduction of its level in the cytoplasmic compartments. The percentage of cells displaying abnormal cell division is shown on the right. Two independent experiments were analysed and the mean is shown of measurements from at least 40 cells.

4.2.6. Wapl may be phosphorylated at mitosis

Studies to date have provided no insight into the mechanism by which Wapl regulates cohesin removal at prophase. To address this question, I examined the mobility shift of Wapl protein at various times after release from nocodazole block. The Western blot shown in Figure 4.10 indicates that the Wapl mobility shift occurred only in mitotically arrested cells and was then reduced when the cells completed mitosis after 9 hrs, accompanied by a reduction in the level of Wapl protein. The mobility shift of Wapl during this period suggests that it may be regulated by phosphorylation during mitosis, which has not been previously reported. The decline in Wapl protein expression at the end of mitosis may be due to its degradation, possibly mediated by APC^{cdh1} as a KEN-box is present in the Wapl protein sequence.

4.2.7. Plk1 is a candidate for Wapl phosphorylation at mitosis

Mitosis is a process that is highly regulated by several serine/threonine protein kinases. Plk1 and Aurora B have been the focus of intensive studies because of their strong association with several mitotic events, including their requirement in the prophase pathway (Andrews et al., 2003, Barr et al., 2004). In order to identify the factor potentially responsible for Wapl phosphorylation, I sought to inhibit the function of the mitotic kinases, PlK1 and Aurora B, using their selective inhibitors BI 2536 (Lenart et al., 2007) and ZM 447439 (Gadea and Ruderman, 2005) respectively. For this purpose, I compared the gel mobility shift of Wapl in nocodazole-arrested cells (control) with that of cells treated with a combination of nocodazole and increasing concentrations of either BI 2536 or ZM 447439.

A concentration-dependent reduction of the Wapl gel mobility shift was observed in cells treated with the Plk1 inhibitor, BI 2536, with full efficacy at 0.1 μM (Figure 4.11A), whereas the Aurora B inhibitor, ZM 447439, did not prevent the gel mobility shift of Wapl even at concentration upto 2μM (Figure 4.11B), although ZM 447439 was functionally active as it caused G2/M-phase arrest as anlysed by FACS (Figure 4.11C). These results indicate that Wapl may be a target of Plk1 phosphorylation upon Plk1 activation. I further investigated Wapl localization using immunofluorescence microscopy to assess whether its localization is phosphorylation-dependent. Compared with nocodazole-arrested cells, Wapl was found to be stably associated with unresolved sister chromatids in both BI 2536-arrested cells and in nocodazole plus BI 2536-arrested cells (Figure 4.12A). To confirm this result, I sought to isolate the cytoplasmic and the nuclear fraction (as describe in the material and methods) from HeLa cells being subjected to 10 μg/ml aphidicolin or 20 nM nocodazole in the presence or absence of 1 μM Plk1 inhibitor BI 2536 for 18 hrs. The fractions were obtain is

pure as judged by Western blot with Histone H3 and α-tubulin (Figure 4.12B). Interestingly, Pds5A, Pds5B, Scc1 and Wapl are still present in the chromatin fraction after the inhibition of Plk1 (Figure 4.12B). Since Wapl is required for sister chromatid resolution (Figure 4.6 on page 95), it may also be required for the dissociation of Pds5A, Pds5B and Scc1 from sister chromatids during mitosis. However, the phosphorylation of Wapl or other cohesin core subunits may be a prerequisite.

4.2.8. Removal of Pds5A and cohesin from chromosomes is dependent on Wapl

The results reported on section 4.2.7 lead me to speculate that whether treatment of HeLa cells with the Plk1 inhibitor BI 2536 to prevent Wapl phosphorylation also prevented the phosphorylation of cohesin and Sororin by Plk1 (Zhang et al., 2011). Therefore, the observed phenotype could also result from the inhibition of cohesin or Sororin phosphorylation by Plk1. To address this question, I monitored the intracellular localization of Pds5A and Pds5B after the siRNA depletion of Wapl in mitotically arrested cells. Under this condition Plk1 would still phosphorylate cohesin and Sororin. However, the results of this experiment indicated that Pds5A, Pds5B and Scc1 remained bound to chromatin in the absence of Wapl. Interestingly, I found that both Pds5A and Pds5B remained associated with sister chromatids in both BI 2536-arrested and nocodazole-BI 2536-arrested cells (Figure 4.13). It is likely that cohesin also remained associated with sister chromatids, because the chromosomes remained attached. This result suggests that phosphorylation of cohesin and Sororin by Plk1 may not be sufficient to remove cohesin and Pds5 proteins upon the loss of Wapl.

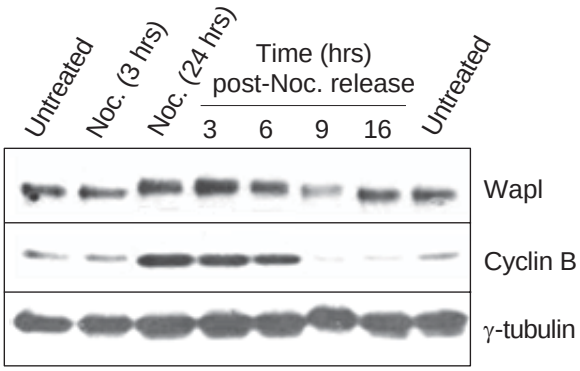

Figure 4.10: Wapl mobility shift is abolished after mitosis.

HeLa cells were treated with 20 nM nocodazole for 3 or 24 hrs. Cells treated for 24 hrs were washed three times with 1 % (v/v) PBS followed by incubation at 37 °C in nocodazole-free medium for 3, 6, 9, 16 hrs. Total proteins were extracted using RIPA buffer supplemented with proteinase inhibitors and 0.1 μM okadaic acid. Wapl, cyclin B1 (as a marker for mitotic cells) and ϒ-tubulin protein levels were analyzed by Western blot. Results are representative of two independent experiments.

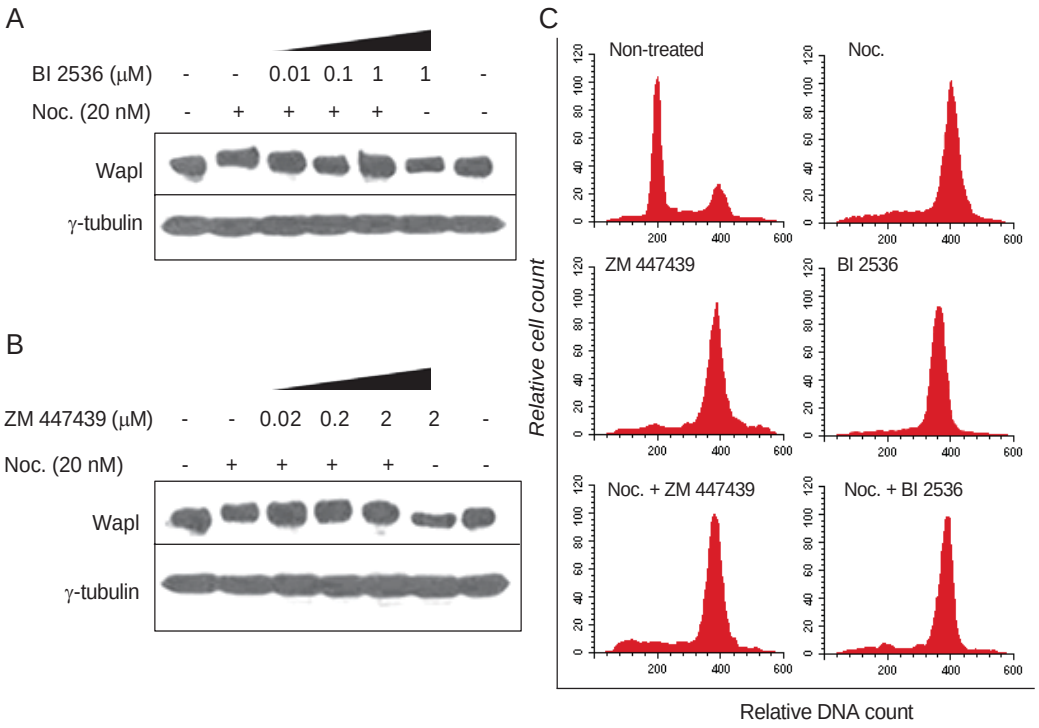

Figure 4.11: Mitosis-specific mobility shift of Wapl is suppressed by inhibition of Plk1.

(A) HeLa cells were incubated either with or without 20 nM nocodazole and either in the presence or absence of the Plk1 inhibitor BI 2536 (0.01, 0.1 and 1 μM) for 18 hrs. Proteins were extracted using RIPA buffer supplemented with proteinase inhibitors and 0.1 μM okadaic acid. Wapl and ϒ-tubulin protein levels were analyzed by Western blot. (B) HeLa cells were incubated either with or without 20 nM nocodazole either in the presence or absence of Aurora B inhibitor, ZM 447439 (0.02, 0.2 and 2 μM). After 18 hrs incubation, proteins were extracted from the cells using RIPA buffer supplemented with proteinase inhibitors and 0.1 μM okadaic acid. Wapl and ϒ-tubulin protein levels were analyzed by Western blot. (C) FACS analysis of propidium iodide-stained nuclei of control cells and cells exposed to 20 nM nocodazole, 0.2 μM ZM 447439, 0.1 μM BI 2536, 20 nM nocodazole + 0.2 μM ZM 447439 and nocodazole + 0.1 μM BI 2536. Results are representative of two independent experiments.

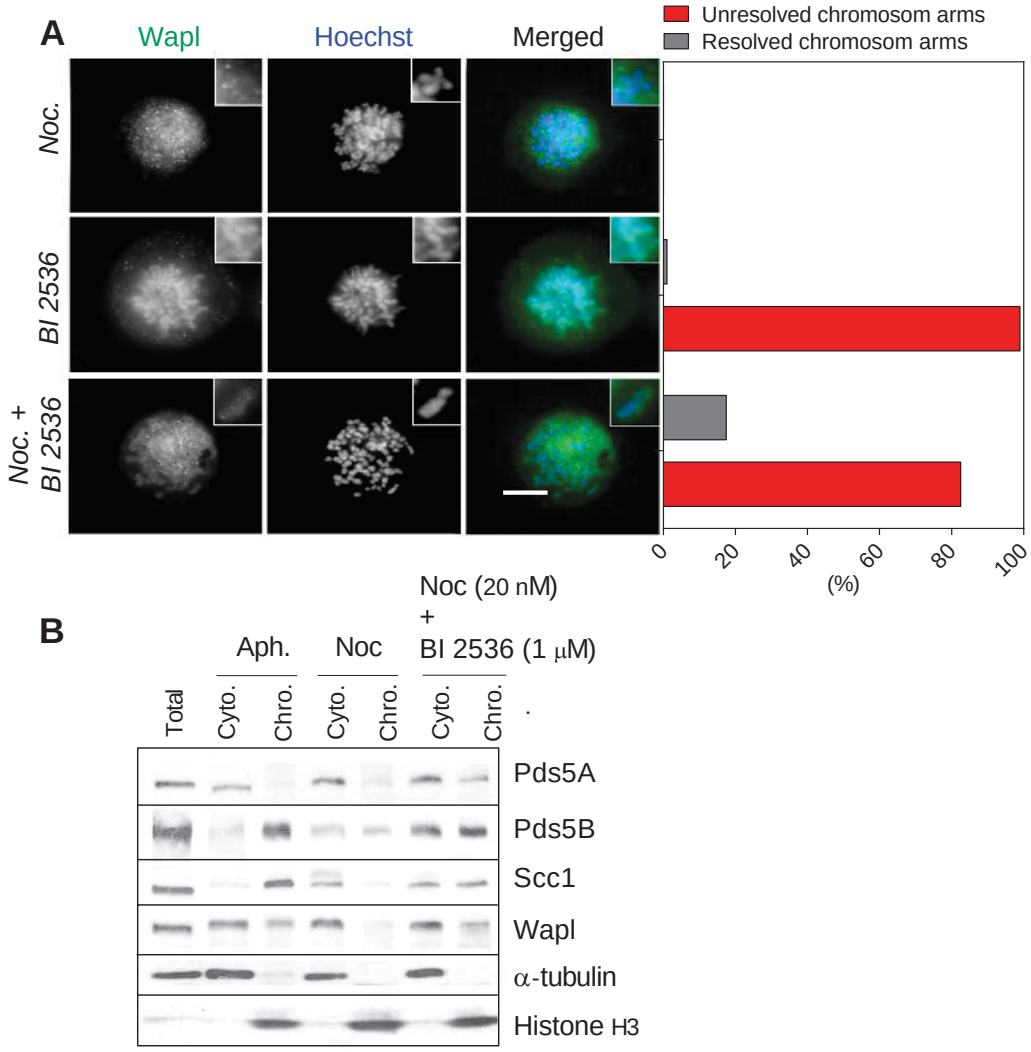

Figure 4.12: Wapl dissociation from chromosomes depends on Plk1.

HeLa cells were incubated with 10 µg/ml aphidicolin or 20 nM nocodazole either in the presence or absence of 1 µM Plk1 inhibitor BI 2536 for 18 hrs Brfor the cells were lysed. The mitotic cells were collected by shake-off and fixed on polylysine coverslips, extracted with a buffer containing Triton X-100 (0.5 % (v/v) Triton X-100, 20 mM HEPES pH 7.4, 3 mM $MgCl_2$, 50 mM NaCl and 300 mM sucrose) for 5 min at 4 °C. The cells were then fixed with 3.7 % (v/v) formaldehyde for 20 min at 4 °C and premeablized with ice-cold 100 % methanol. The cells were then co-stained with the Wapl antibody and Hoechst 33342. (A) Immunofluorescence microscopy images showing the distribution of Wapl chromosomes in prophase cells arrested by treatment with either BI 2536 (1 µM) or a combination of nocodazole (20 nM) and BI 2536 (1 µM). Merged images are shown (right panel). Scale bar: 8 µm. The frequency of unresolved sister chromatids with Wapl on chromosomes is shown on the right of measurements of 100 cells. The histogram represents the mean of two independent experiments. (B) Western blot analysis of cytoplasmic (Cyto) and chromatin (chrom.) fractions using the indicated antibodies. Histone H3 and α-tubulin were used to demonstrate the purity of the chromatin and cytoplasmic fractions, respectively. These results are representative of two independent experiments were conducted.

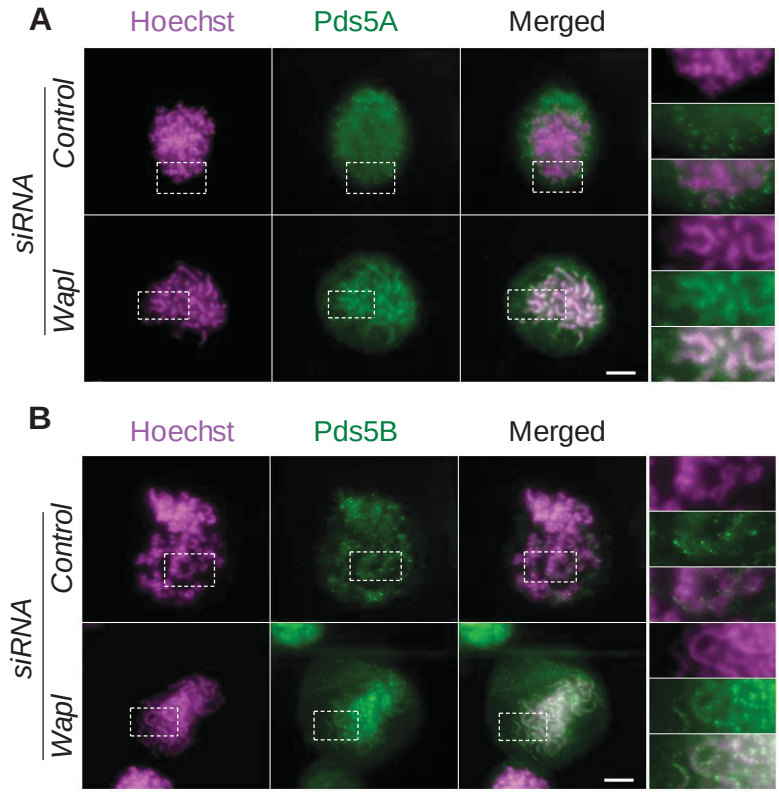

Figure 4.13: Removal of Pds5A and Pds5B proteins from chromatin is dependent on Wapl.

Exponentially growing HeLa cells were transfected with either control siRNA (50 nM) or SMARTpool Wapl siRNAs (50 nM) for 48 hrs. The cells were then treated with nocodazol (20nM) for 18 hrs. The mitotic cells were collected by shake-off and fixed on polylysine coverslips, extracted with a buffer containing Triton X-100 (0.5 % (v/v) Triton X-100, 20 mM HEPES pH 7.4, 3 mM $MgCl_2$, 50 mM NaCl and 300 mM sucrose) for 5 min at 4 °C. The cells were then fixed with 3.7 % (v/v) formaldehyde for 20 min at 4 °C and premeablized with ice-cold 100 % methanol. The cells were then stained with the Pds5A antibody (A) or Pds5B antibody (B). DNA was stained with Hoechst 33342. Merged images are shown (right panel). Scale bar: 5 µm. Magnified views of the boxed regions are shown in order on the right. Three independent experiments were analysed.

4.2.9. Overexpression of Flag-Wapl in HEK 293T cells.

To define and map the possible phosphorylation site in the Wapl sequence, Full length human Wapl was cloned in pLEICS-12 (cloning was performed by Dr. Xiaowen Yang using the In-Fusion technique, Protex, Department of Biochemistry, University of Leicester, www2.le.ac.uk/departments/biochemistry/research-groups/protex, see appendix Figure A. 4 and 5) and overexpressed in HEK 293 cells. 48 hrs after transfection, the lysates were prepared from both the transfected and untransfected HEK 293 cells and subjected to SDS-PAGE and Western blotting with an anti-Flag antibody or immunoprecipitation and colloidal Coomassie Blue staining as described in material and methods. The Western blot results confirm that the Flag-Wapl was expressed and indicate the expected size (Figure 4.14A and B). Further confirmation by immunofluorescence microscopy showed the expression of human Wapl protein in the nucleuse of interphase cells as expected nuclear (Figure 4.14C).

4.2.10. Wapl is associated with cohesin core subunits

To identify Wapl-associated proteins at mitosis, HEK 293 cells were transfected with Flag-Wapl for 48 hrs and synchronised at either G1/S by treatment of 10 µg/ml aphidicolin for 24 hrs or M-phase by treatment of 20 nM nocodazol for 18 hrs. The cells were then lysed and the overexpressed Wapl was immunoprecipitated from the cell extracts using anti-Flag antibody. The immunoprecipitated Flag-Wapl was analysed by SDS-PAGE and Coomassie staining (Figure 4.15), Proteins co-immunoprecipitated with Flag-Wapl were excised from the SDS-PAGE gel and sent to the Protein and Nucleic Acid Chemistry Laboratory (PNACL), University of Leicester, for peptide mass fingerprinting.

4.2.11. Mass spectrometric analysis of Wapl in vivo phosphorylation sites

Previous studies have identified the consensus phosphorylation sites for Plk1 (Nakajima et al., 2003, Barr et al., 2004) and Cdk1 (Nigg, 1993, Harvey et al., 2005). Analysis of human Wapl protein sequences revealed 20 putative Plk1 phosphorylation sites matching the consensus sequence (E/D/Q)-x-(S/T) and only one matching the consensus sequence (E/D)-x-(S/T)Φ-x-(E/D) Φ, where Φ is a hydrophobic amino acid. In addition, I found five putative Cdk1/cyclin B1 phosphorylation sites matching the consensus sequence S/T-P and only one matching the consensus sequence S/T-P-x-K/R. All the predicted plk1 phosphorylation sites are in both C- and N-terminus, whereas the predicted Cdk1/cyclin B1 phosphorylation sites are found in the N-terminus. Plk1 contains two polo-box domain (PBD) in its C-terminus, which is responsible for localizing the catalytic domain in its N-terminus to its substrate by binding to a motif on the substrate itself or a docking protein (Neef et al., 2007, Elia et al., 2003). The Plk1 PBD is known to bind to the consensus motif S(S/T) (P/*X*) (Elia et al., 2003). Further analysis of the

Wapl protein sequence revealed 18 putative PBD binding sites (Figure 4.16). Among these, $ST^{388}P$ is also a Cdk1/cyclin B1 phosphorylation site.

Next, I sought to map the putative phosphorylation sites and to identify Wapl interacting protein using mass spectrometry. To this end, immunoprecipitated Flag-Wapl from HEK 293 which had been synchronized in G1/S or M-phase of the cell cycle was analysed by SDS-PAGE and Coomassie Blue staining (Figure 4.15). Wapl and other bands were excised from the SDS–PAGE gel and sent to the PNACL for peptide mass fingerprinting and phosphopeptide mapping. Liquid chromatography-tandem mass spectrometry (LC-MS/MS) analysis was performed with an LTQ-Orbitrap-Velos-ETD mass spectrometer. Data were searched using Mascot with the Uni-prot Human database, then viewed, filtered and analysed using Scaffold, a visualization program for proteomics data.

I found that only Ser^{221}, a phosphorylation site for Cdk1/cyclin B1, was phosphorylated in a sample prepared from aphidicolin-arrested cells (Table 4.1 and Table 4.2), whereas in samples prepared from mitotically arrested cells, among the 21 putative phosphorylation sites for Plk1, four sites (Ser^{380}, Ser^{904}, Ser^{1069} and Ser^{1076}) were confirmed to be phosphorylated by mass spectrometry analysis; in addition, eleven non-phosphorylated sites were detected and five sites were not identified by mass spectrometry, probably due to poor digestion of the protein (Table 4.3). However, determination of the precise phosphorylation site between the two residues Ser^{68} or Thr^{69} can be ambiguous, because their daughter fragment ions (y and b) were not identified by fragmentation spectrum, although it is definitive that at least one of them was phosphorylated, because the MS/MS fragmentation showed a shift by 80 Da (HPO3 = 80 Da) in mass/charge ratio (m/z) due to peptide modification. In addition, neither of the two could be ruled out, because their positions match the Plk1 consensus sequence (E/D/Q)-x-(S/T).

On the other hand, the mass spectrometry analysis confirmed the phosphorylation of two putative phosphorylation sites for Cdk1/cyclin B1, Ser^{221} and Ser^{226}, and non-phosphorylated sites, Thr^{388}, Ser^{485} and Ser^{1146}, whereas Ser^{549} was not covered by the analysis (Table 4.4; see appendix, Figure A. 10). The mass spectrometry data suggest that Wapl may be a new substrate for both Plk1 and Cdk1/cyclin B1.

4.2.12. Direct phosphorylation of Wapl by Cdk1/cyclin B1 and Plk1 kinases

To confirm whether Wapl is phosphorylated by Cdk1/cyclin B1 and Plk1, I performed an *in vitro* kinase assay using Flag-tagged Wapl immunoprecipitated by anti-Flag antibody from transfected HEK293 cells synchronised in G1/S. The kinase assay was performed using the

methods outlined in section 2.2.3.6 on page 57. Wapl can be phosphorylated by both Cdk1/cyclin B1 and Plk1 (Figure 4.17A). In this assay, Aurora B showed no autophosphorylation with Wapl, whereas the two positive controls, Histone H1 and MBP, were phosphorylated as expected.

Given that Cdk1 cooperates with Plk1 to phosphorylate substrates (Yamaguchi et al., 2005, Zhang et al., 2009b), I speculated that either Cdk1/cyclin B1 or Plk1 requires a priming reaction to facilitate Wapl phosphorylation. To examine this hypothesis, I performed a sequential kinase assay by first using either Cdk1/cyclin B1 or Plk1 to phosphorylate Wapl in the presence of cold ATP, then washing out the kinase or depleting and inhibiting the kinase activity with either Cdk1 inhibitor RO-3306 or Plk1 inhibitor BI 2536 to minimize the incorporation of [ϒ-^{32}P]-ATP by the kinase, finally adding the second kinase to phosphorylate Wapl in the presence of [ϒ-^{32}P]-ATP. In both ways, Cdk1/cyclin B1 and Plk1 phosphorylated Wapl (Figure 4.17B) and the Wapl bands produced by phosphorylation were similar. Taking these results from both *in vitro* kinase assays together, I conclude that Wapl does not require a priming reaction for its phosphorylation.

4.2.13. Phosphorylation of Wapl may enables its interaction with Pds5A

In an attempt to shed light on the function behind Wapl phosphorylation by Plk1 and Cdk1/cyclin B1, I analysed the interaction of Wapl with Pds5A. Having observed that Wapl protein level changed throughout the cell cycle, I decided to immunoprecipitate Pds5A, because the level of Pds5A remains constant throughout the cell cycle and because Wapl interacts preferentially with Pds5A (Kueng et al., 2006). To this end, I prepared cell lysates from HeLa cells synchronized at G1/S by aphidicolin treatment or at mitosis by nocodazole treatment and then released from the block for 3 hrs or 3 and 9 hrs respectively. Alternatively, the lysates were prepared from HeLa cells synchronized at G1/S and released for 1 h before being treated for 18 hrs with either RO-3306 or BI 2536. The lysates were next subjected to Pds5A immunoprecipitation using anti-Pds5A polyclonal and the immunoprecipitates were then resolved by SDS-PAGE and analyzed by immunoblotting (Figure 4.18; appendix Figure A. 11). Anti-Pds5A co-precipitated Scc1 and Wapl with less detectable Wapl in G1/S arrested cells compared to Scc1 (Figure 4.18, lane 9). Three hours after release from aphidicolin block, more Wapl was detectable in this precipitate (Figure 4.18 lane 10); however, it is not clear whether this indicates a direct interaction. During mitosis, however, Wapl is found in a complex with Pds5A and cohesin and undergoes the process of post-translational modification, as judged by the rapid migration of the Wapl band (Figure 4.18 lane 11), followed by the dissociation of Wapl (Figure 4.18 lane 12) and then the dissociation of Scc1

(Figure 4.18 lane 13). This may be because Wapl and Scc1 were degraded after phosphorylation; however, the inhibition of Plk1 and Cdk1 abolish the interaction of Pds5A with Wapl but not with Scc1 (Figure 4.18 lane 14 and 15), suggesting that the phosphorylation of either Wapl, Sororin or both may trigger the interaction between Wapl and Pds5A.

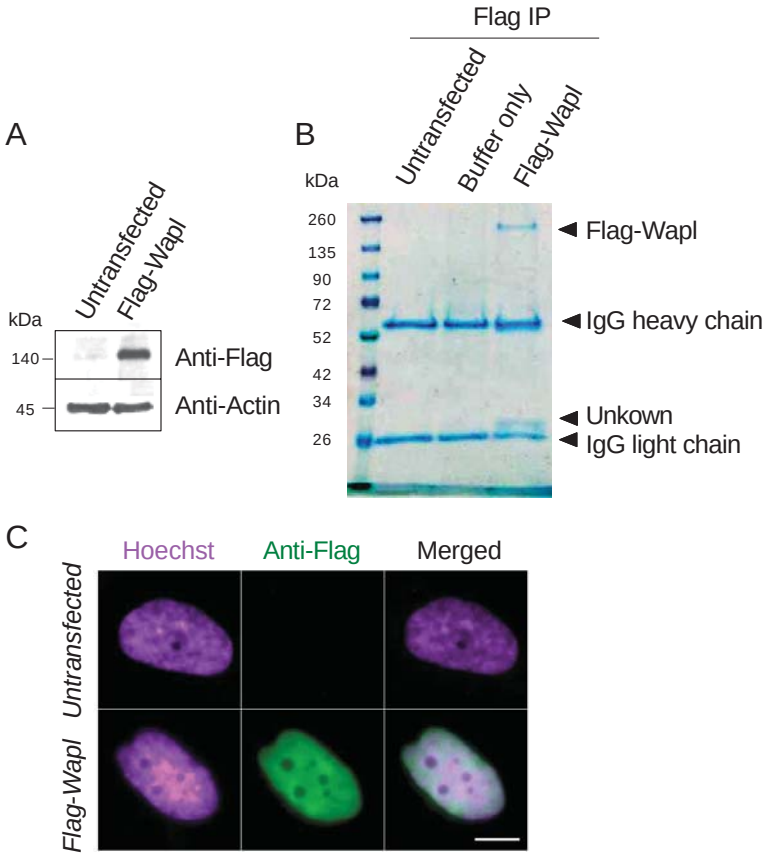

Figure 4.14: Expression and interacellular localization of Flag-tagged Wapl protein.

Flag-tagged Wapl was transiently co-transfected into HEK 293T cells using FuGENE 6 and after 24 hrs the expression was confirmed either by Western blot using anti-Flag antibody (A) or immunoprecipitated with anti-Flag antibody and analysed by SDS-PAGE and colloidal Coomassie staining (B). Untransfected cells and buffer only served as negative control. Molecular wights (kDa) are indicated in the right othe Western blot and the Coomassie gel. (C) Alternatively cells were fixed with 3.7 % (v/v) formaldehyde for 20 min and treated with 0.1 % (v/v) Triton X-100 for 10 min. After blocking with 5 % (w/v) BSA, cells were stained with antibody against Flag (green). DNA was stained with Hoechst 33342 (blue) and then analysed by Immunofluorescence microscopy. Merged images are shown in the right panels. Scale bar: 8 µm. This is representative of two independent experiments.

.

.

A

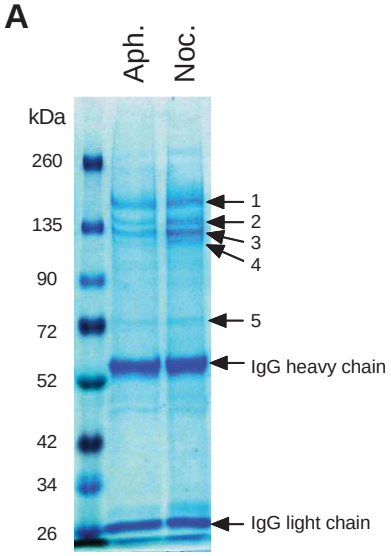

B

No	Protein	Moscot score	Peptide no	Seq Cov (%)
1	Wapl	5399	302	78
2	Smc1A	136	14	14
3	Smc3	95	10	10
4	Rad21 (Scc1)	79	7	13
5	No Seq matched	34	2	12

Figure 4.15: Wapl is associated with the cohesin core subunits.

Flag-tagged Wapl was transiently co-transfected into HEK 293T cells for 24 hrs. The cells were then synchronised at either the G1/S by treatment with aphidicolin (10 µg/ml) or M-phase by treatment with nocodazole (20 nM). The cells were lysed and Wapl was immunoprecipitated using anti-Flag antibody. (A) Wapl-Immunoprecipitates were analysed by SDS-PAGE and Coomassie staining; bands (1-5) were excised from the SDS-PAGE gel and sent to PNACL, University of Leicester, for peptide mass fingerprinting and phosphopeptide mapping. (B) Mass spectrometry analysis of Wapl immunoprecipitates. Mascot scores, number of peptides and sequence coverage are shown. This is representative of one experiment.

Table 4.1: Mapping of Plk1 phosphorylation sites in Wapl by mass spectrometry of aphidicolin-arrested cells.

Phosphosites	*Predicted site*	*Consensus sequence*	*Confirmed by mass spectrometry*	*Peptide sequence*	*Actual Mass*	*Observed (m/z)*
1*	Thr^{39}	ETTF	-			
2*	Ser^{68}	EEST	-			
3*	Thr^{69}	ESTG	-			
4	Ser^{81}	DESL	Not phosphorylated	E.SLPVSSKNLAQVKCSSYSESSE.A	796.39	2,386.13
5	Thr^{127}	EDTV	Not phosphorylated	E.DTVVSDKCFPLE.D	1408.6549	705.3347
6	Thr^{139}	EDTL	Not phosphorylated	E.DTLLGKEKSTNRIVE.D	1701.9264	851.9705
7	Ser^{146}	EKST	Not phosphorylated	E.DTLLGKEKSTNRIVE.D	1701.9264	851.9705
8*	Ser^{156}	DASI	-			
9*	Ser^{190}	DDST	-			
10	Thr^{199}	ETTV	Not phosphorylated	E.TTVASEIKE.T	489.26	976.51
11*	Ser^{330}	ESSK	-			
12	Thr^{359}	DYTV	Not phosphorylated	D.YTVLHPSCLSVCNVTIQDTMERSMDE.F	3084.3671	1029.1296
13	Ser^{380}	ERSMDE	Not phosphorylated	D.YTVLHPSCLSVCNVTIQDTMERSMDE.F	3084.3671	1029.1296
14	Thr^{385}	EFTA	Not phosphorylated	E.FTASTPADLGE.A	1107.5086	554.7616
15*	Ser^{535}	DKSK	-			
16*	Ser^{904}	EDSI	-			
17*	Ser^{1008}	ETSC	-			
18*	Ser^{1013}	DSSI	-			
19	Ser^{1069}	DKSG	Not phosphorylated	E.LIKDAPTTQHDKSGEWQE.T	2082.0033	1042.0089
20*	Ser^{1076}	ETSG	-			
21*	Ser^{1153}	DFSI	-			

*No sequence coverage

Table 4.2: Mapping of Cdk1/cyclin B1 phosphorylation sites in Wapl by mass spectrometry of aphidicolin-arrested cells.

Phosphosites	*Predicted site*	*Consensus sequence*	*Confirmed by mass spectrometry*	*Peptide sequence*	*Actual Mass*	*Observed*
1	Ser^{221}	SP	Phosphorylated	E.TNDTWNSQFGKRPESPSE.I	2158.8966	1080.4556
2	Ser^{226}	SPIK	Not phosphorylated	E.ISPIKGSVRTGLFE.W	1502.8462	501.9560
3	Thr^{388}	TP	Not phosphorylated	E.FTASTPADLGE.A	1107.5086	554.7616
4*	Ser^{485}	SP	-			
5*	Ser^{549}	SP	-			
6	Ser^{1146}	SP	Not phosphorylated	E.SPINVTTVRE.Y	1114.5985	558.3065

*No sequence coverage

Table 4.3: Putative and confirmed Plk1 phosphorylation sites in Wapl by mass spectrometry of nocodazole-arrested HeLa cells.

Phosphosites	*Predicted site*	*Consensus sequence*	*Confirmed by mass spectrometry*	*Peptide sequence*	*Actual Mass*	*Observed (m/z)*
1	Thr^{39}	ETTF	Not phosphorylated	K.WGETTFMAK.L		
2	Ser^{68}	EEST	Might be phosphorylated	K.VEEESTGDPFGFDSDDESLPVSSK.N	2,652.07	1,327.04
3	Thr^{69}	ESTG	Might be phosphorylated	K.VEEESTGDPFGFDSDDESLPVSSK.N	2,652.07	1,327.04
4	Ser^{81}	DE SL	Not phosphorylated	K.VEEESTGDPFGFDSDDESLPVSSK.N	2,652.07	1,327.04
5	Thr^{127}	EDTV	Not phosphorylated	K.ISHVVVEDTVVSDK.C	1525.7996	763.9071
6	Thr^{139}	EDTL	Not phosphorylated	K.CFPLEDTLLGK.E	1291.6485	646.8315
7*	Ser^{146}	EKST	-			
8*	Ser^{156}	DASI	-			
9*	Ser^{190}	DDST	-			
10	Thr^{199}	ETTV	Not phosphorylated	K.KPNAETTVASEIK.E	1386.7359	694.3752
11*	Ser^{330}	ESSK	-			
12	Thr^{359}	DYTV	Not phosphorylated	R.DYTVLHPSCLSVCNVTIQDTMER.S	2737.2537	913.4252
13	Ser^{380}	ERSMDE	Phosphorylated	R.SMDEFTASTPADLGEAGR.L	1,933.78	967.90
14	Thr^{385}	EFTA	Not phosphorylated	R.SMDEFTASTPADLGEAGR.L	1,933.78	967.90
15*	Ser^{535}	DKSK	-			
16	Ser^{904}	EDSI	Phosphorylated	R.AEDSICLADSK.P	1,287.51	644.76
17	Ser^{1008}	ETSC	Not phosphorylated	R.HCLVNMETSCSFDSSICSGEGDDSLR.I	2978.1795	993.7338
18	Ser^{1013}	DSSI	Not phosphorylated	R.HCLVNMETSCSFDSSICSGEGDDSLR.I	2978.1795	993.7338
19	Ser^{1069}	DKSG	Phosphorylated	K.DAPTTQHDKSGEWQETSGEIQWVSTEK.T	3,153.32	1,052.13
20	Ser^{1076}	ETSG	Phosphorylated	K.DAPTTQHDKSGEWQETSGEIQWVSTEK.T	3,233.32	1,078.78
21	Ser^{1153}	DFSI	Not phosphorylated	R.EYLPEGDFSIMTEMLK.K	1917.8755	959.9450

*No sequence coverage

Table 4.4: Putative and confirmed Cdk1/cyclin B1 phosphorylation sites in Wapl by mass spectrometry of nocodazole-arrested HeLa cells.

Phosphosites	*Predicted site*	*Consensus sequence*	*Confirmed by mass spectrometry*	*Peptide sequence*	*Actual Mass*	*Observed*
1	Ser^{221}	SP	Phosphorylated	E.TNDTWNSQFGKRPESPSE.I	2158.8963	1080.4554
2	Ser^{226}	SPIK	Phosphorylated	K.RPESPSEISPIK.G	1418.6806	473.9008
3	Thr^{388}	TP	Not phosphorylated	R.SMDEFTASTPADLGEAGR.L	1933.7755	967.8950
4	Ser^{485}	SP	Not phosphorylated	K.TAPSPSLQPPPES…GVPESVK.K	4609.0715	1153.2751
5*	Ser^{549}	SP	-			
6	Ser^{1146}	SP	Not phosphorylated	K.HMEDCIVASYTALLLGCLCQESPINVTTVR.E	3449.6519	1150.8912

*No sequence coverage

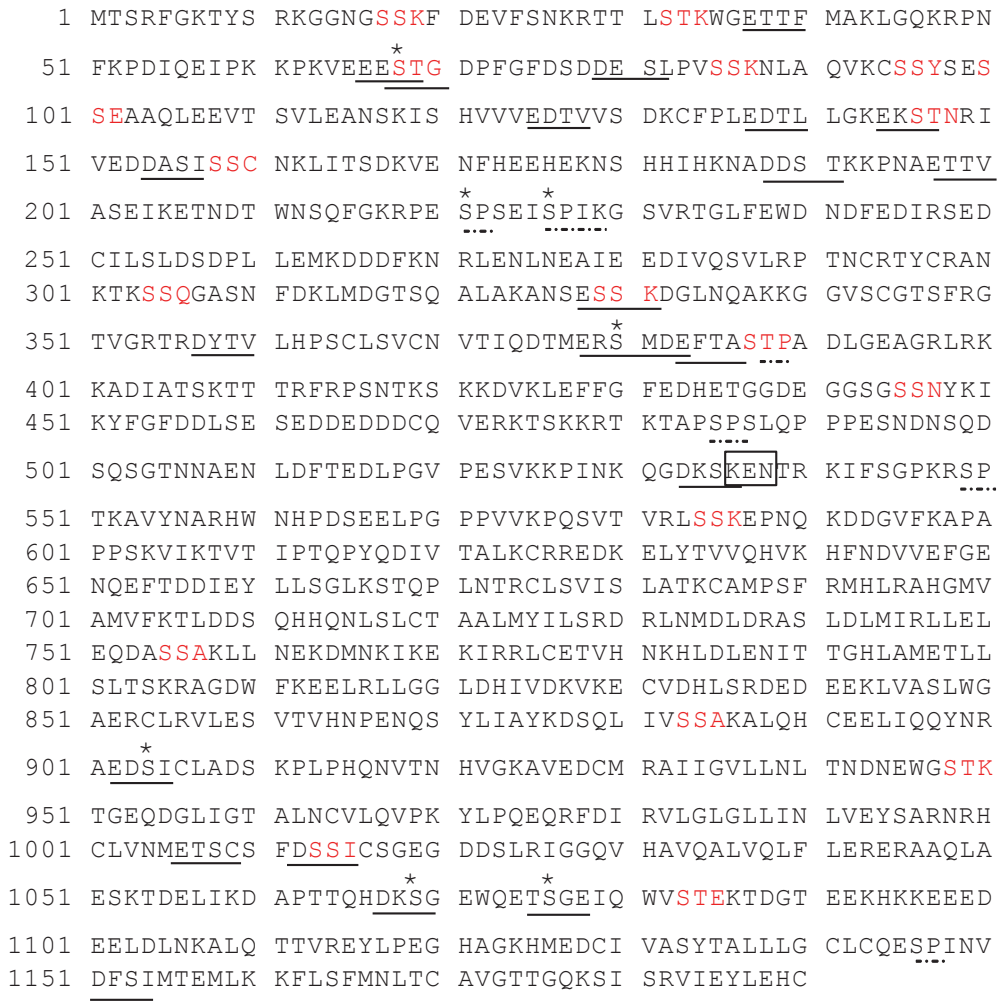

Figure 4.16: Putative PBD binding motifs in human Wapl.

The red letters indicate the putative PBD binding motifs. The phosphorylation sites that have been confirmed by mass spectrometry are labelled with *. The solid lines (—) underneath the letters show the putative Plk1 phosphorylation sites, whereas the dashed lines (-------) show the Cdk1/cyclin B1 phosphorylation sites. The box shows the KEN box.

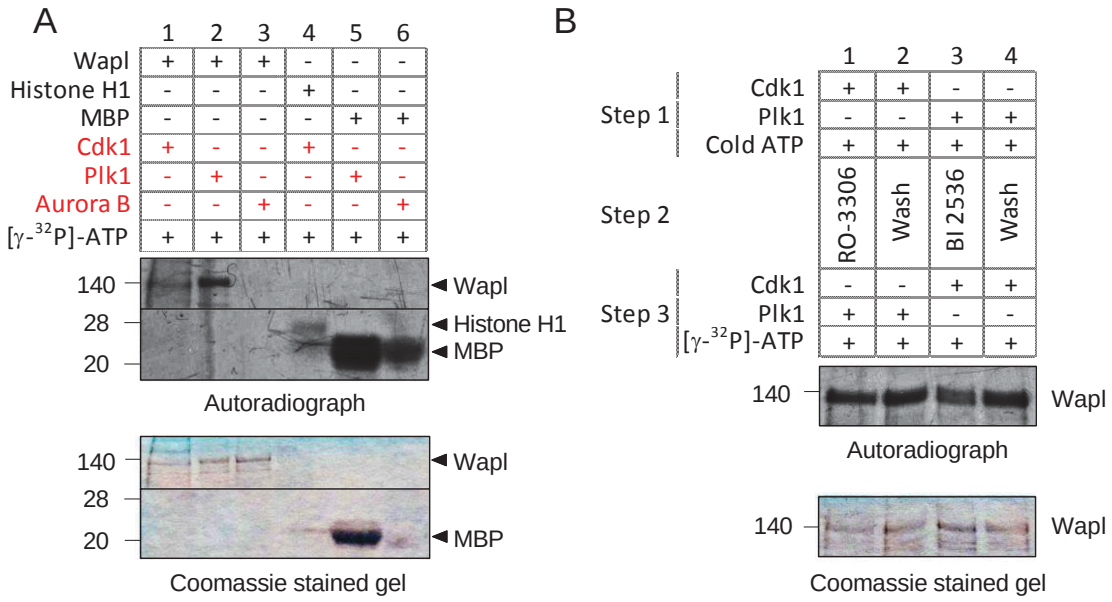

Figure 4.17: Phosphorylation of Wapl by Cdk1 and Plk1 using *in vitro* kinase assay.

HEK 293 cells were transfected with Flag-tagged Wapl for 48 hrs. Cells were then arrested at G1/S by treatment with 10 µg/ml aphidicolin for 24 hrs. The cells were then lysed and Wapl was immunoprecipitated from the cell lysates using an anti-Flag antibody. The immunoprecipitated Flag-tagged Wapl was then used as a substrate for *in vitro* kinase assay. (A) Lanes 1-3; Wapl was used as a substrate for Cdk1/cyclin B1, Plk1 and Aurora B respectively in the presence of [ϒ-^{32}P]-ATP. Lanes 4-6; Histone H1 was used as positive control for Cdk1/cyclin B1 and MBP and was used as positive control for both Plk1 and Aurora B. Samples were analysed by 10 % SDS-PAGE and Coomassie staining and dried for autoradiography. (B) Sequential kinase assay for immunoprecipitated Wapl. Lanes 1 and 2; Wapl was first phosphorylated by Cdk1/cyclin B1 with cold ATP (Step 1), then Cdk1/cyclin B1 was inhibited by adding RO-3306 (0.1 µg/µl) or removed by washing the beads (Step 2) before Plk1 and [ϒ-^{32}P]-ATP were added to phosphorylate Wapl (Step 3). Lanes 3 and 4; Wapl was first phosphorylated by Plk1 with cold ATP (Step 1), then Plk1 was inhibited by adding BI 2536 (1 µM) or removed by washing the beads (Step 2) before Cdk1/cyclin B1 and [ϒ-^{32}P]-ATP were added to phosphorylate Wapl. Samples were analysed by 10 % SDS-PAGE and Coomassie Blue staining. The gel was then dried for autoradiography.

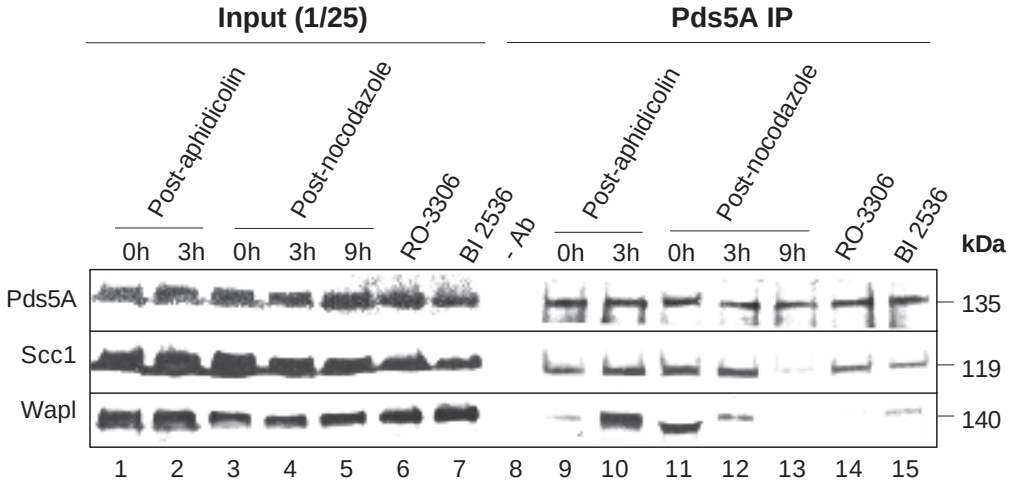

Figure 4.18: Wapl co-immunoprecipitates with Pds5A.

HeLa cells were synchronised at either the G1/S by treatment with 10 µg/ml aphidicolin for 24 hrs or at M-phase by treatment with nocodazole (20 nM). The cells were then released for the indicated time. Alternatively HeLa cells were synchronized at G1/S and released for 1 h before being treated for 18 hrs with either RO-3306 or BI 2536. The cells were then lysed and the total extract (combination of soluble and chromatin associated proteins) were prepared before being subjected to Pds5A immunoprecipitation using an anti-Pds5A antibody. The immunoprecipitates (lanes 9–15) along with input (lanes 1–7) were analysed by SDS-PAGE and Western blotting using Pds5A, Scc1 and Wapl antibodies. Asynchronous HeLa cells plus beads and without antibody (–Ab) was used as negative control for IP. This is representative of one experiment.

4.3. Discussion

Recent studies have demonstrated that Wapl is a cohesin-binding protein that regulates sister chromatid resolution (Gandhi et al., 2006, Kueng et al., 2006). The present study found that Wapl exhibited a localization pattern reminiscent of the localization of Pds5A and cohesin (Figure 4.3 on page 92). In contrast with a previous report showing that the total level of Wapl protein was constant throughout the cell cycle (Gandhi et al., 2006), the present study has found that the level of Wapl protein was slightly elevated during mitosis, followed by a reduction at exit from mitosis (Figure 4.4 on page 93). The reduction of Wapl protein expression may be due to degradation of the protein, as a KEN-box is present in the Wapl protein sequence, suggesting that Wapl is required during mitosis to regulate cohesin removal at prophase, but it may not be required after mitosis.

Depletion of Wapl by siRNA from HeLa cells prevented chromosome separation, as judged by the quantification of the chromosome spreads in Figure 4.6 on page 95. This is consistent with previous findings that Wapl promotes the release of cohesin from chromosomes during mitosis (Gandhi et al., 2006, Shintomi and Hirano, 2009). Unlike Pds5, Wapl seems not to be involved in DNA damage response, because Wapl knockdown did not influence any defect in cell cycle progression or induction of apoptosis (Figure 4.7 on page 97). As a consequence, cells exhibit abnormal chromosome separation accompanied by chromosomal bridge formation. It may be that those cells failed to progress to prophase and Wapl seems to be an important factor that is required for proper prophase progression and for the removal of Pds5A, Pds5B and Scc1, because I observed that in the absence of Wapl these three proteins were still associated with chromosomes when the cells underwent division. The presence of of Pds5A, Pds5B and Scc1 on chromatin at prophase may have promoted the formation of an anaphase bridge, because cohesion was maintained between the sister chromatids. However, how the micronuclei in Wapl-depleted cells are formed is still unclear. It is most likely that the micronuclei are remnants of the chromosomal bridge formed during anaphase after the loss of Wapl.

Budding yeast depleted of Wapl exhibits cohesion defects and impaired loading of cohesin onto chromosomes (Rolef Ben-Shahar et al., 2008, Rowland et al., 2009, Sutani et al., 2009), whereas fission yeast depleted of Wapl has no effect on the establishment and maintenance of SCC (Feytout et al., 2011). At first glance, the phenotypes observed in budding and fission yeast are different from the defect observed in *Xenopus* egg extracts (Shintomi and Hirano, 2009) and in HeLa cells depleted of Wapl (this study). The FGF motifs present at the N-terminus of Wapl are functionally important, because they facilitate the interaction of Wapl

with Pds5 proteins and the cohesin subunits SA1 and Scc1. Mutations in the FGF motifs of Wapl prevent its interaction with Pds5, SA1 or Scc1 and the resolution of sister chromatids (Shintomi and Hirano, 2009). Consistent with this, I have demonstrated that in HeLa cells, Smc1, Smc3, Scc1 and Pds5A were co-immunoprecipitated with Wapl. Since the Wapl orthologs in budding and fission yeast lack the FGF motifs (Figure 1.7 on page 28), it may be that Wapl is not an essential protein in these organisms, whereas in the vertebrates, Wapl may have gained the ability to interact with cohesin and Pds5 in a more efficient way to release cohesin during mitosis. Therefore, the function of Wapl seems to differ substantially among different organisms.

In this study, the mobility shift of the Wapl band on Western blots from mitotic cell lysates is considered to be a major indicator of the post-translational modification of Wapl by phosphorylation. Plk1 and Aurora B are thought to be strongly associated with several mitotic events, including their requirement in the prophase pathway (Andrews et al., 2003, Barr et al., 2004). As a first attempt to identify the mitotic kinases responsible for Wapl phosphorylation, I have provided evidence that following the inhibition of the function of PlK1 using its selective inhibitor, BI 2536, the gel mobility shift of Wapl was reduced, whereas inhibition of the function of Aurora B did not have the same effect, suggesting that Wapl may be a new target of Plk1.

A comparison of my results with the observation that BI 2536 suppresses cohesin release from chromosomes (Lenart et al., 2007) indicates strongly that Wapl dissociation from chromosomes is Plk1-dependent phosphorylation. Wapl was found to be stably associated with the mitotic chromatin after the inhibition of Plk1 and the chromosomes remained attached (Figure 4.12A on page 104). Moreover, the Pds5 proteins, Scc1 and Wapl were still present in the mitotic chromatin fraction after the inhibition of Plk1 (Figure 4.12B on page 104). Because these results did not exclude the possibility that the inhibition of cohesin or Sororin phosphorylation by Plk1 or Cdk1 may lead to similar phenotypes, I sought to maintain phosphorylation of these proteins upon the loss of Wapl. Interestingly, the results obtained, allowed me to suggest that phosphorylation of cohesin or Sororin by Plk1 or Cdk1 does not rescue the phenotype caused by the loss of Wapl, because the Pds5 proteins were detected on the chromosomes in mitotically-arrested cells and the sister chromatids remained attached (Figure 4.13 on page 105). This suggests that Plk1 acts upstream of the removal of Pds5A, Scc1 and Wapl from chromosomes at mitosis, which could be thruogh the phosphorylation of Scc1, Sororin and Wapl. However, it remains to be determined whether mutations in the Plk1 phosphorylation sites of Wapl also lead to sister chromatid non-disjunction.

The data in the present study demonstrate that Wapl is substrate for Cdk1/cyclin B1 and Plk1. Analysis of the Wapl protein sequence for consensus motifs with potential Plk1 and Cdk1/cyclin B1 phosphorylation indicates that there are 21 putative Plk1 phosphorylation sites and six putative Cdk1/cyclin B1 phosphorylation sites. Only four putative Plk1 phosphorylation sites (Ser^{380}, Ser^{904}, Ser^{1069} and Ser^{1076}), one ambiguous site (Ser^{68} or Thr^{69}) and two putative Cdk1/cyclin B1 phosphorylation sites were confirmed by mass spectrometric analysis in this study, suggesting that Wapl is a kinase-regulated protein. Most known functions of Plk1 are dependent on the PBD present on its C-terminus. The PBD of Plk1 binds to substrates previously phosphorylated (primed), often by Cdk1/cyclin B1 or by Plk1 itself (Elia et al., 2003, Lowery et al., 2007, Liu et al., 2012). It has also been reported that the PBD is responsible for localizing the N-terminal catalytic domain of Plk1 to its substrate by binding to a motif on the substrate itself or a docking protein (Elia et al., 2003, Neef et al., 2007). Accordingly, I found 18 putative PBD binding sites on Wapl (Figure 4.16 on page 116). Among these, $ST^{388}P$ is also a Cdk1/cyclin B1 phosphorylation site. However, it is still unknown which PBD binding sites on Wapl have the potential for Plk1 interaction with Wapl. Using an *in vitro* kinase assay, I demonstrated that Wapl is directly phosphorylated by Plk1 and Cdk1/cyclin B1, suggesting that phosphorylation of Wapl by Plk1 does not require the PBD binding motif on Wapl to be previously phosphorylated by Cdk1/cyclin B1.

It has been shown previously that Plk1 can phosphorylate Scc1 and SA1/SA2 (Sumara et al., 2002), although Plk1 contributes to cohesin dissociation from chromosome arms only after SA2 phosphorylation (Hauf et al., 2005). However, no PBD binding site has been found on SA2 or other cohesin core subunits; therefore, it has been suggested that Sororin acts as a docking protein and recruits Plk1 to phosphorylate SA2 during prophase (Zhang et al., 2011). I can speculate similarly that Wapl may also act as a docking protein to facilitate SA2 and Sororin phosphorylation by Plk1, which is essential for the dissociation of cohesin from the chromosome arms at prophase. This hypothesis is supported by the observation that Wapl is found in a complex with the cohesin core subunits Smc1, Smc3 and Scc1 (Figure 4.15B on page 111).

My co-immunoprecipitation experiment shows that the inhibition of Plk1 and Cdk1/cyclin B1 prevented the interaction between Wapl and Pds5A, while conversely, the interaction between Pds5A and cohesin was not prevented after the inhibition of Plk1 and Cdk1/cyclin B1, although I was unable to provide evidence of a direct interaction. Furthermore, I cannot conclude that Wapl phosphorylation enables the Wapl-Pds5A interaction, because it may be that the phosphorylation of both Wapl and Sororin is a key step in enabling Wapl-Pds5A interaction.

Given that Plk1 is essential for the removal of sister chromatid arm cohesion (Sumara et al., 2002), it will be particularly important to investigate the phenotypic results of mutating these phosphorylation sites on Wapl and to shed light on the function behind Wapl phosphorylation by Plk1 or Cdk1/cyclin B1. I can speculate that mutating the PBD binding motif on Wapl may abolish its interaction with Plk1 and Wapl phosphorylation *in vitro*. However, *in vivo*, Sororin may rescue the phenotype caused by disrupting the PBD binding motif of Wapl and this is possible only if Sororin is bound to Wapl at mitosis, because in humans, the PBD of Plk1 also interacts with Sororin via its $ST^{159}P$ consensus motif after the T^{159} is phosphorylated by Cdk1/cyclin B1 (Zhang et al., 2011). Therefore, PBD may interact with Sororin to allow the Plk1 catalytic domain to phosphorylate Wapl.

Based on my data it is, therefore, likely that there is a link between Wapl phosphorylation and its interaction with Wapl's partner Pds5 in regulating cohesin removal. For instance, phosphorylation of Wapl (and perhaps Sororin) may release Wapl from its inhibition, enabling its interaction with Pds5 via its FGF motifs. These conserved motifs at the N-terminus of Wapl are known to be important for the interaction of Wapl with Pds5 and the cohesin subunit SA1 (Shintomi and Hirano, 2009) and subsequently for conformational changes of the cohesin complex to dissociate cohesin from prophase chromosomes.

Chapter 5

Time-lapse imaging of the HeLa cells following depletion of Pds5 or Wapl

5.1. Introduction

Given the sister chromatid resolution defects observed in Pds5 and Wapl-depleted cells, we reasoned that Pds5 and Wapl might be required to ensure the normal fidelity of sister chromatid resolution during mitosis. The data obtained from metaphase chromosome spreads suggest that when Pds5A, Pds5B or Wapl proteins were depleted, they may have caused a cell cycle arrest at metaphase, because these cells were unable to segregate their chromosomes properly during anaphase, or because those chromosomes failed to align properly at the metaphase plate. Furthermore, by examining the fixed cells, we observed an increase in the frequency of micronuclei formation in Pds5-depleted cells and increased frequency of chromosomal bridge formation in Wapl-depleted cells, a hallmark of aneuploidy (Heddle, 1973, Eastmond and Tucker, 1989).

Aneuploidy is often caused by a defect in chromosome segregation through the gain and/or loss of chromosomes in a cell, thereby paving the way for malignant growth and cancer (Griffin, 1996). Thus, equal and accurate chromosome segregation is important to maintain genome stability. Cells have evolved elaborate control mechanisms that ensure the accurate segregation of chromosomes during cell division. From yeast to humans, the sister chromatids of replicated chromosomes are paired from their synthesis during S-phase until their segregation during anaphase. This sister chromatid cohesion is essential for equal distribution of the genetic material into two daughters (Nasmyth, 2001). Defects in SCC and separation could potentially cause the formation of cells with abnormal ploidy, such as aneuploidy or tetraploidy (Mayer et al., 2001, Hauf et al., 2001, Hayashi and Karlseder, 2013). Tetraploid cells are generated when cells exit mitosis without undergoing cytokinesis. They are unstable compared with their diploid counterparts and frequently become aneuploid upon continued cell division (Hayashi and Karlseder, 2013).

In vertebrates, most cohesin is removed from chromosome arms by a mechanism that depends neither on the separase pathway nor on cleavage of the human ortholog of Scc1 (Sumara et al., 2000). A small amount of Scc1 remains in the centromeric regions until it is cleaved during metaphase by separase, following its activation by anaphase-promoting complex (APC/C), which allows the transition to anaphase (Rivera and Losada, 2009). Mutation of the separase cleavage sites abolished Scc1 cleavage by separase *in vitro* and revealed an increased frequency of anaphase bridges, micronuclei and multiple nuclei in HeLa cells (Hauf et al., 2001). Identical results were observed after depletion of separase (Chestukhin et al., 2003), suggesting that this is a direct effect of failing to cleave cohesin and the presence of unseparated sister chromatids.

In this study, I directly characterized the roles of the cohesin regulators Pds5 and Wapl during mitosis and found that knocking down these proteins prevented cohesin removal from mitotic chromosomes and increased the frequency of mitotic abnormalities. However, this does not provide a full picture of this dynamic process. Furthermore, it is not clear whether cells depleted of Pds5 or Wapl are sensitive to mitotic arrest by the spindle assembly checkpoint. To address these points, I monitored the separation of mitotic chromosomes after the depletion of Pds5 and Wapl using time-lapse confocal microscopy.

5.2. Results

Prior to performing the time-lapse imaging experiments using HeLa cells that stably express mCherry-histone H2B and α-tubulin-EGFP (provided by Prof. Andrew Fry's Lab, University of Leicester). I first sought to examine HeLa cell cycle of control untreated cells in order to optimize conditions such as temperature stability, CO_2, humidity and other critical parameters such as the loss of focus of the cells during mitosis (during mitosis there is rounding of cells). However, after performing the live cell imaging experiment, I found that cells were very likely to grow on top of each other after cell division which made it hard to observe cellular details.

Next, I tried a new batch of HeLa cells that stably express mCherry-histone H2B and α-tubulin-EGFP (again provided by Prof. Andrew Fry's Lab, University of Leicester). I found that the new cells grew in dispersed groups as single cells on the tissue culture plate after 24 hrs after seeding and displayed a distinct morphological shape. Therefore I examined the control untreated cells to estimate the time for cells to complete mitosis. However, some problems were still encountered when imaging the cells. This included cell confluence and cell death when imaging, because frequent imaging every 5 min over a long time (18 – 24 hrs) resulted in cell damage via the laser and the cells failed to divide. Therefore I increased the time intervals between images from 5 min to 8 min.

After 3 months of optimization, I was able to achieve the optimum condition for live-cell imaging. First, siRNA and Western blotting was performed in this cell line to determine if the level of Pds5A, Pds5B and Wapl could be depleted in the same manner as described for the normal HeLa cells. The level of Mad2, the regulator of the spindle assembly checkpoint (SAC), was not affected by the siRNA treatment (Figure 5.1). After that, the time-lapse imaging experiments were carried out to monitor the mitotic defects upon loss of either Pds5A, Pds5B or Wapl, and to determine whether depletion of these proteins increased sensitive of the cells to mitotic arrest by the spindle assembly checkpoint. This might also reveal at what stage of the cell cycle the micronuclei and multiple nuclei were formed.

The time-lapse images of cells progressing through mitosis revealed that the average duration of mitosis (from prophase until completion of cytokinesis) was increased after the loss of Pds5A, Pds5B or Wapl proteins compared with control siRNA-treated cells. The control cells had completed mitosis within 96 min ± 35 min (mean ± SD) (Figure 5.2C) or 94 min (Figure 5.3B). In comparison, cells depleted of Pds5A, Pds5B or Wapl required 189 min ± 77 min, 159 min ± 67 min and 132 min, respectively, (mean ± SD), to complete mitosis. However, a number of arrested cells became apoptotic (mean ± SD = 64 % ± 19 %, $P < 0.01$

for Pds5A siRNA; 45 % ± 26 %, *P < 0.01* for Pds5B siRNA and 54 % for Wapl siRNA), as indicated by chromatin condensation and nuclear fragmentation (Figure 5.2A, middle panel, and Figure 5.3A, middle panel). This may have been a result of the activation of the spindle assembly checkpoint as assessed by the localization of Mad2 at kinetochores in Pds5A-depleted cells (Figure 5.4).

During the course of time-lapse observation of cells depleted of Pds5A and Pds5B, the most common defect was the formation of micronuclei, which appeared after mitosis. However, no micronuclei formation was oserved in control cells. This abnormality was more frequent (mean ± SD = 19 % ± 10 %; *P < 0.01*) in cells depleted of Pds5B compared to Pds5A-depleted cells (mean ± SD = 8 % ± 6.73 %; *P < 0.01*). Furthermore, a few cells (mean ± SD = 7 % ± 5.35 %) in which Pds5B was depleted initiated tetraploid mitosis without being able to complete cytokinesis and generated abnormal nuclei or multinucleated cells (Figure 5.2A, lower panel and D). The difference in frequency of mitotic defects between cells depleted of Pds5A and Pds5B proteins may be explained by higher mitotic arrest in cells depleted of Pds5A. On the other hand, the frequency of anaphase bridge and lagging chromosomes was greater in Wapl-depleted cells (Figure 5.3A, lower panel). The anaphase bridge became detectable during the metaphase-to-anaphase transition (t = 72 min) and may have remained as a nuclear bud after cytokinesis. Although a majority of cells appeared to undergo normal anaphase, it is possible that cells suffered mitotic defects which were difficult to observe.

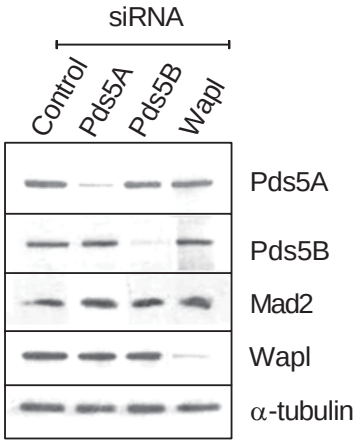

Figure 5.1: siRNA-mediated down-regulation of Pds5A, Pds5B and Wapl.

HeLa cells stably expressing mCherry-histone H2B and α-tubulin-EGFP were transfected with siRNAs as indicated. After 48 hrs the total proteins were extracted and analysed by Western blot using the antibodies indicated. This figure is representative of one experiment.

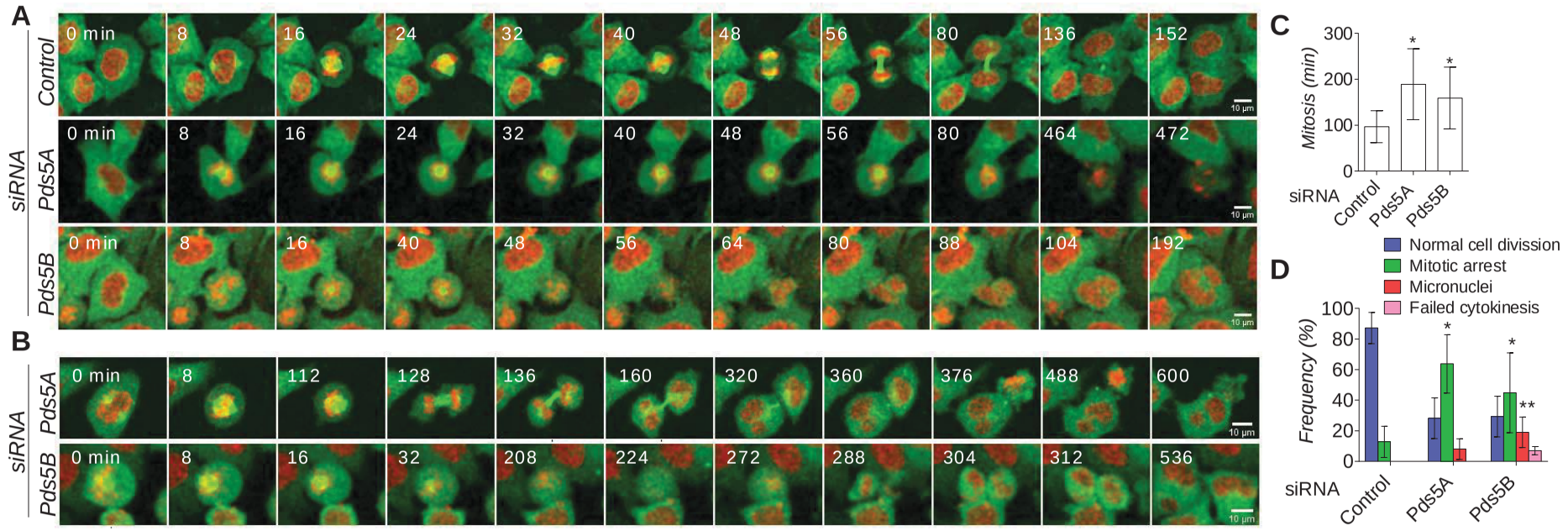

Figure 5.2: Time-lapse confocal microscopy of Pds5A and Pds5B-depleted cells.

HeLa cells stably expressing mCherry-histone H2B and α-tubulin-EGFP were transfected with siRNAs as indicated. After 48 hrs, cells were subjected to time lapse recording and imaged every 8 min to monitor their progression through mitosis. Selected images are depicted from prophase until completion of cytokinesis. (A) Upper panel: Control siRNA (50 nM)-treated cells; Middle panel: Pds5A siRNA (50 nM)-treated cells showing progression to cell death; Lower panel: Pds5B siRNA (50 nM)-treated cells showing exit from mitosis without cytokinesis. (B) Micronucleus formation after defective anaphase in Pds5A siRNA (50 nM)-treated cells (Upper panel) and in Pds5B siRNA (50 nM)-treated cells (Lower panel). Scale bar: 10 µm. (C and D) Quantification of the cell cycle defects seen in (A) and (B). Error bars represent the mean values and standard deviations of counts of at least 122 cells for each condition from four independent experiments; *$P < 0.01$; **$P < 0.05$. P values were calculated using one-way ANOVA in (C) and two-way ANOVA in (D).

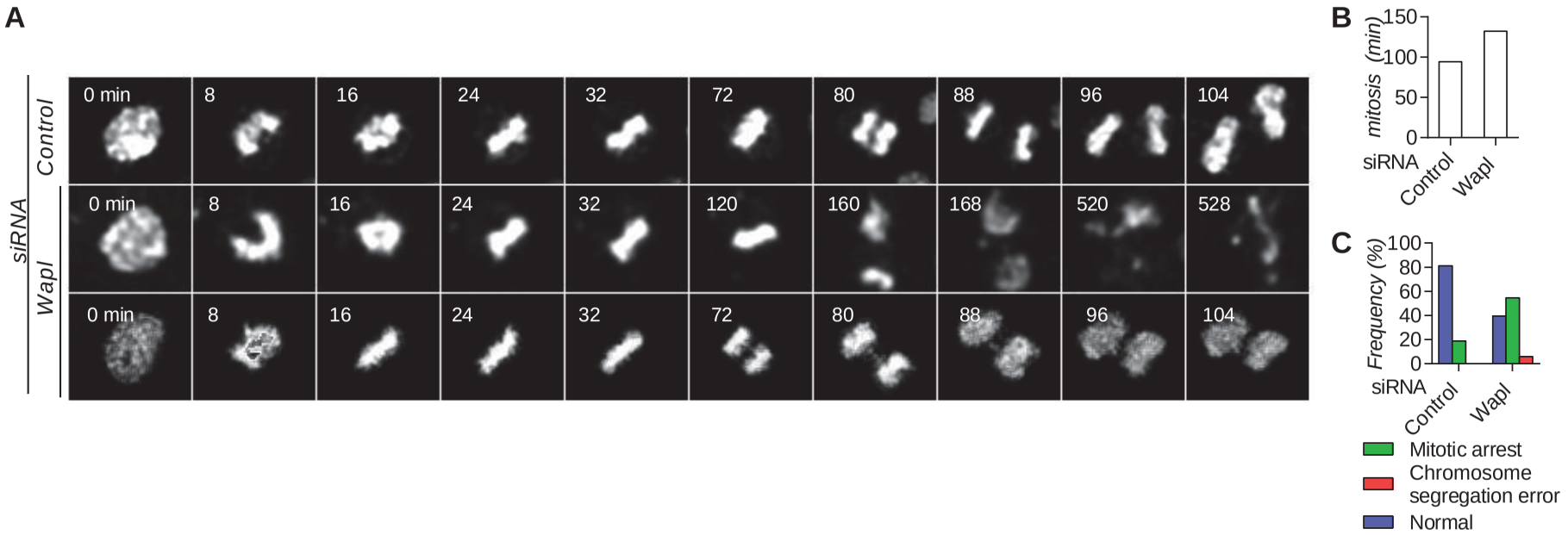

Figure 5.3: Time-lapse confocal microscopy of Wapl-depleted cells.

HeLa cells stably expressing mCherry-histone H2B and α-tubulin-EGFP were transfected either with control siRNAs (50 nM) or Wapl siRNAs (50 nM). After 48 hrs, cells were subjected to time lapse recording and imaged every 8 min to monitor their progression through mitosis. (A) Selected images are presented starting from prophase until completion of cytokinesis. Upper panel: Control siRNA-treated cells showing normal cell dicission; Middle panel: Wapl siRNA-treated cells showing the progression to cell death; Lower panel: Wapl siRNA-treated cells showing the anaphase bridge formation. Scale bar: 10 μm. (C and D) Quantification of the cell cycle defects seen in (A) of counts of at least 70 cells from two independent experiments.

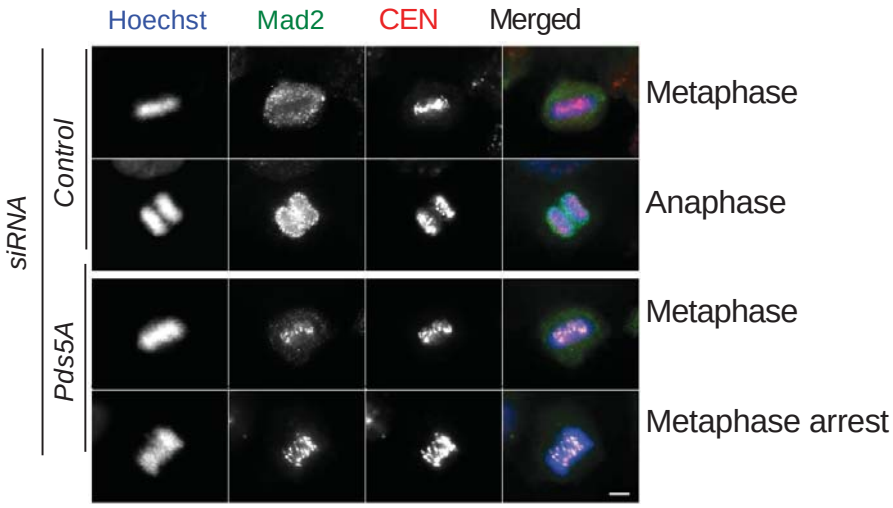

Figure 5.4: Depletion of Pds5A activates the spindle assembly checkpoint.

HeLa cells were transfected with either the control or Pds5A siRNAs (50 nM) for 48 hrs, fixed with -20 °C methanol and analyzed by immunofluorescence microscopy using a Mad2 antibody (green), an centromere antibody (red) and Hoechst 33342 (blue) to visualize the chromosomes. In control siRNA-treated cells, Mad2 dissociated from metaphase and anaphase kinetochores, whereas in Pds5A-depleted cells, Mad2 attached at centromeres at metaphase and anaphase. Merged images are shown for all panels. Scale bar: 8 µm. This is representative of two independent experiments.

5.3. Discussion

The complete separation of sister chromatids at the metaphase-to-anaphase transition is a mitotic event essential for faithful chromosome segregation during cell division. Sister chromatid separation in anaphase depends on the removal of cohesin complexes from chromosomes (Losada et al., 1998, Waizenegger et al., 2000, Haering and Nasmyth, 2003). In humans, depletion of separase or expression of non-cleavable Scc1 blocks sister chromatid separation and leads to abnormal mitosis (Hauf et al., 2001, Chestukhin et al., 2003). Given that the mechanism of sister chromatid separation might differ in some respects between yeast and vertebrate cells, the removal of cohesin from the chromosome arms in vertebrates is initiated at prophase in a separase-independent pathway, which relies on cohesin-regulatory proteins Pds5 and Wapl (Uhlmann et al., 1999, Shintomi and Hirano, 2009), whereas the centromeric cohesin is cleaved in a separase-dependent pathway at the transition from metaphase to anaphase (Uhlmann et al., 1999, Waizenegger et al., 2000). In this study, we observed a virtually identical effect of depleting the cohesin regulators Pds5 and Wapl on sister chromatid separation as that seen in cells lacking separase or expressing non-cleavable Scc1 (Hauf et al., 2001, Chestukhin et al., 2003).

Consistent with our observation that depletion of Pds5A, Pds5B and Wapl by siRNA prevents the dissociation of cohesin, the time-lapse images revealed that the depletion of those proteins was also sufficient to produce prolonged mitotic arrest, which is associated with the failure of chromosome separation and may eventually lead to apoptosis, as identified by chromatin condensation and nuclear fragmentation. In particular, the mitotic arrest was significantly ($P < 0.001$) greater in Pds5A and Pds5B-depleted cells (by 400 % and 250 % respectively) and by 187 % in Wapl-depleted cells compared to control cells, suggesting that the spindle assembly checkpoint was activated.

In mitosis, the SAC functions as a critical surveillance mechanism to detect misaligned sister chromatids and to delay the onset of anaphase until the proper bi-orientation of all sister chromatids (Musacchio and Salmon, 2007). In humans, Bub1 is required for precise chromosome alignment (Klebig et al., 2009); knockdown of Bub1 by RNAi causes errors in chromosome alignment and delays mitosis (Meraldi and Sorger, 2005). The misalignment defects caused by depletion of Pds5 and Wapl proteins were difficult to observe during time-lapse observation, however, examination by immunofluorescence microscopy, as reported in chapter 4, revealed an increased frequency of chromosome misalignment in cells depleted of Pds5 proteins (Figure 3.11 on page 76). Although I did not examine the interaction between Pds5 and Bub1, others have shown that this interaction occurs in fission yeast (Wang et al.,

2002) and there is no reason to believe that this would not be the case in humans. Therefore, it is possible that cells lacking any cohesin regulators, specifically at the centromere, may affect Bub1 localization or its function in kinetochore bi-orientation, which then triggers SAC activation. However, these cells may escape the SAC by the fact that vertebrate cells do not arrest the mitotic process permanently. Instead, they drive through mitosis by a proteasome-dependent degradation of cyclin B (Brito and Rieder, 2006). If this is the case, it is possible that during anaphase, the misaligned sister chromatids are left in the spindle midzone and excluded from both daughter nuclei, generating micronuclei.

On the other hand, if correctly bi-orientated sister chromatids are allowed to progress through anaphase, with persistent SCC on chromosomes, then the two sister chromatids would fail to be equally distributed between the two daughter cells, one being deposited into one daughter cell and none into the other. This might be explained by defects in sister chromatid separation and an increase in the residence time of cohesin on chromatin during mitosis. If this is the case, then karyotyping might be applicable to identify the number and shape of chromosomes after depletion of Pds5 and Wapl.

The abnormal shape of interphase nuclei seen in fixed cells (Figure 3.10A, panel c on page 75) leads me to speculate that this abnormality might be caused by defective cytokinesis which leads cells to enter interphase, often containing enlarged and irregularly shaped nuclei. This is consistent with the abnormality caused by Pds5B depletion shown in Figure 5.2A, lower panel, on page 129. In comparison, anaphase bridges were frequently observed in cells depleted of Wapl; it is possible that these cells initiated anaphase with less defective sister chromatid separation, eventually, chromosomal bridge becom constricted by an ingressing cytoplasmic bridge (cleavage furrow).

Chapter 6

General discussion and concluding remarks

Sister chromatid resolution requires the bulk release of cohesin from chromosomes at the onset of prophase (Losada et al., 2002, Sumara et al., 2002, Lenart et al., 2007). In *Xenopus* egg extracts, this process is prompted by the direct interaction of Wapl with Pds5 to directly modulate conformational changes of cohesin (Shintomi and Hirano, 2009), although Pds5 function seems to be required for SCC in budding yeast (Zhang et al., 2005) and SCC maintenance in fungi (Panizza et al., 2000). In light of the controversial data reported in the literature prior to commencing this study, the work presented in this thesis was conducted with the aim of comprehensively characterising the role of the human cohesin regulatory proteins, Pds5 and Wapl, in the regulation of sister chromatid cohesion and to shed light on the mechanism that triggers sister chromatid separation in early mitosis. To achieve these aims, three principal approaches were taken: (i) the depletion of Pds5 and Wapl proteins using an siRNA approach, followed by phenotypic analysis; (ii) the generation of Flag-tagged Wapl, Flag-tagged Pds5A (full length) and Flag-tagged Pds5A (N-terminus and C-terminus) to overexpress Pds5A, Pds5B and Wapl; (iii) *in vitro* kinase assay to confirm the phosphorylation of Wapl by Cdk1/cyclin B1 and Plk1. The data collected during this study suggest that the functions of Pds5 and Wapl in regulating sister chromatid cohesion are identical to those seen in *Xenopus* egg extracts (Shintomi and Hirano, 2009).

6.1. Cell cycle-dependent dynamic localization of Pds5 and Wapl

The data presented in chapter 3 show no changes in the levels of Pds5 proteins throughout the HeLa cell cycle; however, they highlight the first important difference between Pds5A and Pds5B localization. Pds5A is localized to the interphase chromosomes, dissociates during prophase and rebinds to chromatin in telophase, which is consistent with observations made in human Caco cells (Sumara et al., 2000). However, Pds5B only partially dissociated from chromosomes during prophase to metaphase and could still be detected clearly on chromosomes, but not at anaphase. The higher binding affinity of Pds5B for chromatin could be due to the presence of two AT-hook-type high mobility group (HMG) box motifs in the Pds5B protein sequence, compared to only one in Pds5A (Zhang et al., 2009a). This was confirmed by further analysis using Western blot of cytoplasmic and nuclear fractions reported in chapter 4, which shows that higher levels of Pds5B than of Pds5A were detected in interphase nuclear fractions.

Consistent with the fact that Wapl interacts preferentially with Pds5A (Kueng et al., 2006), the low levels of Pds5B which remained associated with the chromosomes from prophase to metaphase were probably not associated with Wapl, because Wapl, like Pds5A and cohesin, is already dissociated from chromosomes during prophase and rebinds to chromatin in

telophase. In chapter 4, however, there was an attempt to describe the mechanism by which Pds5A and Pds5B are dissociated. Inhibition of Cdk1/cyclin B1 and Plk1 prevented removal of Pds5A and Pds5B from mitotic chromosomes. A similar phenotype was seen after Wapl depletion by siRNA, suggesting that Pds5A and Pds5B act as downstream effectors of Wapl phosphorylation.

Taken together, the evidence indicates that Pds5B is bound to chromatin and cohesin during telophase, however, its binding with cohesin is probably weak (Sumara et al., 2000). Pds5A binding to chromatin might be weak also, but may be stronger with other proteins such as Wapl through the interaction via its FGF motif. Pds5B bound to both cohesin is dissociated during prophase following post-translational modification of Wapl by phosphorylation. At the metaphase-to-anaphase transition, Pds5B-bound chromatin may be subject to an unknown second wave of post-translational modification, causing a complete dissociation of Pds5B from chromatin.

6.2. The roles of Pds5 and Wapl in the mammalian cell cycle

The data presented in this study demonstrate that chromosome separation requires Pds5A, Pds5B and Wapl, and that their loss prevented cohesin removal from chromatin. As a consequence of the loss of either Pds5A or Pds5B, cells are capable of delaying the cell cycle progression through S-phase and eventually undergo apoptosis. It has been reported that the DNA damage checkpoints enable cells to delay cell cycle progression in the presence of DNA damage (Melo and Toczyski, 2002). Accordingly, Chk1 protein is thought to act as a major effector in DNA damage checkpoint signalling, and it was found phosphorylated at Ser^{317} after the loss Pds5A or Pds5B, suggesting that Pds5 proteins are required during S-phase, perhaps for their ability to recruit cohesin establishment factor Ctf7/Esco1 (Tanaka et al., 2001, Skibbens et al., 1999).

On the other hand, neither the activation of the DNA damage checkpoints nor the induction of apoptosis was detected after the loss of Wapl, suggesting that Wapl may not be essential for the DNA synthesis machinery. Instead, it has been proposed that Wapl and Esco1/2 display opposing activities and that the anti-establishment activity of Wapl-Pds5 is relaxed by Eco1 during S-phase to maintain SCC (Skibbens, 2009). However, after DNA synthesis and SCC, Wapl may be required to counteract Esco1/2, because the data from the co-IP performed in this study show an increased level of Wapl associated with Pds5A after DNA synthesis (3 hrs after release from aphidicolin block). This is also consistent with the fact that Eco1 acetyltransferase activity is generally restricted to S-phase and the suggestion that post-

replication DNA damage may promote Eco1/ESCO1 activity via DNA damage checkpoint kinase Mec1/ATR (Strom et al., 2004, Unal et al., 2007). However, Wapl-Pds5 may gain full anti-establishment activity in prophase by the phosphorylation of Wapl mediated by the upstream effectors Cdk1/cyclin B1 and Plk1, inducing conformational changes of cohesin to make it competent for dissociation from chromosome arms and allowing them to separate.

The data presented in this study also demonstrate that chromosome separation requires both Pds5 and Wapl, whose loss results in cells containing chromosomes with unresolved arms. The explanation for this observation is the high level of chromatin-bound cohesin, which prevents chromosome separation. Live cell imaging, however, demonstrated that Pds5 and Wapl-treated cells undergo a prolonged mitosis due to the activation of SAC. In many cases, it was possible to observe mitotic arrest and eventual apoptosis, as identified by nuclear fragmentation. One possible explanation for not being able to detect apoptotic markers in Wapl-depleted cells is the low level of apoptosis caused by mitotic arrest compared to that seen with Pds5A- and Pds5B-depleted cells as a consequence of both defects during interphase and mitosis.

It has been shown that vertebrate cells do not arrest permanently at mitosis, but are driven through mitosis by a proteasome-dependent degradation of cyclin B (Brito and Rieder, 2006). In some cases, however, Pds5- and Wapl-depleted cells may segregate their chromosomes after prolonged mitosis, although not correctly, eventually resulting in chromosomal abnormalities as shown by live cell imaging, which are similar to those seen in cells lacking separase or expressing non-cleavable Scc1 (Hauf et al., 2001, Chestukhin et al., 2003). This suggests that Pds5 and Wapl proteins are required for faithful chromosome segregation. Morphological examination of fixed cells showed a significant increase of chromosomal abnormalities in Pds5- and Wapl-depleted cells, namely chromosomal misalignment, micronuclei, multinucleated cells and chromosomal bridges, although the possibility of witnessing such events using live cell imaging was slight, due to the low-resolution imaging. Furthermore, some cells were not depicted during the emergence of chromosomal abnormalities, because a limited number of cells can be analysed during a single time-consuming experiment. Therefore, it is better to rely on fixed cell analyses, especially for quantitating the frequency of chromosomal abnormalities.

6.3. Cell cycle-dependent phosphorylation of Wapl

What remains to be determined are the molecular mechanisms by which Pds5 and Wapl modulate the conformational changes of the cohesin complex and contribute to chromosome

segregation during prophase. Several attempts have been made to understand the molecular mechanisms of the prophase pathway and it has been proposed that Sororin competes with Wapl to bind Pds5 and inhibit Wapl to maintain SCC (Nishiyama et al., 2010). In this study, I have considered potential mechanisms of action of Pds5 and Wapl, supported by the fact that Wapl is phosphorylated during mitosis. Therefore, Wapl may regulate a biological process of cell division when it reaches the optimum level during G2/M through selective recruitment of Cdk1/cyclin B1 and Plk1.

The association of Wapl with Pds5 may be Wapl phosphorylation-dependent as judged by the observation that inhibition of Plk1 and Cdk1 abolish the interaction between Pds5A and Wapl (Figure 4.18 on page 118). Since the interaction between Pds5A and Wapl occurs during interphase, there is a possibility that Wapl may be phosphorylated by S-phase cyclin-dependent kinases when cyclin concentrations rise and the CKIs are degraded (Mendenhall and Hodge, 1998). However, sequential activation of Wapl may be required to induce conformational changes of cohesin that eventually lead to its dissociation from chromatin. Supporting this idea, Plk1 is activated by the accumulation of Aurora A kinase and its activator bora in G2 before peaking at G2/M (Seki et al., 2008, Macurek et al., 2008). Plk1 activates the Cdk1/cyclin B1 by phosphorylating cyclin B1 and targeting it to the nucleus (Toyoshima-Morimoto et al., 2001). As a key process for mitotic entry, Wapl is targeted by Plk1 and Cdk1/cyclin B1 at G2/M, converting it to the hyperphosphorylated form and causing it to become dissociated from its partner Pds5. This eventually induces conformational changes of cohesin to make it competent for dissociation from chromosome arms during prophase.

6.4. Pds5 activity rises above that of Wapl during G1 and G1/S

Since Wapl has been shown to be required to regulate a vital biological process, viz. chromosome separation, other processes may also be governed by its ubiquitin/proteasome-dependent degradation. The total protein levels of Wapl observed in this study decreased as cells exited from mitosis. The timing of non-APC substrate degradation is thought to be regulated in part by the phosphorylation of the substrate that allows it to interact selectively with the F-box protein in the SCF complex (Skp1-Cullin1/F-box) (Skowyra et al., 1997, Ang and Wade Harper, 2005). The APC/C and SCF complex, members of the Ring-H2-finger-containing E3 Ub-ligase family, are two ubiquitin ligases (E3) that mediate the degradation of numerous substrates (Deshaies, 1999, Peters, 2002). Under different cellular conditions, APC/C engages with its substrates through the recognition of destruction box motifs by Cdc20 or by KEN boxes in the case of Cdh1.

In mammalian cells, the APC^{Cdc20} is activated in early mitosis by Cdk1/cyclin B1 and Plk1, whereas APC^{Cdh1} is kept inactive by phosphorylation (Blanco et al., 2000, Peters, 2002). Activation of APC^{Cdc20} promotes the proteolysis of Pds1/Securin, which directly enables separase to destroy centromeric cohesin and allows the metaphase-to-anaphase transition (Cohen-Fix and Koshland, 1997). Although cyclin activates cdk1 in prophase, it sows the seeds of its own destruction by APC^{Cdc20} (Clute and Pines, 1999). Cyclin B degradation by APC^{Cdc20} lowers overall Cdk1 activity through APC^{Cdc20} and raises that of APC^{Cdh1} by dephosphorylation. Activated APC^{Cdh1} is able to mediate the destruction of Cdc20 and Plk1 during mitotic exit (Prinz et al., 1998, Peters, 2002, Lindon and Pines, 2004).

Furthermore, APC^{Cdh1} recognizes the F-box protein Skp2 and mediates its proteolysis, resulting in low SCF complex activity and the accumulation of CKIs (Bashir et al., 2004, Wei et al., 2004); therefore the feedback loop ultimately raises APC^{Cdh1} activity over that of the SCF complex and APC^{Cdc20}. During the activity of APC^{Cdh1}, the KEN box motif on Wapl is presumably responsible for targeting Wapl for APC^{Cdh1}-dependent degradation in a cell cycle-dependent manner. The fall in Wapl protein level during telophase and its proteolysis during the subsequent G1 period at least allows Pds5 to gain its function in regulation of sister chromatid cohesion. This could be by the ability of Pds5 to recruit the establishment factor, Ctf7/Esco1 (Tanaka et al., 2001).

The data presented in chapter 3 highlight the importance of Pds5 proteins for the integrity of the DNA replication machinery, as their loss was found to induce apoptosis through the DNA damage signalling pathway. However, Wapl seems not to be essential to the G1-phase or to the establishment of cohesion, because of the low level of Wapl protein associated with the Pds5-cohesin complex before DNA synthesis and the fact that Wapl depletion did not induce the DNA damage checkpoint. On the other hand, the increase in Wapl level after DNA synthesis requires the activation of Cdk1 and this in turn depends on the accumulation of S-phase Cdk2/cyclin E, which is not destroyed by APC^{Cdh1}. Activated Cdk2/cyclin E is known to phosphorylate and inactivate APC^{Cdh1} (Zachariae and Nasmyth, 1999). After DNA synthesis, the increased recruitment of Wapl to Pds5 may antagonize Ctf7/Esco1 and finally switch cells back to a state in which mitotic cyclin B kinases can re-accumulate.

6.5. Concluding remarks

Cohesin is a key element in regulating sister chromatid cohesion. In vertebrates, the interaction between cohesin and chromatin is destabilized in prophase by Pds5-Wapl interaction. Most of the knowledge of Pds5 function derives from studies of yeasts and humans, and its role in cell cycle regulation has largely been elucidated with some controversial data reported in the literature. The overall work presented in this thesis has fulfilled the main aim of the study, which was to characterize the function of Pds5 in regulating SCC in HeLa cells. The data presented here indicate that Pds5 proteins are functionally important in mitotic cell division, apoptosis, DNA replication and repair processes. I have shown that Pds5A and Pds5B dissociate from chromatin in a consecutive manner during mitosis. The loss of either Pds5A or Pds5B slows the cell cycle progression through the activation of DNA damage checkpoints and subsequently induces apoptosis.

While Pds5 has been identified as a binding partner of Wapl, characterization of the function of Wapl in HeLa cells has brought further insight into the mechanisms by which those two proteins regulate sister chromatid separation. Work reported in this thesis has demonstrated that Wapl is cell cycle regulated and has highlighted the importance of the roles of Wapl and Pds5 in chromosome separation, as the loss of Wapl or Pds5 suppresses sister chromatid separation by induction of the spindle assembly checkpoint. However, unlike Pds5, Wapl seems not to be required for the integrity of DNA damage checkpoints. Furthermore, the immunofluorescence microscopy data show that the loss of Pds5 or Wapl increases the frequency of chromosomal abnormalities, while live cell imaging analysis has justified those abnormalities as the eventual causes of defects in anaphase or cytokinesis, suggesting that both Pds5 and Wapl are required for normal chromosome separation.

Interestingly, this work also provides the first evidence that Wapl undergoes post-translational modification by phosphorylation at mitosis, while identification of Wapl phosphorylation sites and upstream kinases has cast further light on the role of the cohesion anti-establishment activity of Wapl-Pds5. This finding has added some weight to the proposed mechanism regulating the prophase pathway in vertebrates. My final model highlighted that the anti-establishment activity of Wapl-Pds5 is regulated by phosphorylation and the APC/C-dependent proteolysis of Wapl (Figure 6.1). However, further work is required, particularly on the validation of the Wapl phosphorylation sites through mutagenesis studies and on the importance of Wapl phosphorylation in regulating sister chromatid separation, which could be demonstrated by overexpressing the phosphorylation-defective and phosphomimetic mutants of Wapl.

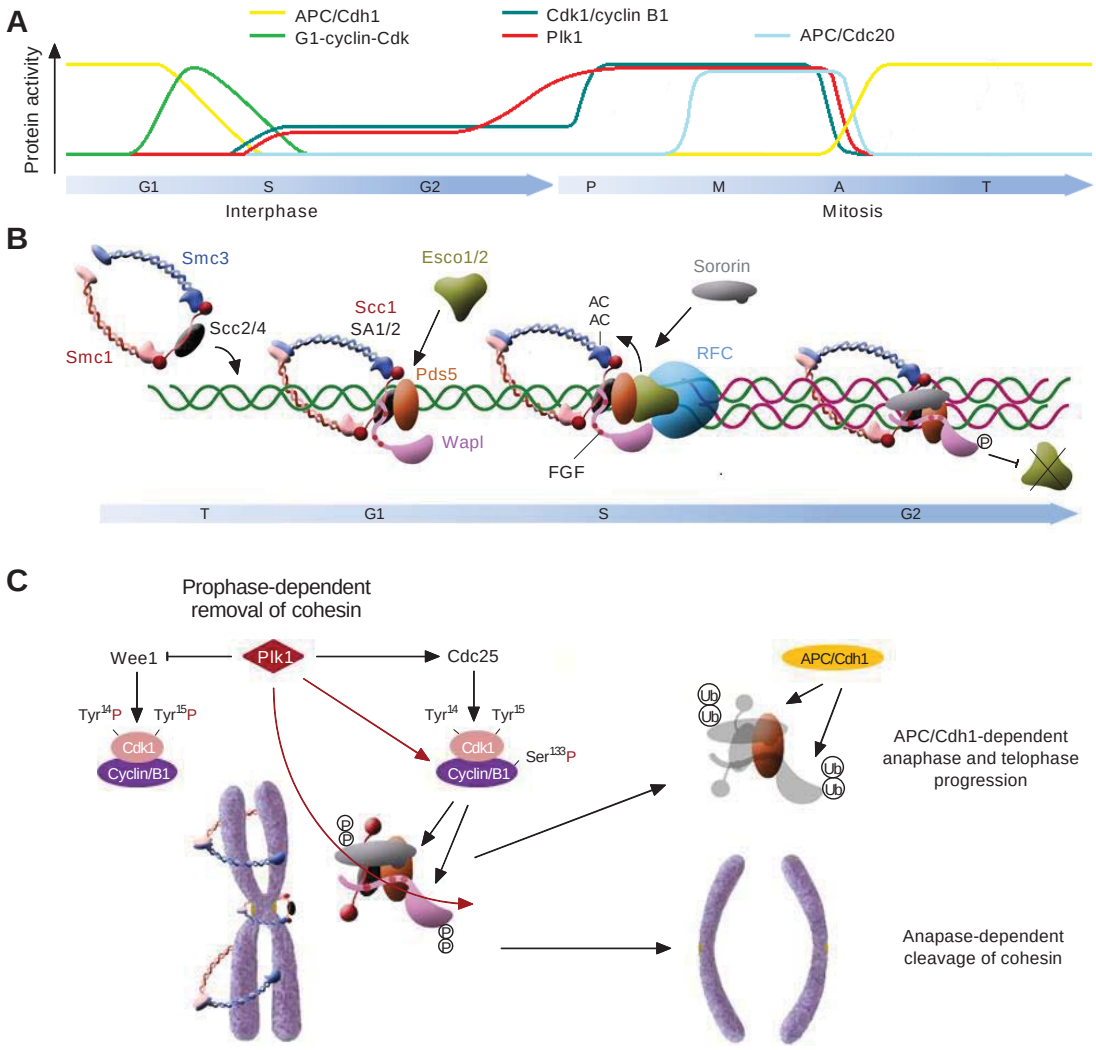

Figure 6.1: Model of the role of Pds5 and Wapl in regulation of the cohesin complex during the mammalian cells cycle.

(A) Schematic diagram of the temporal pattern of activation of the Cdks, Plk1 and the APC/C. (B) During telophase, cohesin is loaded onto chromatin with the aid of the loading factor Scc2 and Scc4. In vertebrates, either Pds5A or Pds5B associates with SA1/2 and Scc1 (Losada et al., 2005), however, this association is unstable (Sumara et al., 2000). Wapl interacts directly with non-Smc subunits SA1 and Scc1 via an FGF motifs present in the N-terminus of Wapl (Gandhi et al., 2006, Shintomi and Hirano, 2009). Association of Esco1/Ctf7 with Pds5 promotes Smc3 acetylation that resides in front of the DNA replication fork to allow for fork progression (Tanaka et al., 2001, Zhang et al., 2008, Unal et al., 2008). Other models suggest that Esco1/Ctf7 interacts with Replication Factor C (RFC) protein, Ctf18, to coordinate the emergence of new sister chromatids (Skibbens et al., 1999, Skibbens, 2000, Lengronne et al., 2006, Skibbens, 2011). Sororin is recruited to chromatin in a manner that depends on cohesin and Smc3 acetylation to stabilize the bound cohesin (Nishiyama et al., 2010). I propose that after S-phase Wapl binds Pds5 and this binding may be regulated by Wapl phosphorylation by Cdks, which may convert the unphosphorylated Wapl to the

hypophosphorylated form and enable its interaction with Pds5 which counteracts the function of Esco1/Ctf7 during G2. This notion is supported by the evidence that Esco1/Ctf7 acetyltransferase activity is generally restricted to S-phase (Strom et al., 2004). (C) The mechanism of cohesin removal during prophase by Wapl-Pds5 complex. Plk1 activity accumulates during G2/M and converts the inactive state of Cdk1/cyclin B1 into the active state by targeting the Cdk1-inhibitory kinase, Wee1 (Watanabe et al., 2004). Plk1 also phosphorylates Cdc25 on Ser^{198} (Toyoshima-Morimoto et al., 2002) and cyclin B1 on Ser^{133} (Jackman et al., 2003). The activity of the phosphorylated Cdc25 and the cyclin B1 overcomes the effect of the Cdk1-inhibitory kinase, Wee1, which results in the dephosphorylation and activation of Cdk1/cyclin B1. Wapl-Pds5 gains full anti-establishment activity by the hyperphosphorylation of Wapl mediated by Cdk1/cyclin B1 and Plk1. This is also combined with the phosphorylation of Sororin by Cdk1/cyclin B1 and Plk1. The phosphorylation of Sororin by Cdk1/cyclin B1 can create docking sites to bring Plk1 into proximity with SA2, resulting in the phosphorylation of SA2 (Zhang et al., 2011, Zhang and Pati, 2012). Phosphorylation of Wapl, Sororin and SA2 is now sufficient to induce conformational changes of cohesin to make it competent for dissociation from chromosome arms and allowing them to separate. During metaphase/anaphase transition the centromeric cohesin is removed by separase, following its activation by APC^{Cdc20} which allows the transition to anaphase (Peters et al., 2008). Cyclin B1 degradation by APC^{Cdc20} lowers overall Cdk1 activity and activates APC^{Cdh1} by dephosphorylation in late mitosis until the next S-phase. Activated APC^{Cdh1} is able to mediate the destruction of Cdc20 and Plk1 during mitotic exit (Prinz et al., 1998, Peters, 2002, Lindon and Pines, 2004). APC^{Cdh1} is also responsible for destruction of Sororin (Rankin et al., 2005) and possibly Wapl (this study). The KEN box present in Sororin (Rankin et al., 2005) (and Wapl) targets Sororin (and Wapl) for APC^{Cdh1}-dependent degradation after mitosis.

Chapter 7

References

ADACHI, Y., KOKUBU, A., EBE, M., NAGAO, K. & YANAGIDA, M. 2008. Cut1/separase-dependent roles of multiple phosphorylation of fission yeast cohesion subunit Rad21 in post-replicative damage repair and mitosis. *Cell Cycle,* 7**,** 765-76.

ADAMS, R. R., WHEATLEY, S. P., GOULDSWORTHY, A. M., KANDELS-LEWIS, S. E., CARMENA, M., SMYTHE, C., GERLOFF, D. L. & EARNSHAW, W. D. 2000. INCENP binds the Aurora-related kinase AIRK2 and is required to target it to chromosomes, the central spindle and cleavage furrow. *Current Biology,* 10**,** 1075-1078.

ALBERGHINA, L., ROSSI, R. L., QUERIN, L., WANKE, V. & VANONI, M. 2004. A cell sizer network involving Cln3 and Far1 controls entrance into S phase in the mitotic cycle of budding yeast. *J Cell Biol,* 167**,** 433-43.

ALBERTS, B. 2002. *Molecular biology of the cell,* New York, Garland Science.

ALEEM, E., KIYOKAWA, H. & KALDIS, P. 2005. Cdc2-cyclin E complexes regulate the G1/S phase transition. *Nature Cell Biology,* 7**,** 831-U93.

ALEXANDRU, G., UHLMANN, F., MECHTLER, K., POUPART, M. A. & NASMYTH, K. 2001. Phosphorylation of the cohesin subunit Scc1 by Polo/Cdc5 kinase regulates sister chromatid separation in yeast. *Cell,* 105**,** 459-472.

ANDERSON, D. E., LOSADA, A., ERICKSON, H. P. & HIRANO, T. 2002. Condensin and cohesin display different arm conformations with characteristic hinge angles. *J Cell Biol,* 156**,** 419-24.

ANDREWS, P. D., KNATKO, E., MOORE, W. J. & SWEDLOW, J. R. 2003. Mitotic mechanics: the auroras come into view. *Current Opinion in Cell Biology,* 15**,** 672-83.

ANG, X. L. & WADE HARPER, J. 2005. SCF-mediated protein degradation and cell cycle control. *Oncogene,* 24**,** 2860-70.

ARUMUGAM, P., NISHINO, T., HAERING, C. H., GRUBER, S. & NASMYTH, K. 2006. Cohesin's ATPase activity is stimulated by the C-terminal Winged-Helix domain of its kleisin subunit. *Current Biology,* 16**,** 1998-2008.

BARR, F. A., SILLJE, H. H. & NIGG, E. A. 2004. Polo-like kinases and the orchestration of cell division. *Nat Rev Mol Cell Biol,* 5**,** 429-40.

BARTEK, J. & LUKAS, J. 2003. Chk1 and Chk2 kinases in checkpoint control and cancer. *Cancer Cell,* 3**,** 421-9.

BASHIR, T., DORRELLO, N. V., AMADOR, V., GUARDAVACCARO, D. & PAGANO, M. 2004. Control of the SCF(Skp2-Cks1) ubiquitin ligase by the APC/C(Cdh1) ubiquitin ligase. *Nature,* 428**,** 190-3.

BECKER, M., STOLZ, A., ERTYCH, N. & BASTIANS, H. 2010. Centromere localization of INCENP-aurora B is sufficient to support spindle checkpoint function. *Cell Cycle,* 9**,** 1360-1372.

BHARADWAJ, R. & YU, H. 2004. The spindle checkpoint, aneuploidy, and cancer. *Oncogene,* 23**,** 2016-27.

BIRKENBIHL, R. P. & SUBRAMANI, S. 1992. Cloning and characterization of rad21 an essential gene of Schizosaccharomyces pombe involved in DNA double-strand-break repair. *Nucleic Acids Research,* 20**,** 6605-11.

BLANCO, M. A., SANCHEZ-DIAZ, A., DE PRADA, J. M. & MORENO, S. 2000. APC(ste9/srw1) promotes degradation of mitotic cyclins in G(1) and is inhibited by cdc2 phosphorylation. *Embo Journal,* 19**,** 3945-3955.

BRANDS, A. & SKIBBENS, R. V. 2008. Sister chromatid cohesion role for CDC28-CDK in Saccharomyces cerevisiae. *Genetics,* 180**,** 7-16.

BRITO, D. A. & RIEDER, C. L. 2006. Mitotic checkpoint slippage in humans occurs via cyclin B destruction in the presence of an active checkpoint. *Curr Biol,* 16**,** 1194-200.

CAMPBELL, J. L. & COHEN-FIX, O. 2002. Chromosome cohesion: ring around the sisters? *Trends in Biochemical Sciences,* 27**,** 492-5.

CARMENA, M., RUCHAUD, S. & EARNSHAW, W. C. 2009. Making the Auroras glow: regulation of Aurora A and B kinase function by interacting proteins. *Curr Opin Cell Biol,* 21**,** 796-805.

CHEN, M. S., RYAN, C. E. & PIWNICA-WORMS, H. 2003. Chk1 kinase negatively regulates mitotic function of Cdc25A phosphatase through 14-3-3 binding. *Mol Cell Biol,* 23**,** 7488-97.

CHESTUKHIN, A., PFEFFER, C., MILLIGAN, S., DECAPRIO, J. A. & PELLMAN, D. 2003. Processing, localization, and requirement of human separase for normal anaphase progression. *Proc Natl Acad Sci U S A,* 100**,** 4574-9.

CLUTE, P. & PINES, J. 1999. Temporal and spatial control of cyclin B1 destruction in metaphase. *Nat Cell Biol,* 1**,** 82-7.

COHEN-FIX, O. 2001. The making and breaking of sister chromatid cohesion. *Cell,* 106**,** 137-40.

COHEN-FIX, O. & KOSHLAND, D. 1997. The anaphase inhibitor of Saccharomyces cerevisiae Pds1p is a target of the DNA damage checkpoint pathway. *Proceedings of the National Academy of Sciences of the United States of America,* 94**,** 14361-14366.

COHEN, P. 1989. The Structure and Regulation of Protein Phosphatases. *Annual Review of Biochemistry,* 58**,** 453-508.

COOKE, C. A., HECK, M. M. S. & EARNSHAW, W. C. 1987. The Inner Centromere Protein (Incenp) Antigens - Movement from Inner Centromere to Midbody during Mitosis. *Journal of Cell Biology,* 105**,** 2053-2067.

DARWICHE, N., FREEMAN, L. A. & STRUNNIKOV, A. 1999. Characterization of the components of the putative mammalian sister chromatid cohesion complex. *Gene,* 233**,** 39-47.

DENISON, S. H., KAFER, E. & MAY, G. S. 1993. Mutation in the bimD gene of Aspergillus nidulans confers a conditional mitotic block and sensitivity to DNA damaging agents. *Genetics,* 134**,** 1085-96.

DESHAIES, R. J. 1999. SCF and Cullin/Ring H2-based ubiquitin ligases. *Annu Rev Cell Dev Biol,* 15**,** 435-67.

DOBIE, K. W., KENNEDY, C. D., VELASCO, V. M., MCGRATH, T. L., WEKO, J., PATTERSON, R. W. & KARPEN, G. H. 2001. Identification of chromosome inheritance modifiers in Drosophila melanogaster. *Genetics,* 157**,** 1623-37.

DORSETT, D. 2007. Roles of the sister chromatid cohesion apparatus in gene expression, development, and human syndromes. *Chromosoma,* 116**,** 1-13.

DORSETT, D., EISSENBERG, J. C., MISULOVIN, Z., MARTENS, A., REDDING, B. & MCKIM, K. 2005. Effects of sister chromatid cohesion proteins on cut gene expression during wing development in Drosophila. *Development,* 132**,** 4743-53.

DREIER, M. R., BEKIER, M. E. & TAYLOR, W. R. 2011. Regulation of sororin by Cdk1-mediated phosphorylation. *Journal of Cell Science,* 124**,** 2976-2987.

EASTMOND, D. A. & TUCKER, J. D. 1989. Identification of Aneuploidy-Inducing Agents Using Cytokinesis-Blocked Human-Lymphocytes and an Antikinetochore Antibody. *Environmental and Molecular Mutagenesis,* 13**,** 34-43.

ELIA, A. E., CANTLEY, L. C. & YAFFE, M. B. 2003. Proteomic screen finds pSer/pThr-binding domain localizing Plk1 to mitotic substrates. *Science,* 299**,** 1228-31.

FEYTOUT, A., VAUR, S., GENIER, S., VAZQUEZ, S. & JAVERZAT, J. P. 2011. Psm3 Acetylation on Conserved Lysine Residues Is Dispensable for Viability in Fission Yeast but Contributes to Eso1-Mediated Sister Chromatid Cohesion by Antagonizing Wpl1. *Molecular and Cellular Biology,* 31**,** 1771-1786.

FORD, J. H., SCHULTZ, C. J. & CORRELL, A. T. 1988. Chromosome elimination in micronuclei: a common cause of hypoploidy. *American Journal of Human Genetics,* 43**,** 733-40.

FURNARI, B., RHIND, N. & RUSSELL, P. 1997. Cdc25 mitotic inducer targeted by chk1 DNA damage checkpoint kinase. *Science,* 277**,** 1495-7.

GADEA, B. B. & RUDERMAN, J. V. 2005. Aurora kinase inhibitor ZM447439 blocks chromosome-induced spindle assembly, the completion of chromosome condensation, and the establishment of the spindle integrity checkpoint in Xenopus egg extracts. *Molecular Biology of the Cell,* 16**,** 1305-18.

GANDHI, R., GILLESPIE, P. J. & HIRANO, T. 2006. Human Wapl is a cohesin-binding protein that promotes sister-chromatid resolution in mitotic prophase. *Current Biology,* 16**,** 2406-17.

GARLAND, L. L., TAYLOR, C., PILKINGTON, D. L., COHEN, J. L. & VON HOFF, D. D. 2006. A phase I pharmacokinetic study of HMN-214, a novel oral stilbene derivative with polo-like kinase-1-interacting properties, in patients with advanced solid tumors. *Clinical Cancer Research,* 12**,** 5182-5189.

GECK, P., SZELEI, J., JIMENEZ, J., SONNENSCHEIN, C. & SOTO, A. M. 1999. Early gene expression during androgen-induced inhibition of proliferation of prostate cancer cells: a new suppressor candidate on chromosome 13, in the BRCA2-Rb1 locus. *J Steroid Biochem Mol Biol,* 68**,** 41-50.

GERHARD, D. S., WAGNER, L., FEINGOLD, E. A., SHENMEN, C. M., GROUSE, L. H., SCHULER, G., KLEIN, S. L., OLD, S., RASOOLY, R., GOOD, P., GUYER, M., PECK, A. M., DERGE, J. G., LIPMAN, D., COLLINS, F. S., JANG, W., SHERRY, S., FEOLO, M., MISQUITTA, L., LEE, E., ROTMISTROVSKY, K., GREENHUT, S. F., SCHAEFER, C. F., BUETOW, K., BONNER, T. I., HAUSSLER, D., KENT, J., KIEKHAUS, M., FUREY, T., BRENT, M., PRANGE, C., SCHREIBER, K., SHAPIRO, N., BHAT, N. K., HOPKINS, R. F., HSIE, F., DRISCOLL, T., SOARES, M. B., CASAVANT, T. L., SCHEETZ, T. E., BROWN-STEIN, M. J., USDIN, T. B., TOSHIYUKI, S., CARNINCI, P., PIAO, Y., DUDEKULA, D. B., KO, M. S., KAWAKAMI, K., SUZUKI, Y., SUGANO, S., GRUBER, C. E., SMITH, M. R., SIMMONS, B., MOORE, T., WATERMAN, R., JOHNSON, S. L., RUAN, Y., WEI, C. L., MATHAVAN, S., GUNARATNE, P. H., WU, J., GARCIA, A. M., HULYK, S. W., FUH, E., YUAN, Y., SNEED, A., KOWIS, C., HODGSON, A., MUZNY, D. M., MCPHERSON, J., GIBBS, R. A., FAHEY, J., HELTON, E., KETTEMAN, M., MADAN, A., RODRIGUES, S., SANCHEZ, A., WHITING, M., MADARI, A., YOUNG, A. C., WETHERBY, K. D., GRANITE, S. J., KWONG, P. N., BRINKLEY, C. P., PEARSON, R. L., BOUFFARD, G. G., BLAKESLY, R. W., GREEN, E. D., DICKSON, M. C., RODRIGUEZ, A. C., GRIMWOOD, J., SCHMUTZ, J., MYERS, R. M., BUTTERFIELD, Y. S., GRIFFITH, M., GRIFFITH, O. L., KRZYWINSKI, M. I., LIAO, N., MORIN, R., PALMQUIST, D., et al. 2004. The status, quality, and expansion of the NIH full-length cDNA project: the Mammalian Gene Collection (MGC). *Genome Res,* 14**,** 2121-7.

GERLICH, D., KOCH, B., DUPEUX, F., PETERS, J. M. & ELLENBERG, J. 2006. Live-cell imaging reveals a stable cohesin-chromatin interaction after but not before DNA replication. *Current Biology,* 16**,** 1571-8.

GIET, R. & GLOVER, D. M. 2001. Drosophila Aurora B kinase is required for histone H3 phosphorylation and condensin recruitment during chromosome condensation and to organize the central spindle during cytokinesis. *Journal of Cell Biology,* 152**,** 669-681.

GILLESPIE, P. J. & HIRANO, T. 2004. Scc2 couples replication licensing to sister chromatid cohesion in Xenopus egg extracts. *Current Biology,* 14**,** 1598-603.

GOEPFERT, T. M., ADIGUN, Y. E., ZHONG, L., GAY, J., MEDINA, D. & BRINKLEY, W. R. 2002. Centrosome amplification and overexpression of aurora A are early events in rat mammary carcinogenesis. *Cancer Res,* 62**,** 4115-22.

GORBSKY, G. J., CHEN, R. H. & MURRAY, A. W. 1998. Microinjection of antibody to Mad2 protein into mammalian cells in mitosis induces premature anaphase. *Journal of Cell Biology,* 141**,** 1193-1205.

GOTO, H., YASUI, Y., NIGG, E. A. & INAGAKI, M. 2002. Aurora-B phosphorylates histone H3 at serine28 with regard to the mitotic chromosome condensation. *Genes to Cells,* 7**,** 11-17.

GRIFFIN, D. K. 1996. The incidence, origin, and etiology of aneuploidy. *Int Rev Cytol,* 167**,** 263-96.

GRIFFITH, J. D., LINDSEY-BOLTZ, L. A. & SANCAR, A. 2002. Structures of the human Rad17-replication factor C and checkpoint Rad 9-1-1 complexes visualized by glycerol spray/low voltage microscopy. *J Biol Chem,* 277**,** 15233-6.

GRUBER, S., HAERING, C. H. & NASMYTH, K. 2003. Chromosomal Cohesin Forms a Ring. *Cell,* 112**,** 765-777.

GUACCI, V., KOSHLAND, D. & STRUNNIKOV, A. 1997. A direct link between sister chromatid cohesion and chromosome condensation revealed through the analysis of MCD1 in S. cerevisiae. *Cell,* 91**,** 47-57.

HAERING, C. H., LOWE, J., HOCHWAGEN, A. & NASMYTH, K. 2002. Molecular architecture of SMC proteins and the yeast cohesin complex. *Mol Cell,* 9**,** 773-88.

HAERING, C. H. & NASMYTH, K. 2003. Building and breaking bridges between sister chromatids. *Bioessays,* 25**,** 1178-1191.

HAERING, C. H., SCHOFFNEGGER, D., NISHINO, T., HELMHART, W., NASMYTH, K. & LOWE, J. 2004. Structure and stability of cohesin's Smc1-kleisin interaction. *Mol Cell,* 15**,** 951-64.

HANSEN, D. V., LOKTEV, A. V., BAN, K. H. & JACKSON, P. K. 2004. Plk1 regulates activation of the anaphase promoting complex by phosphorylating and triggering SCFbetaTrCP-dependent destruction of the APC Inhibitor Emi1. *Mol Biol Cell,* 15**,** 5623-34.

HARTMAN, T., STEAD, K., KOSHLAND, D. & GUACCI, V. 2000. Pds5p is an essential chromosomal protein required for both sister chromatid cohesion and condensation in Saccharomyces cerevisiae. *Journal of Cell Biology,* 151**,** 613-26.

HARTWELL, L. H. 1974. Saccharomyces cerevisiae cell cycle. *Bacteriol Rev,* 38**,** 164-98.

HARTWELL, L. H., MORTIMER, R. K., CULOTTI, J. & CULOTTI, M. 1973. Genetic Control of the Cell Division Cycle in Yeast: V. Genetic Analysis of cdc Mutants. *Genetics,* 74**,** 267-86.

HARVEY, S. L., CHARLET, A., HAAS, W., GYGI, S. P. & KELLOGG, D. R. 2005. Cdk1-dependent regulation of the mitotic inhibitor Wee1. *Cell,* 122**,** 407-420.

HAUF, S., COLE, R. W., LATERRA, S., ZIMMER, C., SCHNAPP, G., WALTER, R., HECKEL, A., VAN MEEL, J., RIEDER, C. L. & PETERS, J. M. 2003. The small molecule Hesperadin reveals a role for Aurora B in correcting kinetochore-microtubule attachment and in maintaining the spindle assembly checkpoint. *J Cell Biol,* 161**,** 281-94.

HAUF, S., ROITINGER, E., KOCH, B., DITTRICH, C. M., MECHTLER, K. & PETERS, J. M. 2005. Dissociation of cohesin from chromosome arms and loss of arm cohesion during early mitosis depends on phosphorylation of SA2. *PLoS Biol,* 3**,** e69.

HAUF, S., WAIZENEGGER, I. C. & PETERS, J. M. 2001. Cohesin cleavage by separase required for anaphase and cytokinesis in human cells. *Science,* 293**,** 1320-3.

HAYASHI, M. T. & KARLSEDER, J. 2013. DNA damage associated with mitosis and cytokinesis failure. *Oncogene*.

HEDDLE, J. A. 1973. A rapid in vivo test for chromosomal damage. *Mutat Res,* 18**,** 187-90.

HEGARAT, N., SMITH, E., NAYAK, G., TAKEDA, S., EYERS, P. A. & HOCHEGGER, H. 2011. Aurora A and Aurora B jointly coordinate chromosome segregation and anaphase microtubule dynamics. *J Cell Biol,* 195**,** 1103-13.

HEIDINGER-PAULI, J. M., UNAL, E. & KOSHLAND, D. 2009. Distinct targets of the Eco1 acetyltransferase modulate cohesion in S phase and in response to DNA damage. *Molecular Cell,* 34**,** 311-21.

HEO, S. J., TATEBAYASHI, K. & IKEDA, H. 1999. The budding yeast cohesin gene SCC1/MCD1/RHC21 genetically interacts with PKA, CDK and APC. *Curr Genet,* 36**,** 329-338.

HEWITT, L., TIGHE, A., SANTAGUIDA, S., WHITE, A. M., JONES, C. D., MUSACCHIO, A., GREEN, S. & TAYLOR, S. S. 2010. Sustained Mps1 activity is required in mitosis to recruit O-Mad2 to the Mad1-C-Mad2 core complex. *Journal of Cell Biology,* 190**,** 25-34.

HINDS, P. W., MITTNACHT, S., DULIC, V., ARNOLD, A., REED, S. I. & WEINBERG, R. A. 1992. Regulation of retinoblastoma protein functions by ectopic expression of human cyclins. *Cell,* 70**,** 993-1006.

HIRANO, T. 2005a. Condensins: organizing and segregating the genome. *Current Biology,* 15**,** R265-75.

HIRANO, T. 2005b. SMC proteins and chromosome mechanics: from bacteria to humans. *Philos Trans R Soc Lond B Biol Sci,* 360**,** 507-14.

HOCHEGGER, H., TAKEDA, S. & HUNT, T. 2008. Cyclin-dependent kinases and cell-cycle transitions: does one fit all? *Nat Rev Mol Cell Biol,* 9**,** 910-6.

HOLT, L. J., TUCH, B. B., VILLEN, J., JOHNSON, A. D., GYGI, S. P. & MORGAN, D. O. 2009. Global Analysis of Cdk1 Substrate Phosphorylation Sites Provides Insights into Evolution. *Science,* 325**,** 1682-1686.

HOYT, M. A., TOTIS, L. & ROBERTS, B. T. 1991. S. cerevisiae genes required for cell cycle arrest in response to loss of microtubule function. *Cell,* 66**,** 507-17.

IVANOV, D., SCHLEIFFER, A., EISENHABER, F., MECHTLER, K., HAERING, C. H. & NASMYTH, K. 2002. Eco1 is a novel acetyltransferase that can acetylate proteins involved in cohesion. *Current Biology,* 12**,** 323-328.

JACKMAN, M., LINDON, C., NIGG, E. A. & PINES, J. 2003. Active cyclin B1-Cdk1 first appears on centrosomes in prophase. *Nat Cell Biol,* 5**,** 143-8.

JACKSON, L., KLINE, A. D., BARR, M. A. & KOCH, S. 1993. de Lange syndrome: a clinical review of 310 individuals. *Am J Med Genet,* 47**,** 940-6.

JANG, Y. J., MA, S., TERADA, Y. & ERIKSON, R. L. 2002. Phosphorylation of threonine 210 and the role of serine 137 in the regulation of mammalian polo-like kinase. *J Biol Chem,* 277**,** 44115-20.

JORDAN, M. A., THROWER, D. & WILSON, L. 1992. Effects of vinblastine, podophyllotoxin and nocodazole on mitotic spindles. Implications for the role of microtubule dynamics in mitosis. *J Cell Sci,* 102 (Pt 3)**,** 401-16.

JORDAN, M. A., TOSO, R. J., THROWER, D. & WILSON, L. 1993. Mechanism of Mitotic Block and Inhibition of Cell-Proliferation by Taxol at Low Concentrations. *Proceedings of the National Academy of Sciences of the United States of America,* 90**,** 9552-9556.

KAGAMI, A., SAKUNO, T., YAMAGISHI, Y., ISHIGURO, T., TSUKAHARA, T., SHIRAHIGE, K., TANAKA, K. & WATANABE, Y. 2011. Acetylation regulates monopolar attachment at multiple levels during meiosis I in fission yeast. *Embo Reports,* 12**,** 1189-1195.

KITADA, K., JOHNSON, A. L., JOHNSTON, L. H. & SUGINO, A. 1993. A multicopy suppressor gene of the Saccharomyces cerevisiae G1 cell cycle mutant gene dbf4 encodes a protein kinase and is identified as CDC5. *Mol Cell Biol,* 13**,** 4445-57.

KITAGAWA, R., BAKKENIST, C. J., MCKINNON, P. J. & KASTAN, M. B. 2004. Phosphorylation of SMC1 is a critical downstream event in the ATM-NBS1-BRCA1 pathway. *Genes & Development,* 18**,** 1423-1438.

KLEBIG, C., KORINTH, D. & MERALDI, P. 2009. Bub1 regulates chromosome segregation in a kinetochore-independent manner. *J Cell Biol,* 185**,** 841-58.

KONDO, T., MATSUMOTO, K. & SUGIMOTO, K. 1999. Role of a complex containing Rad17, Mec3, and Ddc1 in the yeast DNA damage checkpoint pathway. *Mol Cell Biol,* 19**,** 1136-43.

KUENG, S., HEGEMANN, B., PETERS, B. H., LIPP, J. J., SCHLEIFFER, A., MECHTLER, K. & PETERS, J.-M. 2006. Wapl controls the dynamic association of cohesin with chromatin. *Cell,* 127**,** 955-67.

KUMAR, D., SAKABE, I., PATEL, S., ZHANG, Y., AHMAD, I., GEHAN, E. A., WHITESIDE, T. L. & KASID, U. 2004. SCC-112, a novel cell cycle-regulated molecule, exhibits reduced expression in human renal carcinomas. *Gene,* 328**,** 187-96.

KURODA, M., KIYONO, T., OIKAWA, K., YOSHIDA, K. & MUKAI, K. 2005. The human papillomavirus E6 and E7 inducible oncogene, hWAPL, exhibits potential as a therapeutic target. *British Journal of Cancer,* 92**,** 290-293.

KWIATKOWSKI, B. A., RAGOCZY, T., EHLY, J. & SCHUBACH, W. H. 2004. Identification and cloning of a novel chromatin-associated protein partner of Epstein-Barr nuclear protein 2. *Exp Cell Res,* 300**,** 223-33.

LAFONT, A. L., SONG, J. & RANKIN, S. 2010. Sororin cooperates with the acetyltransferase Eco2 to ensure DNA replication-dependent sister chromatid cohesion. *Proc Natl Acad Sci U S A,* 107**,** 20364-9.

LEE, J. M. & GREENLEAF, A. L. 1991. Ctd Kinase Large Subunit Is Encoded by Ctk1, a Gene Required for Normal Growth of Saccharomyces Cerevisiae. *Gene Expression,* 1**,** 149-167.

LEE, M. G. & NURSE, P. 1987. Complementation Used to Clone a Human Homolog of the Fission Yeast-Cell Cycle Control Gene Cdc2. *Nature,* 327**,** 31-35.

LENART, P., PETRONCZKI, M., STEEGMAIER, M., DI FIORE, B., LIPP, J. J., HOFFMANN, M., RETTIG, W. J., KRAUT, N. & PETERS, J.-M. 2007. The Small-Molecule Inhibitor BI 2536 Reveals Novel Insights into Mitotic Roles of Polo-like Kinase 1. *Current Biology,* 17**,** 304-315.

LENGRONNE, A., MCINTYRE, J., KATOU, Y., KANOH, Y., HOPFNER, K. P., SHIRAHIGE, K. & UHLMANN, F. 2006. Establishment of sister chromatid cohesion at the S-cerevisiae replication fork. *Molecular Cell,* 23**,** 787-799.

LERA, R. F. & BURKARD, M. E. 2012. High Mitotic Activity of Polo-like Kinase 1 Is Required for Chromosome Segregation and Genomic Integrity in Human Epithelial Cells. *Journal of Biological Chemistry,* 287**,** 42812-42825.

LI, R. & MURRAY, A. W. 1991. Feedback control of mitosis in budding yeast. *Cell,* 66**,** 519-31.

LI, Y., GORBEA, C., MAHAFFEY, D., RECHSTEINER, M. & BENEZRA, R. 1997. MAD2 associates with the cyclosome/anaphase-promoting complex and inhibits its activity. *Proc Natl Acad Sci U S A,* 94**,** 12431-6.

LIAO, S. M., ZHANG, J. H., JEFFREY, D. A., KOLESKE, A. J., THOMPSON, C. M., CHAO, D. M., VILJOEN, M., VANVUUREN, H. J. J. & YOUNG, R. A. 1995. A Kinase-Cyclin Pair in the Rna-Polymerase-Ii Holoenzyme. *Nature,* 374**,** 193-196.

LIGHTFOOT, J., TESTORI, S., BARROSO, C. & MARTINEZ-PEREZ, E. 2011. Loading of Meiotic Cohesin by SCC-2 Is Required for Early Processing of DSBs and for the DNA Damage Checkpoint. *Current biology : CB,* 21**,** 1421-1430.

LINDON, C. & PINES, J. 2004. Ordered proteolysis in anaphase inactivates Plk1 to contribute to proper mitotic exit in human cells. *J Cell Biol,* 164**,** 233-41.

LIU, F., PARK, J. E., QIAN, W. J., LIM, D., SCHAROW, A., BERG, T., YAFFE, M. B., LEE, K. S. & BURKE, T. R. 2012. Identification of High Affinity Polo-like Kinase 1 (Plk1) Polo-box Domain Binding Peptides Using Oxime-Based Diversification. *Acs Chemical Biology,* 7**,** 805-810.

LIU, J. & KIPREOS, E. T. 2000. Evolution of cyclin-dependent kinases (CDKs) and CDK-activating kinases (CAKs): Differential conservation of CAKs in yeast and metazoa. *Molecular Biology and Evolution,* 17**,** 1061-1074.

LIU, Q., GUNTUKU, S., CUI, X. S., MATSUOKA, S., CORTEZ, D., TAMAI, K., LUO, G., CARATTINI-RIVERA, S., DEMAYO, F., BRADLEY, A., DONEHOWER, L. A. & ELLEDGE, S. J. 2000. Chk1 is an essential kinase that is regulated by Atr and required for the G(2)/M DNA damage checkpoint. *Genes Dev,* 14**,** 1448-59.

LLAMAZARES, S., MOREIRA, A., TAVARES, A., GIRDHAM, C., SPRUCE, B. A., GONZALEZ, C., KARESS, R. E., GLOVER, D. M. & SUNKEL, C. E. 1991. polo encodes a protein kinase homolog required for mitosis in Drosophila. *Genes Dev,* 5**,** 2153-65.

LOPEZ-GIRONA, A., TANAKA, K., CHEN, X. B., BABER, B. A., MCGOWAN, C. H. & RUSSELL, P. 2001. Serine-345 is required for Rad3-dependent phosphorylation and function of checkpoint kinase Chk1 in fission yeast. *Proc Natl Acad Sci U S A,* 98**,** 11289-94.

LORINCZ, A. T. & REED, S. I. 1984. Primary Structure Homology between the Product of Yeast-Cell Division Control Gene Cdc28 and Vertebrate Oncogenes. *Nature,* 307**,** 183-185.

LOSADA, A., HIRANO, M. & HIRANO, T. 1998. Identification of Xenopus SMC protein complexes required for sister chromatid cohesion. *Genes & Development,* 12**,** 1986-1997.

LOSADA, A., HIRANO, M. & HIRANO, T. 2002. Cohesin release is required for sister chromatid resolution, but not for condensin-mediated compaction, at the onset of mitosis. *Genes Dev,* 16**,** 3004-16.

LOSADA, A. & HIRANO, T. 2005. Dynamic molecular linkers of the genome: the first decade of SMC proteins. *Genes Dev,* 19**,** 1269-87.

LOSADA, A., YOKOCHI, T. & HIRANO, T. 2005. Functional contribution of Pds5 to cohesin-mediated cohesion in human cells and Xenopus egg extracts. *Journal of Cell Science,* 118**,** 2133-41.

LOSADA, A., YOKOCHI, T., KOBAYASHI, R. & HIRANO, T. 2000. Identification and characterization of SA/Scc3p subunits in the Xenopus and human cohesin complexes. *J Cell Biol,* 150**,** 405-16.

LOWERY, D. M., CLAUSER, K. R., HJERRILD, M., LIM, D., ALEXANDER, J., KISHI, K., ONG, S. E., GAMMELTOFT, S., CARR, S. A. & YAFFE, M. B. 2007. Proteomic screen defines the Polo-box domain interactome and identifies Rock2 as a Plk1 substrate. *Embo Journal,* 26**,** 2262-2273.

LUNDBERG, A. S. & WEINBERG, R. A. 1998. Functional inactivation of the retinoblastoma protein requires sequential modification by at least two distinct cyclin-cdk complexes. *Mol Cell Biol,* 18**,** 753-61.

LYONS, N. A. & MORGAN, D. O. 2011. Cdk1-Dependent Destruction of Eco1 Prevents Cohesion Establishment after S Phase. *Molecular Cell,* 42**,** 378-389.

MACUREK, L., LINDQVIST, A., LIM, D., LAMPSON, M. A., KLOMPMAKER, R., FREIRE, R., CLOUIN, C., TAYLOR, S. S., YAFFE, M. B. & MEDEMA, R. H. 2008. Polo-like kinase-1 is activated by aurora A to promote checkpoint recovery. *Nature,* 455**,** 119-U88.

MAFFINI, M., DENES, V., SONNENSCHEIN, C., SOTO, A. & GECK, P. 2008. APRIN is a unique Pds5 paralog with features of a chromatin regulator in hormonal differentiation. *Journal of Steroid Biochemistry and Molecular Biology,* 108**,** 32-43.

MALDONADO, M. & KAPOOR, T. M. 2011. Constitutive Mad1 targeting to kinetochores uncouples checkpoint signalling from chromosome biorientation. *Nat Cell Biol,* 13**,** 475-82.

MATSUOKA, S., BALLIF, B. A., SMOGORZEWSKA, A., MCDONALD, E. R., 3RD, HUROV, K. E., LUO, J., BAKALARSKI, C. E., ZHAO, Z., SOLIMINI, N., LERENTHAL, Y., SHILOH, Y., GYGI, S. P. & ELLEDGE, S. J. 2007. ATM and ATR substrate analysis reveals extensive protein networks responsive to DNA damage. *Science,* 316**,** 1160-6.

MATSUOKA, S., HUANG, M. & ELLEDGE, S. J. 1998. Linkage of ATM to cell cycle regulation by the Chk2 protein kinase. *Science,* 282**,** 1893-7.

MATSUOKA, S., ROTMAN, G., OGAWA, A., SHILOH, Y., TAMAI, K. & ELLEDGE, S. J. 2000. Ataxia telangiectasia-mutated phosphorylates Chk2 in vivo and in vitro. *Proc Natl Acad Sci U S A,* 97**,** 10389-94.

MAYER, M. L., GYGI, S. P., AEBERSOLD, R. & HIETER, P. 2001. Identification of RFC(Ctf18p, Ctf8p, Dcc1p): an alternative RFC complex required for sister chromatid cohesion in S. cerevisiae. *Mol Cell,* 7**,** 959-70.

MCALEENAN, A., CLEMENTE-BLANCO, A., CORDON-PRECIADO, V., SEN, N., ESTERAS, M., JARMUZ, A. & ARAGON, L. 2013. Post-replicative repair involves separase-dependent removal of the kleisin subunit of cohesin. *Nature,* 493**,** 250-4.

MEINHART, A., KAMENSKI, T., HOEPPNER, S., BAUMLI, S. & CRAMER, P. 2005. A structural perspective of CTD function. *Genes & Development,* 19**,** 1401-1415.

MELO, J. & TOCZYSKI, D. 2002. A unified view of the DNA-damage checkpoint. *Curr Opin Cell Biol,* 14**,** 237-45.

MENDENHALL, M. D. & HODGE, A. E. 1998. Regulation of cdc28 cyclin-dependent protein kinase activity during the cell cycle of the yeast Saccharomyces cerevisiae. *Microbiology and Molecular Biology Reviews,* 62**,** 1191-+.

MERALDI, P. & SORGER, P. K. 2005. A dual role for Bub1 in the spindle checkpoint and chromosome congression. *EMBO J,* 24**,** 1621-33.

METCALF, C. E. & WASSARMAN, D. A. 2006. DNA binding properties of TAF1 isoforms with two AT-hooks. *Journal of Biological Chemistry,* 281**,** 30015-30023.

MICHAELIS, C., CIOSK, R. & NASMYTH, K. 1997. Cohesins: Chromosomal proteins that prevent premature separation of sister chromatids. *Cell,* 91**,** 35-45.

MOSES, A. M., HERICHE, J. K. & DURBIN, R. 2007. Clustering of phosphorylation site recognition motifs can be exploited to predict the targets of cyclin-dependent kinase. *Genome Biol,* 8.

MUSACCHIO, A. & SALMON, E. D. 2007. The spindle-assembly checkpoint in space and time. *Nat Rev Mol Cell Biol,* 8**,** 379-93.

NAGASE, T., ISHIKAWA, K., KIKUNO, R., HIROSAWA, M., NOMURA, N. & OHARA, O. 1999. Prediction of the coding sequences of unidentified human genes. XV. The complete sequences of 100 new cDNA clones from brain which code for large proteins in vitro. *DNA Res,* 6**,** 337-45.

NAGASE, T., SEKI, N., ISHIKAWA, K., OHIRA, M., KAWARABAYASI, Y., OHARA, O., TANAKA, A., KOTANI, H., MIYAJIMA, N. & NOMURA, N. 1996. Prediction of the coding sequences of unidentified human genes. VI. The coding sequences of 80 new genes (KIAA0201-KIAA0280) deduced by analysis of cDNA clones from cell line KG-1 and brain. *DNA Res,* 3**,** 321-9, 341-54.

NAKAJIMA, H., TOYOSHIMA-MORIMOTO, F., TANIGUCHI, E. & NISHIDA, E. 2003. Identification of a consensus motif for Plk (Polo-like kinase) phosphorylation reveals Myt1 as a Plk1 substrate. *Journal of Biological Chemistry,* 278**,** 25277-80.

NASMYTH, K. 1993. Control of the yeast cell cycle by the Cdc28 protein kinase. *Current Opinion in Cell Biology,* 5**,** 166-179.

NASMYTH, K. 2001. Disseminating the genome: joining, resolving, and separating sister chromatids during mitosis and meiosis. *Annu Rev Genet,* 35**,** 673-745.

NASMYTH, K. 2005. How might cohesin hold sister chromatids together? *Philosophical Transactions of the Royal Society B-Biological Sciences,* 360**,** 483-496.

NASMYTH, K. & HAERING, C. H. 2005. The structure and function of SMC and kleisin complexes. *Annu Rev Biochem,* 74**,** 595-648.

NEEF, R., GRUNEBERG, U., KOPAJTICH, R., LI, X. L., NIGG, E. A., SILLJE, H. & BARR, F. A. 2007. Choice of Plk1 docking partners during mitosis and cytokinesis is controlled by the activation state of Cdk1. *Nature Cell Biology,* 9**,** 436-U132.

NIGG, E. A. 1993. Cellular substrates of p34(cdc2) and its companion cyclin-dependent kinases. *Trends Cell Biol,* 3**,** 296-301.

NIGG, E. A. 2001. Mitotic kinases as regulators of cell division and its checkpoints. *Nature Reviews Molecular Cell Biology,* 2**,** 21-32.

NISHIYAMA, T., LADURNER, R., SCHMITZ, J., KREIDL, E., SCHLEIFFER, A., BHASKARA, V., BANDO, M., SHIRAHIGE, K., HYMAN, A. A., MECHTLER, K. & PETERS, J. M. 2010. Sororin mediates sister chromatid cohesion by antagonizing Wapl. *Cell,* 143**,** 737-49.

OHBAYASHI, T., OIKAWA, K., YAMADA, K., NISHIDA-UMEHARA, C., MATSUDA, Y., SATOH, H., MUKAI, H., MUKAI, K. & KURODA, M. 2007. Unscheduled overexpression of human WAPL promotes chromosomal instability. *Biochem Biophys Res Commun,* 356**,** 699-704.

OIKAWA, K., OHBAYASHI, T., KIYONO, T., NISHI, H., ISAKA, K., UMEZAWA, A., KURODA, M. & MUKAI, K. 2004. Expression of a novel human gene, Human wings apart-like (hWAPL), is associated with cervical carcinogenesis and tumor progression. *Cancer Research,* 64**,** 3545-3549.

OLINS, A. L. & OLINS, D. E. 1974. Spheroid chromatin units (v bodies). *Science,* 183**,** 330-2.

OLINS, D. E. & OLINS, A. L. 2003. Chromatin history: our view from the bridge. *Nat Rev Mol Cell Biol,* 4**,** 809-14.

ONN, I., HEIDINGER-PAULI, J. M., GUACCI, V., UNAL, E. & KOSHLAND, D. E. 2008. Sister chromatid cohesion: a simple concept with a complex reality. *Annual Review of Cell & Developmental Biology,* 24**,** 105-29.

OTA, T., SUZUKI, Y., NISHIKAWA, T., OTSUKI, T., SUGIYAMA, T., IRIE, R., WAKAMATSU, A., HAYASHI, K., SATO, H., NAGAI, K., KIMURA, K., MAKITA, H., SEKINE, M., OBAYASHI, M., NISHI, T., SHIBAHARA, T., TANAKA, T., ISHII, S., YAMAMOTO, J., SAITO, K., KAWAI, Y., ISONO, Y., NAKAMURA, Y., NAGAHARI, K., MURAKAMI, K., YASUDA, T., IWAYANAGI, T., WAGATSUMA, M., SHIRATORI, A., SUDO, H., HOSOIRI, T., KAKU, Y., KODAIRA, H., KONDO, H., SUGAWARA, M., TAKAHASHI, M., KANDA, K., YOKOI, T., FURUYA, T., KIKKAWA, E., OMURA, Y., ABE, K., KAMIHARA, K., KATSUTA, N., SATO, K., TANIKAWA, M., YAMAZAKI, M., NINOMIYA, K., ISHIBASHI, T., YAMASHITA, H., MURAKAWA, K., FUJIMORI, K., TANAI, H., KIMATA, M., WATANABE, M., HIRAOKA, S., CHIBA, Y., ISHIDA, S., ONO, Y., TAKIGUCHI, S., WATANABE, S., YOSIDA, M., HOTUTA, T., KUSANO, J., KANEHORI, K., TAKAHASHI-FUJII, A., HARA, H., TANASE, T. O., NOMURA, Y., TOGIYA, S., KOMAI, F., HARA, R., TAKEUCHI, K., ARITA, M., IMOSE, N., MUSASHINO, K., YUUKI, H., OSHIMA, A., SASAKI, N., AOTSUKA, S., YOSHIKAWA, Y., MATSUNAWA, H., ICHIHARA, T., SHIOHATA, N., SANO, S., MORIYA, S., MOMIYAMA, H., SATOH, N., TAKAMI, S., TERASHIMA, Y., SUZUKI, O., NAKAGAWA, S., SENOH, A., MIZOGUCHI, H., GOTO, Y., SHIMIZU, F., WAKEBE, H., HISHIGAKI, H., WATANABE, T., SUGIYAMA, A., et al. 2004. Complete sequencing and characterization of 21,243 full-length human cDNAs. *Nat Genet,* 36**,** 40-5.

PANIZZA, S., TANAKA, T., HOCHWAGEN, A., EISENHABER, F. & NASMYTH, K. 2000. Pds5 cooperates with cohesin in maintaining sister chromatid cohesion. *Current Biology,* 10**,** 1557-64.

PETERS, J.-M., TEDESCHI, A. & SCHMITZ, J. 2008. The cohesin complex and its roles in chromosome biology. *Genes & Development,* 22**,** 3089-114.

PETERS, J. M. 2002. The anaphase-promoting complex: Proteolysis in mitosis and beyond. *Molecular Cell,* 9**,** 931-943.

PETERS, J. M. 2006. The anaphase promoting complex/cyclosome: a machine designed to destroy. *Nature Reviews Molecular Cell Biology,* 7**,** 644-656.

PEZZI, N., PRIETO, I., KREMER, L., JURADO, L. A. P., VALERO, C., DEL MAZO, J., MARTINEZ, C. & BARBERO, J. L. 2000. STAG3, a novel gene encoding a protein involved in meiotic chromosome pairing and location of STAG3-related genes flanking the Williams-Beuren syndrome deletion. *Faseb Journal,* 14**,** 581-592.

PFAU, S. J. & AMON, A. 2012. Chromosomal instability and aneuploidy in cancer: from yeast to man. *EMBO Rep,* 13**,** 515-27.

PRINZ, S., HWANG, E. S., VISINTIN, R. & AMON, A. 1998. The regulation of Cdc20 proteolysis reveals a role for APC components Cdc23 and Cdc27 during S phase and early mitosis. *Curr Biol,* 8**,** 750-60.

QIAN, Y. W., ERIKSON, E. & MALLER, J. L. 1999. Mitotic effects of a constitutively active mutant of the Xenopus polo-like kinase Plx1. *Mol Cell Biol,* 19**,** 8625-8632.

RANKIN, S., AYAD, N. G. & KIRSCHNER, M. W. 2005. Sororin, a substrate of the anaphase-promoting complex, is required for sister chromatid cohesion in vertebrates (vol 18, pg 185, 2005). *Molecular Cell,* 18**,** 609-609.

RIEDEL, C. G., KATIS, V. L., KATOU, Y., MORI, S., ITOH, T., HELMHART, W., GÁLOVÁ, M., PETRONCZKI, M., GREGAN, J., CETIN, B., MUDRAK, I., OGRIS, E., MECHTLER, K., PELLETIER, L., BUCHHOLZ, F., SHIRAHIGE, K. & NASMYTH, K. 2006. Protein phosphatase 2A protects centromeric sister chromatid cohesion during meiosis I. *Nature,* 441**,** 53-61.

RIEDER, C. L., COLE, R. W., KHODJAKOV, A. & SLUDER, G. 1995. The Checkpoint Delaying Anaphase in Response to Chromosome Monoorientation Is Mediated by an Inhibitory Signal Produced by Unattached Kinetochores. *Journal of Cell Biology,* 130**,** 941-948.

RIEDER, C. L., SCHULTZ, A., COLE, R. & SLUDER, G. 1994. Anaphase onset in vertebrate somatic cells is controlled by a checkpoint that monitors sister kinetochore attachment to the spindle. *J Cell Biol,* 127**,** 1301-10.

RIVERA, T. & LOSADA, A. 2009. Shugoshin regulates cohesion by driving relocalization of PP2A in Xenopus extracts. *Chromosoma,* 118**,** 223-33.

ROLEF BEN-SHAHAR, T., HEEGER, S., LEHANE, C., EAST, P., FLYNN, H., SKEHEL, M. & UHLMANN, F. 2008. Eco1-dependent cohesin acetylation during establishment of sister chromatid cohesion. *Science,* 321**,** 563-6.

ROWLAND, B. D., ROIG, M. B., NISHINO, T., KURZE, A., ULUOCAK, P., MISHRA, A., BECKOUET, F., UNDERWOOD, P., METSON, J., IMRE, R., MECHTLER, K., KATIS, V. L. & NASMYTH, K. 2009. Building sister chromatid cohesion: smc3 acetylation counteracts an antiestablishment activity. *Mol Cell,* 33**,** 763-74.

RUCHAUD, S., CARMENA, M. & EARNSHAW, W. C. 2007. Chromosomal passengers: conducting cell division. *Nat Rev Mol Cell Biol,* 8**,** 798-812.

SANCHEZ, Y., WONG, C., THOMA, R. S., RICHMAN, R., WU, Z., PIWNICA-WORMS, H. & ELLEDGE, S. J. 1997. Conservation of the Chk1 checkpoint pathway in mammals: linkage of DNA damage to Cdk regulation through Cdc25. *Science,* 277**,** 1497-501.

SCHMITZ, J., WATRIN, E., LENART, P., MECHTLER, K. & PETERS, J. M. 2007. Sororin is required for stable binding of cohesin to chromatin and for sister chromatid cohesion in interphase. *Current Biology,* 17**,** 630-636.

SCHWOB, E., BOHM, T., MENDENHALL, M. D. & NASMYTH, K. 1994. The B-type cyclin kinase inhibitor p40SIC1 controls the G1 to S transition in S. cerevisiae. *Cell,* 79**,** 233-44.

SEKI, A., COPPINGER, J. A., JANG, C. Y., YATES, J. R. & FANG, G. W. 2008. Bora and the kinase Aurora A cooperatively activate the kinase Plk1 and control mitotic entry. *Science,* 320**,** 1655-1658.

SHINTOMI, K. & HIRANO, T. 2009. Releasing cohesin from chromosome arms in early mitosis: opposing actions of Wapl-Pds5 and Sgo1. *Genes & Development,* 23**,** 2224-36.

SHIOMI, Y., SHINOZAKI, A., NAKADA, D., SUGIMOTO, K., USUKURA, J., OBUSE, C. & TSURIMOTO, T. 2002. Clamp and clamp loader structures of the human checkpoint protein complexes, Rad9-1-1 and Rad17-RFC. *Genes Cells,* 7**,** 861-8.

SIMON, M., SERAPHIN, B. & FAYE, G. 1986. Kin28, a Yeast Split Gene Coding for a Putative Protein-Kinase Homologous to Cdc28. *Embo Journal,* 5**,** 2697-2701.

SIMONETTA, M., MANZONI, R., MOSCA, R., MAPELLI, M., MASSIMILIANO, L., VINK, M., NOVAK, B., MUSACCHIO, A. & CILIBERTO, A. 2009. The influence of catalysis on mad2 activation dynamics. *PLoS Biol,* 7**,** e10.

SKIBBENS, R. V. 2000. Holding your own: establishing sister chromatid cohesion. *Genome Res,* 10**,** 1664-71.

SKIBBENS, R. V. 2009. Establishment of Sister Chromatid Cohesion Minireview. *Current Biology,* 19**,** R1126-R1132.

SKIBBENS, R. V. 2011. Sticking a fork in cohesin--it's not done yet! *Trends in Genetics,* 27**,** 499-506.

SKIBBENS, R. V., CORSON, L. B., KOSHLAND, D. & HIETER, P. 1999. Ctf7p is essential for sister chromatid cohesion and links mitotic chromosome structure to the DNA replication machinery. *Genes & Development,* 13**,** 307-19.

SKOWYRA, D., CRAIG, K. L., TYERS, M., ELLEDGE, S. J. & HARPER, J. W. 1997. F-box proteins are receptors that recruit phosphorylated substrates to the SCF ubiquitin-ligase complex. *Cell,* 91**,** 209-219.

SMITS, V. A., WARMERDAM, D. O., MARTIN, Y. & FREIRE, R. 2010. Mechanisms of ATR-mediated checkpoint signalling. *Front Biosci,* 15**,** 840-53.

STEAD, K., AGUILAR, C., HARTMAN, T., DREXEL, M., MELUH, P. & GUACCI, V. 2003. Pds5p regulates the maintenance of sister chromatid cohesion and is sumoylated to promote the dissolution of cohesion. *Journal of Cell Biology,* 163**,** 729-741.

STROM, L., LINDROOS, H. B., SHIRAHIGE, K. & SJOGREN, C. 2004. Postreplicative recruitment of cohesin to double-strand breaks is required for DNA repair. *Molecular Cell,* 16**,** 1003-1015.

SUMARA, I., VORLAUFER, E., GIEFFERS, C., PETERS, B. H. & PETERS, J. M. 2000. Characterization of vertebrate cohesin complexes and their regulation in prophase. *Journal of Cell Biology,* 151**,** 749-761.

SUMARA, I., VORLAUFER, E., STUKENBERG, P. T., KELM, O., REDEMANN, N., NIGG, E. A. & PETERS, J.-M. 2002. The dissociation of cohesin from chromosomes in prophase is regulated by Polo-like kinase. *Molecular Cell,* 9**,** 515-25.

SUNKEL, C. E. & GLOVER, D. M. 1988. Polo, a Mitotic Mutant of Drosophila Displaying Abnormal Spindle Poles. *Journal of Cell Science,* 89**,** 25-38.

SUTANI, T., KAWAGUCHI, T., KANNO, R., ITOH, T. & SHIRAHIGE, K. 2009. Budding yeast Wpl1(Rad61)-Pds5 complex counteracts sister chromatid cohesion-establishing reaction. *Curr Biol,* 19**,** 492-7.

TAKAHASHI, T. S., YIU, P., CHOU, M. F., GYGI, S. & WALTER, J. C. 2004. Recruitment of Xenopus Scc2 and cohesin to chromatin requires the pre-replication complex. *Nature Cell Biology,* 6**,** 991-6.

TAKAKI, T., TRENZ, K., COSTANZO, V. & PETRONCZKI, M. 2008. Polo-like kinase 1 reaches beyond mitosis--cytokinesis, DNA damage response, and development. *Curr Opin Cell Biol,* 20**,** 650-60.

TANAKA, K., HAO, Z., KAI, M. & OKAYAMA, H. 2001. Establishment and maintenance of sister chromatid cohesion in fission yeast by a unique mechanism. *EMBO Journal,* 20**,** 5779-90.

TAYLOR, S. & PETERS, J. M. 2008. Polo and Aurora kinases: lessons derived from chemical biology. *Curr Opin Cell Biol,* 20**,** 77-84.

TERADA, Y., TATSUKA, M., SUZUKI, F., YASUDA, Y., FUJITA, S. & OTSU, M. 1998. AIM-1: a mammalian midbody-associated protein required for cytokinesis. *EMBO J,* 17**,** 667-76.

TOHE, A., TANAKA, K., UESONO, Y. & WICKNER, R. B. 1988. Pho85, a Negative Regulator of the Pho System, Is a Homolog of the Protein-Kinase Gene, Cdc28, of Saccharomyces-Cerevisiae. *Molecular & General Genetics,* 214**,** 162-164.

TOMONAGA, T., NAGAO, K., KAWASAKI, Y., FURUYA, K., MURAKAMI, A., MORISHITA, J., YUASA, T., SUTANI, T., KEARSEY, S. E., UHLMANN, F., NASMYTH, K. & YANAGIDA, M. 2000. Characterization of fission yeast cohesin: essential anaphase proteolysis of Rad21 phosphorylated in the S phase. *Genes Dev,* 14**,** 2757-70.

TOTH, A., CIOSK, R., UHLMANN, F., GALOVA, M., SCHLEIFFER, A. & NASMYTH, K. 1999. Yeast Cohesin complex requires a conserved protein, Eco1p(Ctf7), to establish cohesion between sister chromatids during DNA replication. *Genes & Development,* 13**,** 320-333.

TOYOSHIMA-MORIMOTO, F., TANIGUCHI, E. & NISHIDA, E. 2002. Plk1 promotes nuclear translocation of human Cdc25C during prophase. *EMBO Rep,* 3**,** 341-8.

TOYOSHIMA-MORIMOTO, F., TANIGUCHI, E., SHINYA, N., IWAMATSU, A. & NISHIDA, E. 2001. Polo-like kinase 1 phosphorylates cyclin B1 and targets it to the nucleus during prophase. *Nature,* 410**,** 215-20.

TURNER, B. M. 2007. Defining an epigenetic code. *Nature Cell Biology,* 9**,** 2-6.

UBERSAX, J. A., WOODBURY, E. L., QUANG, P. N., PARAZ, M., BLETHROW, J. D., SHAH, K., SHOKAT, K. M. & MORGAN, D. O. 2003. Targets of the cyclin-dependent kinase Cdk1. *Nature,* 425**,** 859-864.

UHLMANN, F., LOTTSPEICH, F. & NASMYTH, K. 1999. Sister-chromatid separation at anaphase onset is promoted by cleavage of the cohesin subunit Scc1. *Nature,* 400**,** 37-42.

UHLMANN, F., WERNIC, D., POUPART, M. A., KOONIN, E. V. & NASMYTH, K. 2000. Cleavage of cohesin by the CD clan protease separin triggers anaphase in yeast. *Cell,* 103**,** 375-86.

UNAL, E., ARBEL-EDEN, A., SATTLER, U., SHROFF, R., LICHTEN, M., HABER, J. E. & KOSHLAND, D. 2004. DNA damage response pathway uses histone modification to assemble a double-strand break-specific cohesin domain. *Molecular Cell,* 16**,** 991-1002.

UNAL, E., HEIDINGER-PAULI, J. M., KIM, W., GUACCI, V., ONN, I., GYGI, S. P. & KOSHLAND, D. E. 2008. A molecular determinant for the establishment of sister chromatid cohesion. *Science,* 321**,** 566-9.

UNAL, E., HEIDINGER-PAULI, J. M. & KOSHLAND, D. 2007. DNA double-strand breaks trigger genome-wide sister-chromatid cohesion through Eco1 (Ctf7). *Science,* 317**,** 245-248.

VAN HEEMST, D., JAMES, F., POGGELER, S., BERTEAUX-LECELLIER, V. & ZICKLER, D. 1999. Spo76p is a conserved chromosome morphogenesis protein that links the mitotic and meiotic programs. *Cell,* 98**,** 261-271.

VAUR, S., FEYTOUT, A., VAZQUEZ, S. & JAVERZAT, J. P. 2012. Pds5 promotes cohesin acetylation and stable cohesin-chromosome interaction. *EMBO Rep,* 13**,** 645-52.

VERNI, F., GANDHI, R., GOLDBERG, M. L. & GATTI, M. 2000. Genetic and molecular analysis of wings apart-like (wapl), a gene controlling heterochromatin organization in Drosophila melanogaster. *Genetics,* 154**,** 1693-1710.

WAIZENEGGER, I. C., HAUF, S., MEINKE, A. & PETERS, J. M. 2000. Two distinct pathways remove mammalian cohesin from chromosome arms in prophase and from centromeres in anaphase. *Cell,* 103**,** 399-410.

WANG, F., ULYANOVA, N. P., DAUM, J. R., PATNAIK, D., KATENEVA, A. V., GORBSKY, G. J. & HIGGINS, J. M. 2012. Haspin inhibitors reveal centromeric functions of Aurora B in chromosome segregation. *J Cell Biol,* 199**,** 251-68.

WANG, S.-W., READ, R. L. & NORBURY, C. J. 2002. Fission yeast Pds5 is required for accurate chromosome segregation and for survival after DNA damage or metaphase arrest. *Journal of Cell Science,* 115**,** 587-98.

WANG, Z. H. & CHRISTMAN, M. F. 2001. Replication-related activities establish cohesion between sister chromatids. *Cell Biochemistry and Biophysics,* 35**,** 289-301.

WATANABE, N., ARAI, H., NISHIHARA, Y., TANIGUCHI, M., WATANABE, N., HUNTER, T. & OSADA, H. 2004. M-phase kinases induce phospho-dependent ubiquitination of somatic Wee1 by SCFbeta-TrCP. *Proc Natl Acad Sci U S A,* 101**,** 4419-24.

WEGENER, A. D. & JONES, L. R. 1984. Phosphorylation-induced mobility shift in phospholamban in sodium dodecyl sulfate-polyacrylamide gels. Evidence for a protein structure consisting of multiple identical phosphorylatable subunits. *J Biol Chem,* 259**,** 1834-41.

WEI, W., AYAD, N. G., WAN, Y., ZHANG, G. J., KIRSCHNER, M. W. & KAELIN, W. G., JR. 2004. Degradation of the SCF component Skp2 in cell-cycle phase G1 by the anaphase-promoting complex. *Nature,* 428**,** 194-8.

WEITZER, S., LEHANE, C. & UHLMANN, F. 2003. A model for ATP hydrolysis-dependent binding of cohesin to DNA. *Current Biology,* 13**,** 1930-1940.

WHITE, G. E. & ERICKSON, H. P. 2006. Sequence divergence of coiled coils - structural rods, myosin filament packing, and the extraordinary conservation of cohesins. *Journal of Structural Biology,* 154**,** 111-121.

WITTENBERG, C. & REED, S. I. 1989. Conservation of Function and Regulation within the Cdc28/Cdc2 Protein-Kinase Family - Characterization of the Human Cdc2hs Protein-Kinase in Saccharomyces-Cerevisiae. *Mol Cell Biol,* 9**,** 4064-4068.

YAMAGUCHI, T., GOTO, H., YOKOYAMA, T., SILLJE, H., HANISCH, A., ULDSCHMID, A., TAKAI, Y., OGURI, T., NIGG, E. A. & INAGAKI, M. 2005. Phosphorylation by Cdk1 induces Plk1-mediated vimentin phosphorylation during mitosis. *J Cell Biol,* 171**,** 431-6.

YAO, S., NEIMAN, A. & PRELICH, G. 2000. BUR1 and BUR2 encode a divergent cyclin-dependent kinase-cyclin complex important for transcription in vivo. *Mol Cell Biol,* 20**,** 7080-7.

YE, X. S., FINCHER, R. R., TANG, A. & OSMANI, S. A. 1997. The G2/M DNA damage checkpoint inhibits mitosis through Tyr15 phosphorylation of p34cdc2 in Aspergillus nidulans. *EMBO J,* 16**,** 182-92.

YU, H. T. 2002. Regulation of APC-Cdc20 by the spindle checkpoint. *Curr Opin Cell Biol,* 14**,** 706-714.

ZACHARIAE, W. & NASMYTH, K. 1999. Whose end is destruction: cell division and the anaphase-promoting complex. *Genes & Development,* 13**,** 2039-2058.

ZHANG, B., CHANG, J., FU, M., HUANG, J., KASHYAP, R., SALAVAGGIONE, E., JAIN, S., KULKARNI, S., DEARDORFF, M. A., UZIELLI, M. L. G., DORSETT, D., BEEBE, D. C., JAY, P. Y., HEUCKEROTH, R. O., KRANTZ, I. & MILBRANDT, J. 2009a. Dosage effects of cohesin regulatory factor PDS5 on mammalian development: implications for cohesinopathies.[Erratum appears in PLoS One. 2009;4(5). doi: 10.1371/annotation/ea5b7eb5-5087-448a-8325-c8efff1f54d9 Note: Shashikant, Kulkarni [corrected to Kulkarni, Shashikant]]. *PLoS ONE [Electronic Resource],* 4**,** e5232.

ZHANG, B., JAIN, S., SONG, H., FU, M., HEUCKEROTH, R. O., ERLICH, J. M., JAY, P. Y. & MILBRANDT, J. 2007. Mice lacking sister chromatid cohesion protein PDS5B exhibit developmental abnormalities reminiscent of Cornelia de Lange syndrome. *Development,* 134**,** 3191-201.

ZHANG, J. L., SHI, X. M., LI, Y. H., KIM, B. J., JIA, J. L., HUANG, Z. W., YANG, T., FU, X. Y., JUNG, S. Y., WANG, Y., ZHANG, P. M., KIM, S. T., PAN, X. W. & QIN, J. 2008. Acetylation of Smc3 by Eco1 is required for S phase sister chromatid cohesion in both human and yeast. *Molecular Cell,* 31**,** 143-151.

ZHANG, N., PANIGRAHI, A. K., MAO, Q. & PATI, D. 2011. Interaction of Sororin protein with polo-like kinase 1 mediates resolution of chromosomal arm cohesion. *J Biol Chem,* 286**,** 41826-37.

ZHANG, N. G. & PATI, D. 2012. Sororin is a master regulator of sister chromatid cohesion and separation. *Cell Cycle,* 11**,** 2073-2083.

ZHANG, X., CHEN, Q., FENG, J., HOU, J., YANG, F., LIU, J., JIANG, Q. & ZHANG, C. 2009b. Sequential phosphorylation of Nedd1 by Cdk1 and Plk1 is required for targeting of the gammaTuRC to the centrosome. *J Cell Sci,* 122**,** 2240-51.

ZHANG, Z., REN, Q., YANG, H., CONRAD, M. N., GUACCI, V., KATENEVA, A. & DRESSER, M. E. 2005. Budding yeast PDS5 plays an important role in meiosis and is required for sister chromatid cohesion. *Molecular Microbiology,* 56**,** 670-80.

ZHAO, H. & PIWNICA-WORMS, H. 2001. ATR-mediated checkpoint pathways regulate phosphorylation and activation of human Chk1. *Mol Cell Biol,* 21**,** 4129-39.

ZURHAUSEN, H. 1996. Papillomavirus infections - A major cause of human cancers. *Biochimica Et Biophysica Acta-Reviews on Cancer,* 1288**,** F55-F78.

Appendix

Supplemental data

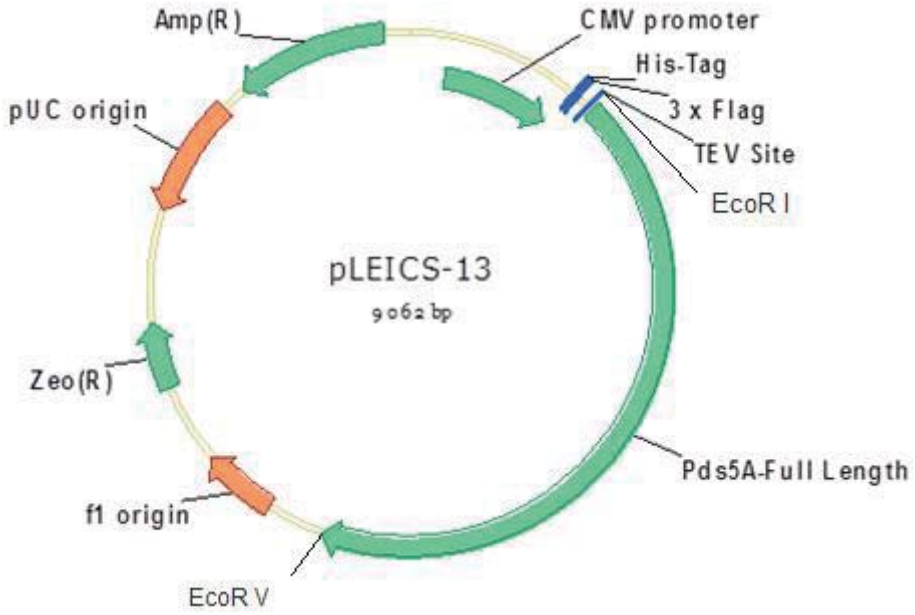

Figure A.1: Circular map of pLEICS-13 (pCMV).

Human Pds5A (full length) was cloned into pLEICS-13 (pCMV) mammalian expression vector by Dr. Xiaowen Yang (Protein Expression Laboratory (Protex), Biochemistry department, University of Leicester), using In-Fusion cloning and was digested with EcoR I and EcoR V. The peptide sequence of the Flag-tag located at the N-terminus of the Pds5A.

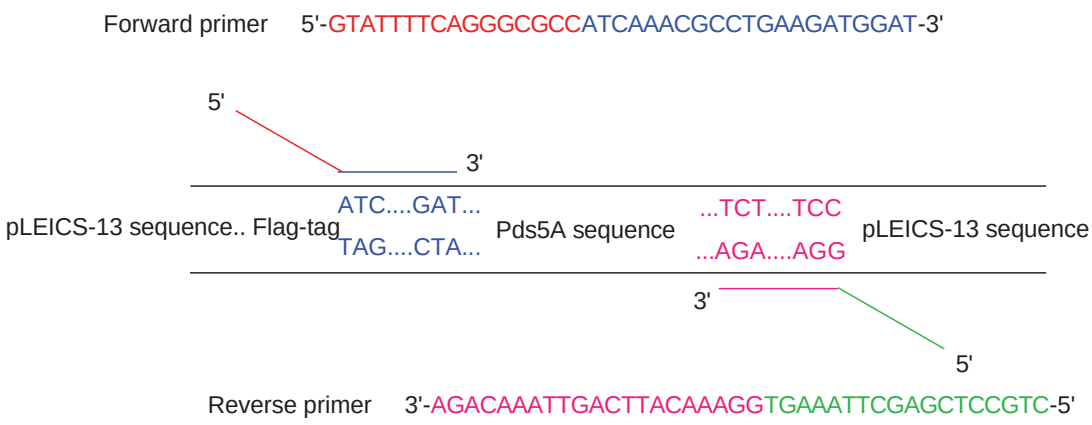

Figure A.2: An example of generation of Flag-tagged Pds5A (full length).

Pds5A cDNA sequence (full length) forward and reverse primers were designed with overhang appropriate 5′ vector homology region, using NCBI primer designing tool (http://www.ncbi.nlm.nih.gov/tools/primer-blast/). Pds5A cDNA sequence was amplified and cleaned as described in material and methods. The cloning was performed by Dr. Xiaowen Yang using the In-Fusion technique (Protein Expression Laboratory (Protex), Department of Biochemistry, University of Leicester). Blue and pink colours indicate the Pds5A homology region, whereas red and green mark the vector homology region.

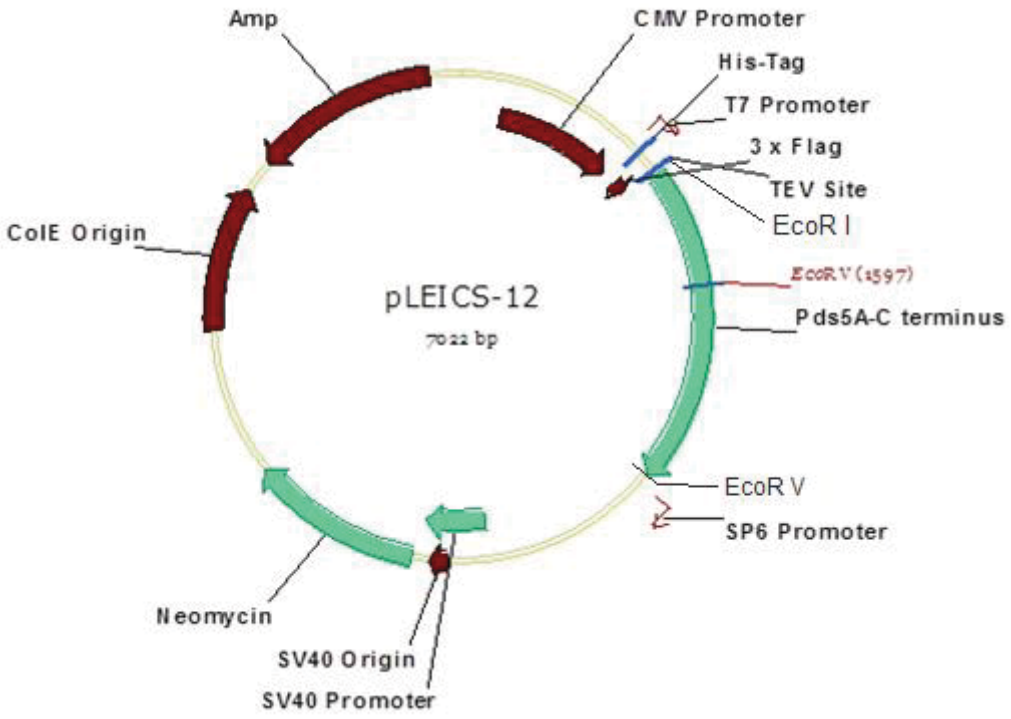

Figure A.3: Circular map of pLEICS-12 (pCMV).

Truncated human Pds5A (C-terminal fragment) was cloned into pLEICS-12 (pCMV) mammalian expression vector by Dr. Xiaowen Yang (Protein Expression Laboratory (Protex), Biochemistry department, University of Leicester), using In-Fusion cloning and was digested with EcoR V and EcoR I. The peptide sequence of the Flag-tag located at the N-terminus of the Pds5A fragment.

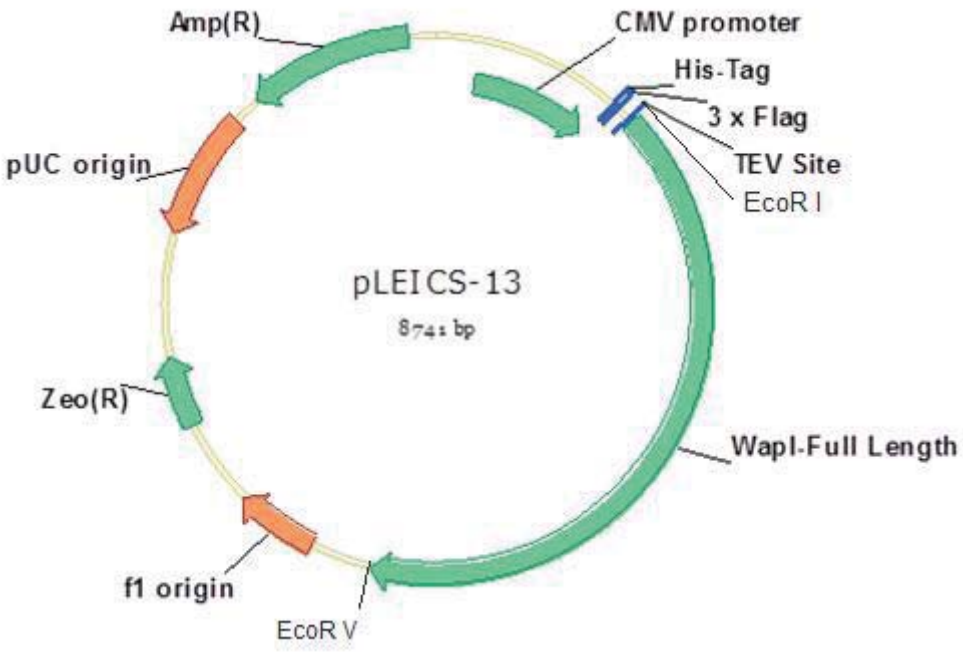

Figure A.4: Circular map of pLEICS-13 (pCMV).

Human Wapl (full length) was cloned into pLEICS-12 (pCMV) mammalian expression vector by Dr. Xiaowen Yang (Protein Expression Laboratory (Protex), Biochemistry department, University of Leicester), using In-Fusion cloning and was digested with EcoR V and EcoR I. The peptide sequence of the Flag-tag located at the N-terminus of the Wapl.

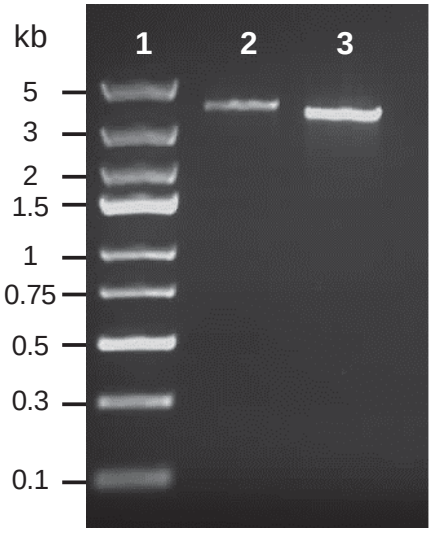

Figure A.5: Succesful amplification of full length Pds5A and Wapl.

Separation of PCR amplicons of full length Pds5A and Wapl fragments by 1 % agarose gel electrophoresis after purification of DNA fragments as described in material and methods. Lanes 1: DNA ladder (1 kb); Lanes 2: Pds5A (3.8 kb); Lanes 3: Wapl (3.6 kb).

```
   1  MDFTAQPKPATALCGVVSADGKIAYPPGVKEITDKITTDEMIKRLKMVVK   50
  51  TFMDMDQDSEDEKQQYLPLALHLASEFFLRNPNKDVRLLVACCLADIFRI  100
 101  YAPEAPYTSHDKLKDIFLFITRQLKGLEDTKSPQFNRYFYLLENLAWVKS  150
 151  YNICFELEDCNEIFIQLFRTLFSVINNSHNKKVQMHMLDLMSSIIMEGDG  200
 201  VTQELLDSILINLIPAHKNLNKQSFDLAKVLLKRTVQTIEACIANFFNQV  250
 251  LVLGRSSVSDLSEHVFDLIQELFAIDPHLLLSVMPQLEFKLKSNDGEERL  300
 301  AVVRLLAKLFGSKDSDLATQNRPLWQCFLGRFNDIHVPVRLESVKFASHC  350
 351  LMNHPDLAKDLTEYLKVRSHDPEEAIRHDVIVTIITAAKRDLALVNDQLL  400
 401  GFVRERTLDKRWRVRKEAMMGLAQLYKKYCLHGEAGKEAAEKVSWIKDKL  450
 451  LHIYYQNSIDDKLLVEKIFAQYLVPHNLETEERMKCLYYLYASLDPNAVK  500
 501  ALNEMWKCQNMLRSHVRELLDLHKQPTSEANCSAMFGKLMTIAKNLPDPG  550
 551  KAQDFVKKFNQVLGDDEKLRSQLELLISPTCSCKQADICVREIARKLANP  600
 601  KQPTNPFLEMVKFLLERIAPVHIDSEAISALVKLMNKSIEGTADDEEEGV  650
 651  SPDTAIRSGLELLKVLSFTHPTSFHSAETYESLLQCLRMEDDKVAEAAIQ  700
 701  IFRNTGHKIETDLPQIRSTLIPILHQKAKRGTPHQAKQAVHCIHAIFTNK  750
 751  EVQLAQIFEPLSRSLNADVPEQLITPLVSLGHISMLAPDQFASPMKSVVA  800
 801  NFIVKDLLMNDRSTGEKNGKLWSPDEEVSPEVLAKVQAIKLLVRWLLGMK  850
 851  NNQSKSANSTLRLLSAMLVSEGDLTEQKRISKSDMSRLRLAAGSAIMKLA  900
 901  QEPCYHEIITPEQFQLCALVINDECYQVRQIFAQKLHKALVKLLLPLEYM  950
 951  AIFALCAKDPVKERRAHARQCLLKNISIRREYIKQNPMATEKLLSLLPEY 1000
1001  VVPYMIHLLAHDPDFTRSQDVDQLRDIKECLWFMLEVLMTKNENNSHAFM 1050
1051  KKMAENIKLTRDAQSPDESKTNEKLYTVCDVALCVINSKSALCNADSPKD 1100
1101  PVLPMKFFTQPEKDFCNDKSYISEETRVLLLTGKPKPAGVLGAVNKPLSA 1150
1151  TGRKPYVRSTGTETGSNINVNSELNPSTGNRSREQSSEAAETGVSENEEN 1200
1201  PVRIISVTPVKNIDPVKNKEINSDQATQGNISSDRGKKRTVTAAGAENIQ 1250
1251  QKTDEKVDESGPPAPSKPRRGRRPKSESQGNATKNDDLNKPINKGRKRAA 1300
1301  VGQESPGGLEAGNAKAPKLQDLAKKAAPAERQIDLQR               1337
```

Figure A.6: Nuclear localization signals (NLSs) prediction in human Pds5A.

The protein sequence alignment of human Pds5A (Accession No in GenBank database is AAI14219.1) contains one nuclear localization signal (underlined) at the C-terminus predicted by NucPred-Predicting Nuclear Localization of Proteins (http://www.sbc.su.se/~maccallr/nucpred/).

```
   1  MAHSKTRTNDGKITYPPGVKEISDKISKEEMVRRLKMVVKTFMDMDQDSE    50
  51  EEKELYLNLALHLASDFFLKHPDKDVRLLVACCLADIFRIYAPEAPYTSP   100
 101  DKLKDIFMFITRQLKGLEDTKSPQFNRYFYLLENIAWVKSYNICFELEDS   150
 151  NEIFTQLYRTLFSVINNGHNQKVHMHMVDLMSSIICEGDTVSQELLDTVL   200
 201  VNLVPAHKNLNKQAYDLAKALLKRTAQAIEPYITNFFNQVLMLGKTSISD   250
 251  LSEHVFDLILELYNIDSHLLLSVLPQLEFKLKSNDNEERLQVVKLLAKMF   300
 301  GAKDSELASQNKPLWQCYLGRFNDIHVPIRLECVKFASHCLMNHPDLAKD   350
 351  LTEYLKVRSHDPEEAIRHDVIVSIVTAAKKDILLVNDHLLNFVRERTLDK   400
 401  RWRVRKEAMMGLAQIYKKYALQSAAGKDAAKQIAWIKDKLLHIYYQNSID   450
 451  DRLLVERIFAQYMVPHNLETTERMKCLYYLYATLDLNAVKALNEMWKCQN   500
 501  LLRHQVKDLLDLIKQPKTDASVKAIFSKVMVITRNLPDPGKAQDFMKKFT   550
 551  QVLEDDEKIRKQLEVLVSPTCSCKQAEGCVREITKKLGNPKQPTNPFLEM   600
 601  IKFLLERIAPVHIDTESISALIKQVNKSIDGTADDEDEGVPTDQAIRAGL   650
 651  ELLKVLSFTHPISFHSAETFESLLACLKMDDEKVAEAALQIFKNTGSKIE   700
 701  EDFPHIRSALLPVLHHKSKKGPPRQAKYAIHCIHAIFSSKETQFAQIFEP   750
 751  LHKSLDPSNLEHLITPLVTIGHIALLAPDQFAAPLKSLVATFIVKDLLMN   800
 801  DRLPGKKTTKLWVPDEEVSPETMVKIQAIKMMVRWLLGMKNNHSKSGTST   850
 851  LRLLTTILHSDGDLTEQGKISKPDMSRLRLAAGSAIVKLAQEPCYHEIIT   900
 901  LEQYQLCALAINDECYQVRQVFAQKLHKGLSRLRLPLEYMAICALCAKDP   950
 951  VKERRAHARQCLVKNINVRREYLKQHAAVSEKLLSLLPEYVVPYTIHLLA  1000
1001  HDPDYVKVQDIEQLKDVKECLWFVLEILMAKNENNSHAFIRKMVENIKQT  1050
1051  KDAQGPDDAKMNEKLYTVCDVAMNIIMSKSTTYSLESPKDPVLPARFFTQ  1100
1101  PDKNFSNTKNYLPPEMKSFFTPGKPKTTNVLGAVNKPLSSAGKQSQTKSS  1150
1151  RMETVSNASSSSNPSSPGRIKGRLDSSEMDHSENEDYTMSSPLPGKKSDK  1200
1201  RDDSDLVRSELEKPRGRKKTPVTEQEEKLGMDDLTKLVQEQKPKGSQRSR  1250
1251  KRGHTASESDEQQWPEEKRLKEDILENEDEQNSPPKKGKRGRPPKPLGGG  1300
1301  TPKEEPTMKTSKKGSKKKSGPPAPEEEEEEERQSGNTEQKSKSKQHRVSR  1350
1351  RAQQRAESPESSAIESTQSTPQKGRGRPSKTPSPSQPKKNVRVGRSKQAA  1400
1401  TKENDSSEEVDVFQGSSPVDDIPQEETEEEEVSTVNVRRRSAKRERR     1447
```

Figure A.7: Nuclear localization signals (NLSs) prediction in human Pds5B.

The protein sequence alignment of human Pds5B (NCBI Reference Sequence: NP_055847.1) contains three nuclear localization signals (underlined) at the C-terminus predicted by NucPred-Predicting Nuclear Localization of Proteins, (http://www.sbc.su.se/~maccallr/nucpred/).

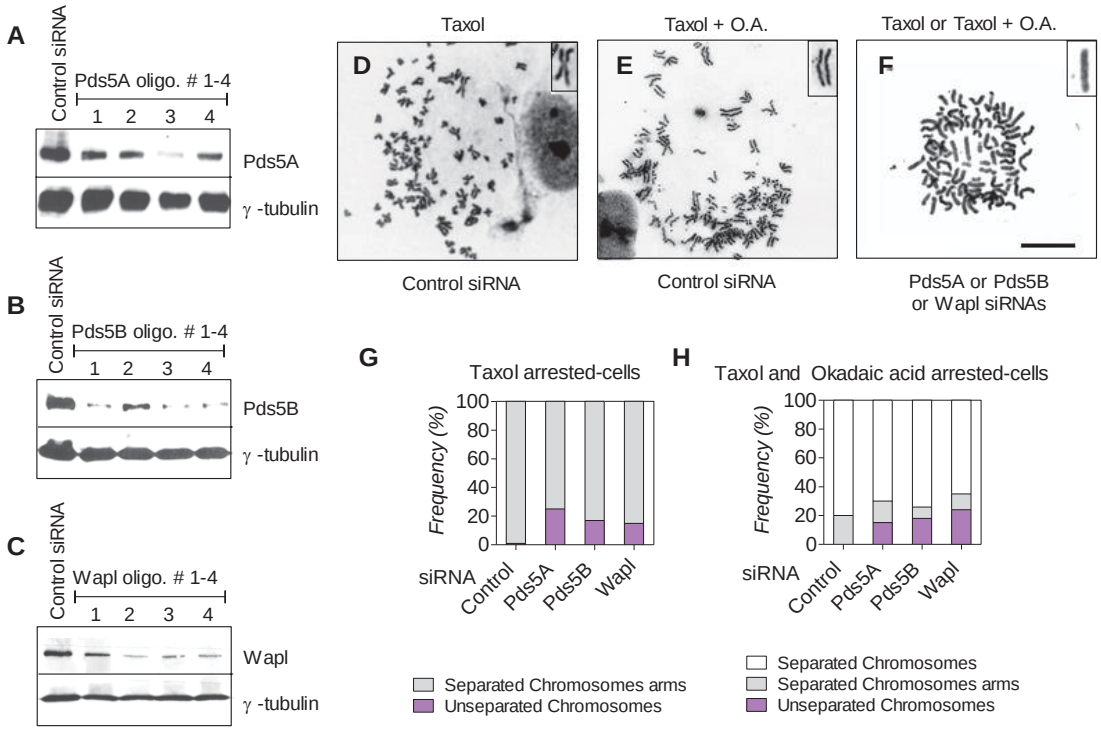

Figure A.8: Single oligonucleotide-mediated Pds5A, Pds5B or Wapl down-regulation.

HeLa cells were transfected for 48 hrs with 50 nM control or individual siRNA (oligonucleotide # 1-4) specific to Pds5A, Pds5B or Wapl (see 2.1.2.1 on page 39). (A-C) Western blots showing the levels of Pds5A, Pds5B or Wapl after depletion; ϒ-tubulin antibody was used for loading controls in Western blot. (D-F) Metaphase chromosome spreads were prepared from cells treated with 10 μM Taxol or 10 μM Taxol and 0.1 μM okadaic acid, in which Pds5A or Pds5B or Wapl proteins were depleted by oligonucleotide # 3 or 1 or 2 respectively. (G and H) Quantification of the chromosome spreads obtained in (D-F) and classified according to their morphology. One experiment was performed and 100 nuclei examined for each treatment.

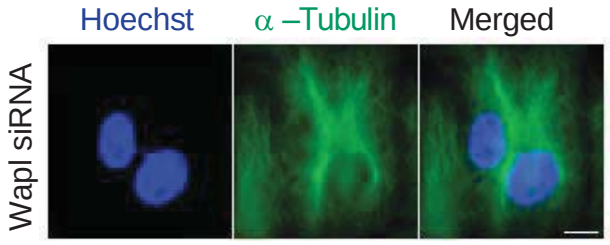

Figure A.9: Formation of chromosomal bridge in cells depleted of Wapl.

HeLa cells were transfected with Wapl siRNA 48 hrs, fixed with -20 °C methanol before being co-stained with anti-α-tubulin (green) to visualize the microtubules and Hoechst 33342 (blue) to visualize the chromosomes, and observed by immunofluorescence microscopy. Scale bar: 10 μm.

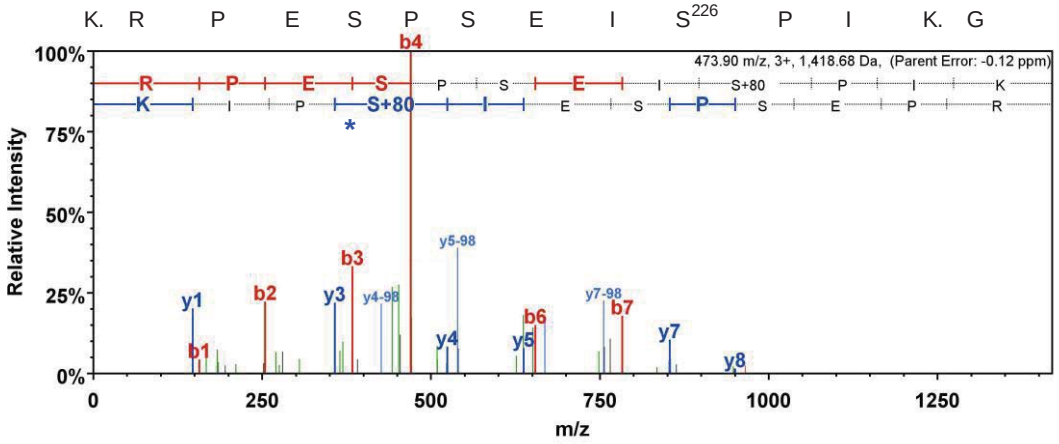

Figure A.10: Example of an *in vivo* Cdk1/cyclin B1 phosphorylation site.

Mass spectrum of peptide K.RPESPSEISPIK.G containing phosphorylated Ser^{226} is shown. The fragment ions along the amino acid backbone recognized by LTQ-Orbitrap-Velos-ETD mass spectrometer are indicated as b-ions (red) having the charge retained on the N-terminal fragment or y-ions (blue) having the charge retained on the C-terminal. Ser^{226} phosphorylation was recognized by 80 Da mass shifts in m/z and indicated with an asterisk.

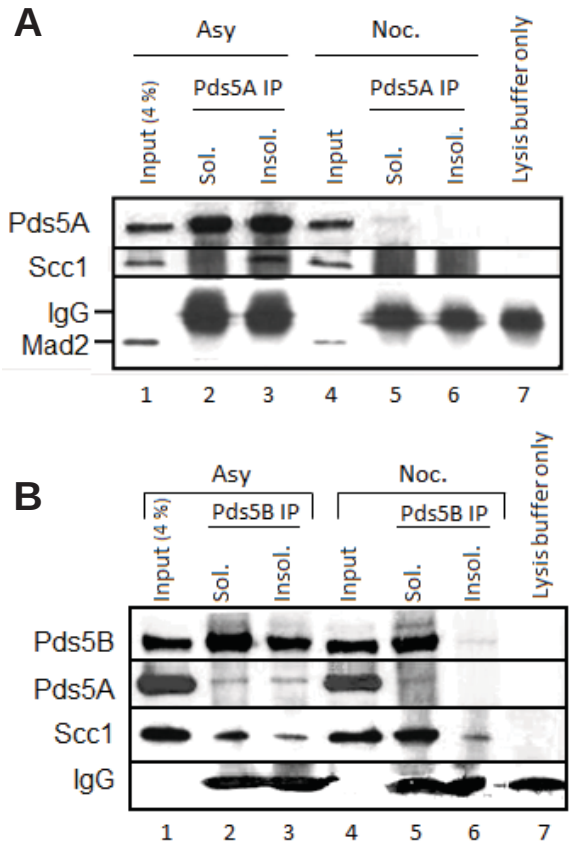

Figure A.11: Investigation of Pds5 interacting proteins.

Soluble (Sol.) and insoluble (Insol.) protein fractions (prepared as described in material and methods) from asynchronous and nocodazole-arrested HeLa cells were subjected to Pds5A or Pds5B immunoprecipitation using specific anti-Pds5A polyclonal (A) or anti-Pds5B polyclonal (B) respectively. The immunoprecipitates (lanes 2–7) along with input (4 %; lane 1) were analysed by SDS-PAGE and Western blotting using Pds5A, Pds5B, Scc1 and Mad2 antibodies. Lysis buffer plus beads and antibody (Ab) was used as negative controls for IP. Data shown from one experiment.